



DUDLEY KNOX LIBRARY
NAVAL POSTGRADUATE SCHOOL
MONTEREY CA 93943-5101

DUDLEY KNOX LIBRARY
NAVAL POSTGRADUATE SCHOOL
MONTEREY CA 93943-5101

Approved for public release; distribution is unlimited.

CONTROL VANE GUIDANCE FOR
A DUCTED-FAN UNMANNED AIR VEHICLE

by

Patrick J. Moran
Lieutenant Commander, United States Coast Guard
B.S., United States Coast Guard Academy, 1981

Submitted in partial fulfillment
of the requirements for the degree of

MASTER OF SCIENCE IN AERONAUTICAL ENGINEERING

from the

NAVAL POSTGRADUATE SCHOOL
June 1993

REPORT DOCUMENTATION PAGE

| | | | |
|--|--|--|-----------------------------------|
| 1a Report Security Classification: Unclassified | | 1b Restrictive Markings | |
| 2a Security Classification Authority | | 3 Distribution/Availability of Report Approved for public release; distribution is unlimited. | |
| 2b Declassification/Downgrading Schedule | | | |
| 4 Performing Organization Report Number(s) | | 5 Monitoring Organization Report Number(s) | |
| 6a Name of Performing Organization Naval Postgraduate School | 6b Office Symbol (if applicable) 31 | 7a Name of Monitoring Organization Naval Postgraduate School | |
| 6c Address (city, state, and ZIP code) Monterey CA 93943-5000 | | 7b Address (city, state, and ZIP code) Monterey CA 93943-5000 | |
| 8a Name of Funding/Sponsoring Organization | 6b Office Symbol (if applicable) | 9 Procurement Instrument Identification Number | |
| Address (city, state, and ZIP code) | | 10 Source of Funding Numbers | |
| | | Program Element No | Project No |
| | | Task No | Work Unit Accession |
| 11 Title (include security classification) Control Vane Guidance for a Ducted-fan Unmanned Air Vehicle | | | |
| 12 Personal Author(s) Patrick J. Moran | | | |
| 13a Type of Report Master's Thesis | 13b Time Covered From To | 14 Date of Report (year, month, day) June 1993 | 15 Page Count 112 |
| 16 Supplementary Notation The views expressed in this thesis are those of the author and do not reflect the official policy or position of the Department of Defense or the U.S. Government. | | | |
| 17 Cosati Codes | | 18 Subject Terms (continue on reverse if necessary and identify by block number) AROD, Aquila, UAV, control, Pulse-width Modulation, Archytas, Humphrey Sensors, Futaba Servo Control, SISO control | |
| 19 Abstract (continue on reverse if necessary and identify by block number) Control of airborne vehicles was originally conceived to be done entirely by human pilots. Improvements in electronics in last 50 years have allowed many flight control functions to become automated, with the pilot continuously monitoring flight parameters from within the vehicle cockpit. With the advent of small unmanned air vehicles (UAV's), which are limited in size and weight-carrying capacity, a pilot is now able to fly an airborne vehicle from a distant ground-fixed position. Miniature electronic instruments control or direct vehicle movements either through pilot commands or autonomously. In order to accomplish reliable, continuous control of a UAV, many sensors are necessary aboard the vehicle. This thesis designed and installed necessary hardware and developed software to guide a UAV's aerodynamic control vanes, with feedback from sensors aboard the vehicle, in order to facilitate ground-based pilot control. Previous thesis work accomplished on this project achieved control of a UAV, named Archytas, in one degree-of-freedom, roll, while mounted on a test stand. Umbilical-controlled guidance of Archytas' control vanes from a forward-mounted sensor pod was set as the goal for this phase of the Archytas project. This work focused on modification of hardware to generate and access required signals, programming of analog-to-digital (A/D) and counter/timer peripheral boards mounted in a personal computer to control electrical and signal flow, and implementation of single input-single-output (SISO) control equations developed concurrently in another thesis. | | | |
| 20 Distribution/Availability of Abstract <input type="checkbox"/> unclassified/unlimited <input type="checkbox"/> same as report <input type="checkbox"/> DTIC users | | 21 Abstract Security Classification Unclassified | |
| 22a Name of Responsible Individual Richard M. Howard and Michael K. Shields | | 22b Telephone (include Area Code) (408) 656-2870, 656-2979 | 22c Office Symbol AA/Ho, EC/Sh |

ABSTRACT

Control of airborne vehicles was originally conceived to be done entirely by human pilots. Improvements in electronics in the last 50 years have allowed many flight control functions to become automated, with the pilot continuously monitoring flight parameters from within the vehicle cockpit. With the advent of small unmanned air vehicles (UAV's), which are limited in size and weight-carrying capacity, a pilot is now able to fly an airborne vehicle from a distant ground-fixed position. Miniature electronic instruments control or direct vehicle movements either through pilot commands or autonomously. In order to accomplish reliable, continuous control of a UAV, many sensors are necessary aboard the vehicle. This thesis designed and installed necessary hardware and developed software to guide a UAV's aerodynamic control vanes, with feedback from sensors aboard the vehicle, in order to facilitate ground-based pilot control. Previous thesis work accomplished on this project achieved control of a UAV, named Archytas, in one degree-of-freedom, roll, while mounted on a test stand. Umbilical-controlled guidance of Archytas' control vanes from a forward-mounted sensor pod was set as the goal for this phase of the project. This work focused on modification of hardware to generate and access required signals, programming of analog-to-digital (A/D) and counter/timer peripheral boards mounted in a personal computer to control electrical and signal flow, and implementation of single-input-single-output (SISO) control equations developed concurrently in another thesis.

Thesis
1981/954
C.I.

TABLE OF CONTENTS

| | |
|--|----|
| I. INTRODUCTION | 1 |
| II. BACKGROUND | 4 |
| A. GENERAL INFORMATION ON UAV'S | 4 |
| B. ARCHYTAS CONCEPT EVOLUTION | 6 |
| 1. AROD | 7 |
| 2. Aquila | 9 |
| 3. The Archytas UAV | 11 |
| III. GROUND CONTROL EQUIPMENT | 15 |
| A. COMPUTERS | 17 |
| B. PC PERIPHERAL BOARDS | 17 |
| 1. Counter/timers: 'Quartz' and 'CIO-CTR' | 17 |
| 2. A/D Boards: 'CIO-AD16jr' and 'DAS-16' | 19 |
| C. CONTROL JUNCTION BOARD AND UMBILICAL CORD | 20 |
| IV. ON-BOARD VEHICLE EQUIPMENT | 25 |
| A. FOREBODY | 25 |

| | | |
|----|--|----|
| 1. | SAS Sensors | 28 |
| a. | Angular Rate Sensors | 30 |
| b. | Vertical Gyroscope | 30 |
| 2. | SAS Sensor Modeling | 32 |
| a. | Angular Rate Sensors | 32 |
| b. | Vertical Gyroscope | 33 |
| 3. | Forebody Interconnections | 34 |
| B. | CHASSIS | 34 |
| 1. | Diode Rectifier Board | 35 |
| 2. | Signal Distribution Buses | 35 |
| 3. | Engine | 38 |
| C. | REARBODY | 38 |
| 1. | Control Vane and Throttle Servos | 40 |
| a. | Futaba Servos | 40 |
| b. | Condor Servos | 42 |
| c. | Servo Modeling | 42 |
| d. | PWM Servo Control | 43 |
| 2. | Ignition and Tachometer | 45 |
| 3. | Alternator | 45 |
| D. | VEHICLE INTERCONNECTIONS | 46 |

| | |
|---|----|
| V. CONTROL VANE GUIDANCE 'C' ROUTINES | 50 |
| A. PWM VANE CONTROL ROUTINES | 51 |
| 1. Basic PWM Control Using Counter/timer Board | 51 |
| 2. PWM Signal Control Via A/D Board | 54 |
| B. SISO ROLL CONTROLLER ROUTINE | 55 |
| C. MIXED CONTROL SURFACE GUIDANCE ROUTINE | 55 |
| VI. SYSTEM EVALUATION AND RESULTS | 60 |
| A. VEHICLE AND GROUND CONTROL EQUIPMENT EVALUATION | 60 |
| 1. Ground Control Equipment | 60 |
| 2. On-board Vehicle Equipment | 61 |
| B. CONTROL ROUTINE EVALUATION | 64 |
| 1. Implementation of SISO Controller | 65 |
| 2. Dual Joystick Control Vane Guidance | 66 |
| C. SUMMARY OF RESULTS | 66 |
| VII. CONCLUSIONS AND RECOMMENDATIONS | 68 |
| APPENDIX A: 'C' PROGRAMS DEVELOPED FOR THE ARCHYTAS UAV | 70 |
| APPENDIX B: HARDWARE SPECIFICATIONS | 80 |

| | |
|---|-----|
| APPENDIX C: SCHEMATICS- AROD-3 AND ARCHYTAS | 95 |
| APPENDIX D: ARCHYTAS UAV ENGINE RUN CHECKLIST | 99 |
| LIST OF REFERENCES | 100 |
| INITIAL DISTRIBUTION LIST | 102 |

LIST OF FIGURES

| | | |
|-----------|---|----|
| Figure 1 | Three-view Sketch of Archytas UAV General Configuration | 8 |
| Figure 2 | AROD UAV Two-view Sketch and Aquila RPV Three-view Sketch | 10 |
| Figure 3 | General Block Diagram of the Archytas UAV Control System | 13 |
| Figure 4 | Archytas UAV Ground Equipment Block Diagram | 16 |
| Figure 5 | Control Junction Board Photograph | 21 |
| Figure 6 | Archytas UAV On-Board Equipment Block Diagram | 26 |
| Figure 7 | Photograph showing Archytas Forebody/Chassis/Rearbody Assembly | 27 |
| Figure 8 | Photograph of SAS Sensors mounted in Forebody | 29 |
| Figure 9 | Axis and Vane Numbering Conventions for the Archytas UAV | 31 |
| Figure 10 | Photo of Chassis-mounted Diode Rectifier Board (TSB5) | 36 |
| Figure 11 | Schematic of Diode Rectifier Board (TSB5) with 3-Phase AC Input | 37 |
| Figure 12 | Photograph of Chassis Bus Board | 39 |
| Figure 13 | Photograph of Rearbody/Chassis Assembly | 41 |
| Figure 14 | Typical PWM Waveform | 44 |
| Figure 15 | Flow Chart for <i>pwm.c</i> Routine | 52 |
| Figure 16 | Flow Chart for <i>atod.c</i> Routine | 53 |
| Figure 17 | Flow Chart for <i>roll.c</i> Routine | 56 |
| Figure 18 | Flow Chart for <i>ai_el_ru.c</i> Routine | 59 |

I. INTRODUCTION

Unmanned air vehicles (UAV's) can offer many benefits to potential users, such as relatively low procurement cost, low cost per flight hour, portability, and simplicity of operation. UAV's are also known as remotely piloted vehicles or RPV's. The term 'UAV' is preferred, denoting an air vehicle often flown autonomously. When studied in an academic environment, such as the Naval Postgraduate School's (NPS) UAV Flight Research Laboratory, UAV's offer students and faculty the ability to safely and inexpensively flight test different aircraft designs, configurations, or technologies. Vehicles can be equipped with radio-frequency (RF) uplinks, allowing thorough command of flight conditions. Additionally, UAV's can be instrumented to send data via RF downlinks so that flight parameters can be observed real-time during flight, or recorded for later analysis. Unique or novel designs can be developed to serve special purposes or missions, which may not be achievable or economically feasible using full-scale piloted aircraft. Safety is another benefit of UAV flight research, as personnel are at minimal risk while a vehicle is airborne during flight testing.

In order to accomplish safe, reliable, and continuous control of UAV platforms, a stability augmentation system (SAS) is often required. A SAS consists of motion sensors, an inertial measurement unit (IMU), a filtering scheme such as Kalman filtering, a navigation system such as GPS (global positioning system), and a microprocessor to perform calculations, all mounted aboard the UAV. The SAS sends command outputs

to the vehicle's aerodynamic control surfaces, which then guide the vehicle's trajectory, either through pilot inputs or autonomously. [Ref. 1]

This thesis details the design and installation of a suite of sensors which provide necessary feedback signals to support the SAS of the prototype Archytas UAV in a hovering flight mode. Later phases of the Archytas project will add additional SAS elements to achieve more complicated flight conditions. Software algorithms which implement the control laws to guide the vehicle's aerodynamic control vanes were developed. Algorithms were encoded using the 'C' programming language. An external personal computer (PC), connected to Archytas through an umbilical cord, served as the onboard microprocessor to test the algorithms. Commands were sent to the control vanes either from two joysticks on a control station via umbilical, which represented the RF transmitter, or as a result of control algorithm feedback from the SAS. The algorithms and control system were tested by simulating various inputs, either joystick or sensor generated, and observing appropriate vane responses.

This project continued work begun by Merz [Ref. 2] and Davis [Ref. 3], which implemented a one degree-of-freedom SAS and core control system for the aerodynamic control vanes. Several concurrent student theses in progress will continue to develop other aspects of the SAS, including the IMU, GPS, MIMO controller and Kalman filters, so that the combined theses will contribute to the final design of the Archytas SAS.

This investigation examined:

- The ground control equipment necessary for umbilical-controlled flight of the Archytas UAV including the PC's required for generation of control signals, the

control junction board on which two joysticks and associated control switches were mounted, and the umbilical cord.

- The redesign of on-board vehicle hardware, including reconfiguration of the previously-designed sensor pod from the vehicle's rearbody to a forebody mounted on struts above the vehicle intake. All wiring harnesses and associated bus boards were connected to accommodate the redesign.
- The modification of 'C'-coded software to generate pulse-width modulated (PWM) signals through programming of counter/timer and analog-to-digital (A/D) boards mounted within the PC's. The PWM signals were used to drive servos which in turn positioned the UAV's four control vanes and throttle.
- The implementation of a single-input-single-output (SISO) and multiple-input-multiple-output (MIMO) controllers as progressive steps toward achieving hovering flight of the Archytas UAV.

This thesis consists of six chapters, including this introduction. Chapter II summarizes evolution of the Archytas project. Chapter III details the ground equipment required for this phase of the project. Chapter IV describes the vehicle's on-board equipment and systems, such as sensors, servos, and signal distribution. Chapter V concerns implementation of control algorithms which develop pulse-width modulated signals to drive the vehicle's control vanes. Finally, Chapter VI deals with system evaluation, results achieved, conclusions derived, and recommendations for future improvements to the system. Appendix A contains 'C' routine listings developed for the project. Appendix B includes plug diagrams, and sensor and peripheral hardware specifications. Appendix C contains schematic diagrams used extensively in the vehicle's signal and electrical connections. Finally, Appendix D is an engine-run safety checklist developed to ensure that proper safety precautions were adhered to during engine runs.

II. BACKGROUND

This chapter begins with a summary of Close-range UAV requirements, and follows with a development of the history of the Archytas project to date. Archytas UAV project mission and goals are also described.

A. GENERAL INFORMATION ON UAV'S

The DoD Unmanned Aerial Vehicles Joint Project Office (UAV JP), which oversees military unmanned air vehicle programs, classifies UAV's into four categories based on a vehicle's intended operating range or endurance:

- Close-range: 30-50 km range,
- Short-range: 150 km range,
- Medium-range: 650 km range,
- Endurance: up to 24 hour flight time.

Close-range UAV's tend to be small, portable vehicles with minimal support equipment. Short-range UAV's are generally larger, requiring incrementally more support equipment and personnel for operation. Medium-range UAV's rival manned aircraft in size, speed, and endurance, and are similar to non-lethal cruise missiles. Endurance UAV's tend to be large in size with glider-like wingspans, and have a desired endurance on the order of days. [Ref. 4]

The Archytas project is directed toward the Close-range UAV category. A Close-range UAV would ideally be employed at Marine Corps expeditionary unit (MEU) or Army battalion level for battlefield intelligence surveillance. Historically, UAV designs require prepared runway surfaces on which to conduct flight operations. This requirement has tended to limit UAV usefulness in battlefield scenarios, which often do not allow the luxury of a dedicated, prepared runway. Previous designers have overcome this shortcoming by using pneumatic launchers or rocket-assisted takeoffs (RATO), but such methods require numerous personnel and bulky support equipment, severely restricting overall UAV system portability. To that end, the UAV JP Master Plan for 1992 included a requirement for a VTOL (Vertical Take-off and Landing) UAV system, which must be able to operate from U.S. Navy surface combatants. VTOL UAV specifications call for a 135 kt cruise speed, 110 nm radius of action, 3 hour loiter time at 110 nm, and 12,000 ft operating altitude. [Ref. 5, pp. 34-6]

A configuration which could meet UAV JP requirements is a hybrid VTOL, which would take-off vertically, using very little ground/deck space. Once airborne the vehicle would transition to horizontal flight to take advantage of the improvements in speed, range, and loiter time which horizontal fixed-wing flight provide. [Ref. 6]

The Archytas UAV is an NPS UAV Flight Research Laboratory project currently under development. The ducted-fan, tail-sitter configuration of Archytas is a VTOL platform being investigated to explore technologies related to the VTOL UAV mission. Archytas' namesake was a citizen of ancient Greece and colleague of Plato credited with having designed, constructed, and flown the first mechanical bird. [Ref. 6]

The U.S. Coast Guard is closely following the development of prototype vehicles which are designed to meet the VTOL UAV specifications. The potential benefits from UAV technology for the Coast Guard's law enforcement efforts are numerous. UAV's could be operated from strategic island locations throughout the Caribbean much more efficiently than costly manned aircraft. Also, Coast Guard ships are similar in size to the small surface combatants specified in the VTOL UAV specifications. As the Coast Guard's research and development budget is far less than DoD's, any technologies advanced by DoD research facilities, such as the Naval Postgraduate School, are frequently later employed by the Coast Guard.

B. ARCHYTAS CONCEPT EVOLUTION

The Archytas UAV is mainly built from the assets of two previously cancelled DoD developmental UAV programs, the U.S. Marine Corps' AROD program and the U.S. Army's Aquila program, both of which are described below. The Archytas mission requires a lightweight, inexpensive UAV which, due to its VTOL capability, can be operated from very confined locations, including flight decks of ships at sea. In its current configuration, Archytas is not specifically designed to meet VTOL UAV requirements. But as a VTOL technology demonstrator, it has the potential to validate the concept of a ducted-fan, tail-sitter-configured UAV, and to design, test, and validate sensor and software requirements for guidance, navigation, and control of such a platform.

Previous work in the NPS UAV Flight Research Lab achieved design and initial testing of a preliminary half-scale version of the Archytas concept. This work introduced the ducted-fan-in-fuselage configuration, although the original concept had been to keep the wings horizontal during hover, rotating only the duct and engine to transition from hover to forward flight [Ref. 7]. The new Archytas configuration, a tail-sitter design with a rigidly-mounted duct, was chosen due to the availability of useful assets and its design simplicity. The Archytas UAV's current configuration is shown in a three-view sketch with approximate dimensions in Figure 1.

Assets remaining from the cancelled AROD and Aquila programs have been acquired by NPS. Elements of each design are being used to further explore the ducted-fan-in-fuselage, tail-sitter UAV configuration. Positive aspects of each design are combined in the Archytas design to form a more efficient, more capable platform than either AROD or Aquila. The following sections describe each vehicle, then how they are combined to form the Archytas UAV.

1. AROD

The U.S. Marine Corps identified a requirement in the late-1970's for an MEU-level intelligence gathering tool, and so commissioned the development of a Close-range UAV to fill that need. Program development was engineered by Sandia National Laboratory at Albuquerque, New Mexico, in conjunction with the Naval Ocean System Command, in the mid-1980's. The result of their design efforts was the Airborne Remotely Operated Device, or AROD. AROD was built to fly strictly in a hover or vertical flight mode. While filling the requirement for operation from unprepared areas,

Dimensions Approximate

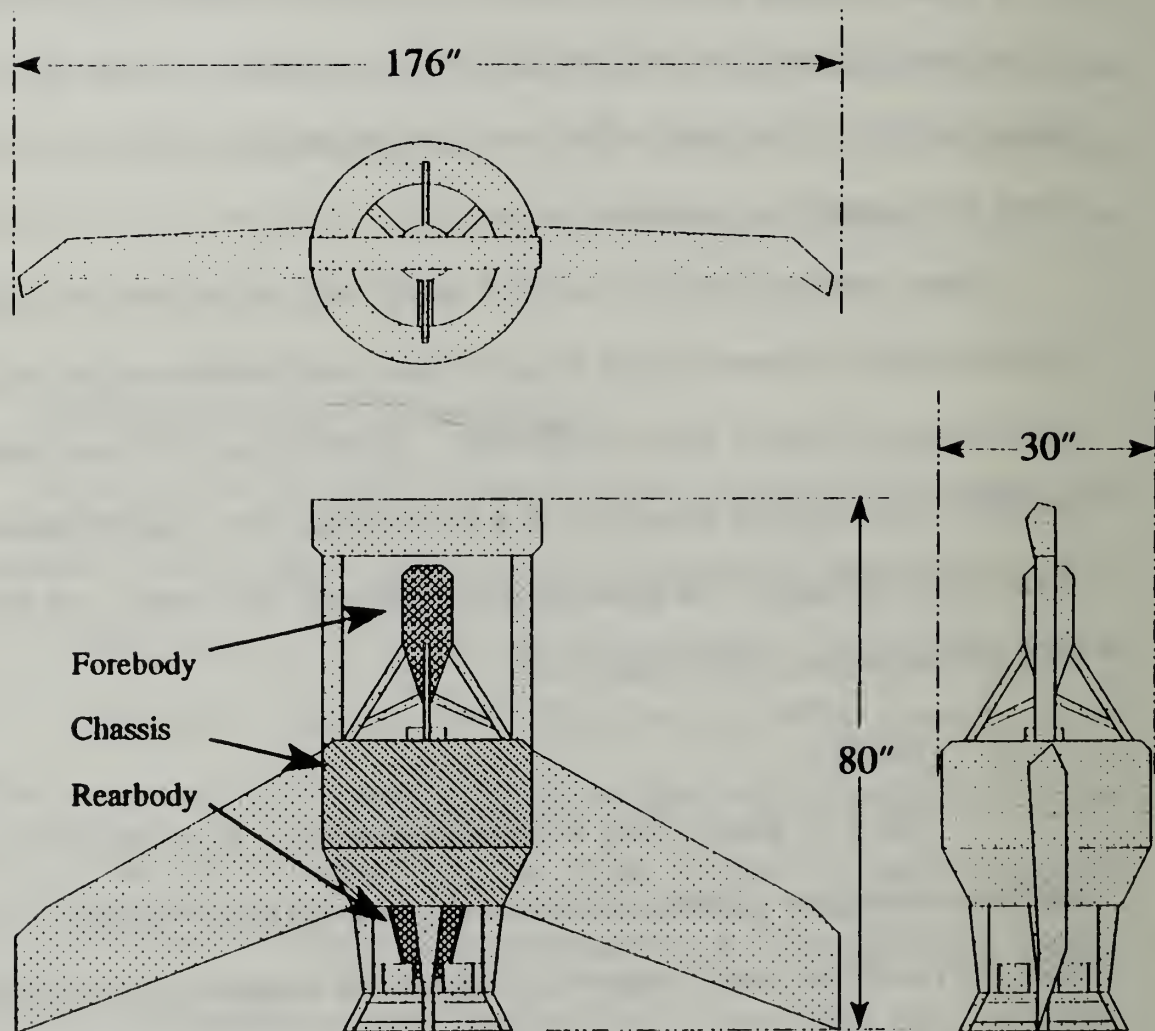


Figure 1 Three-view Sketch of Archytas UAV General Configuration

the configuration was lacking in that its vertical flight mode was inherently inefficient for transitional flight. Its ducted-propeller design did offer the advantage of safety when operated in close proximity to ground personnel, as well as high thrust efficiency. AROD was intended to be controlled primarily through a fiber-optic (FO) link, with RF control available for backup and as a training aide [Ref. 8]. It first flew successfully in 1986, but never went into production. One problem the AROD design suffered from was severe vibration. Also, an updated requirement by the newly-formed UAV JP called for the UAV to be able to achieve translational flight, rather than simply hovering flight, which AROD was not designed to do. The AROD project was cancelled in 1987 due to budget cutbacks [Ref. 6]. Equipment assets remaining from the AROD program were acquired by NPS in 1992. Those assets provide much of the hardware which now makes up Archytas' fuselage and electronics. A two-view sketch of AROD is shown in Figure 2.

2. Aquila

Prior to the AROD program, the U.S. Army developed a short-range UAV, named Aquila, which also never saw operational employment. A pure fixed-wing design engineered by the Lockheed Corporation, Aquila was launched from a pneumatic launch device mounted on a large truck. Aquila was a delta-wing configured RPV, with a wingspan of 12 feet 9 inches. It was powered by a 2-stroke, 2-cylinder gasoline engine, which drove a pusher propeller. Figure 2 shows the general Aquila configuration in a three-view sketch. The Aquila engine, a Dyad 280 made by Herbrandson Engines, Inc., was derived from a commercial chainsaw engine. Coincidentally, the same engine was

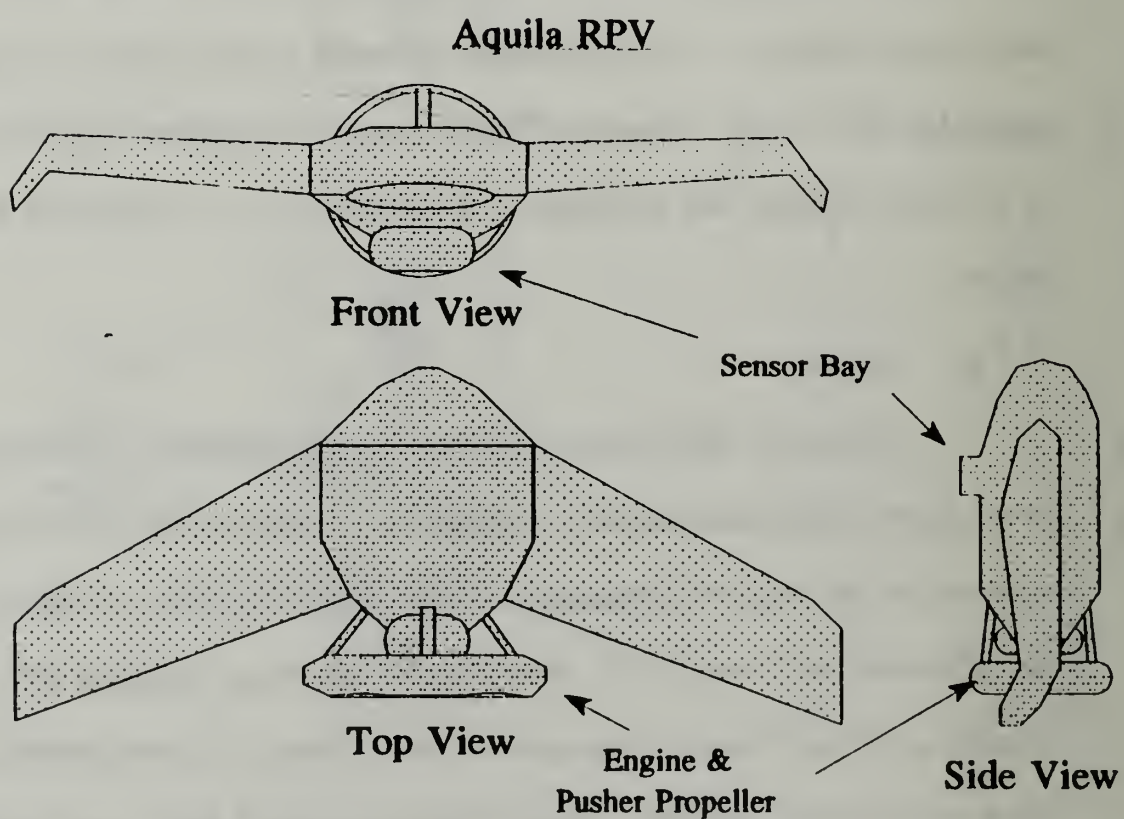
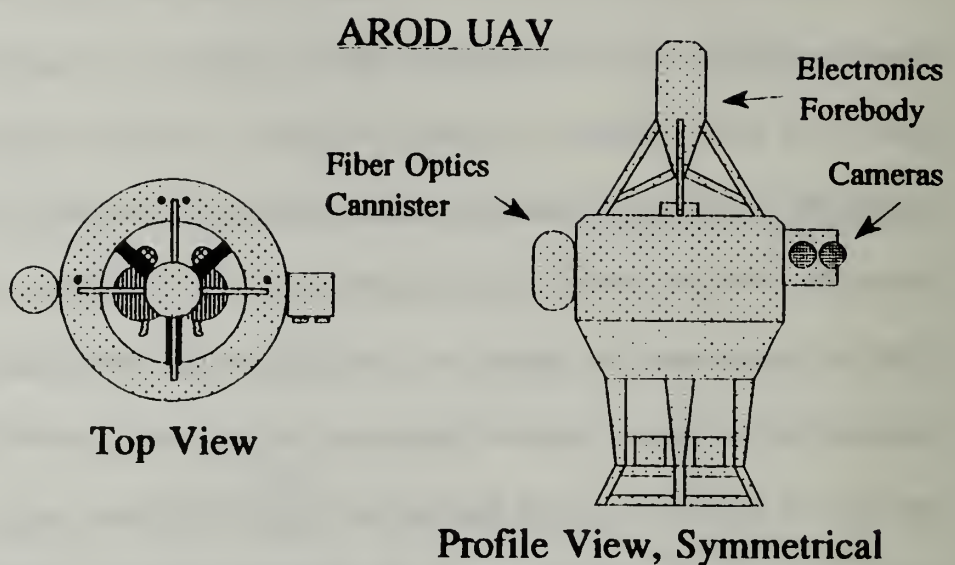


Figure 2 Two-view sketch of AROD UAV and three-view sketch of Aquila RPV

later chosen by Sandia Laboratory for AROD [Ref. 4]. Like the AROD project, the Aquila project was cancelled due to budget cutbacks. The wings from Aquila, which were reflexed to provide longitudinal stability for Aquila's delta-wing shape, are used in the Archytas design by adapting them to mount on an AROD fuselage [Ref. 6]. Figure 2 also shows a three-view sketch of the Aquila RPV.

3. The Archytas UAV

Archytas project goal is to couple the hovering takeoff and landing benefits of AROD with the inherently more efficient and faster horizontal flight characteristics of Aquila. Archytas was designed in a tail-sitter configuration with the AROD body forming the Archytas fuselage and Aquila's wings providing horizontal flight lift. A forward canard was added to provide longitudinal stability in horizontal flight.

AROD's electronics were originally mounted around the exterior shell of its chassis. They were relocated to a pod mounted above its intake duct for center-of-gravity (CG) and vibration considerations. In the initial stages of the Archytas design, the pod was moved aft of the engine and control vanes so as not to impede intake airflow and to ease implementation of the electronics suite [Ref. 2]. Later, longitudinal stability calculations determined that Archytas, like AROD, needed to have the pod forward for CG considerations, despite the potential airflow hinderance [Ref. 9]. Also, experience with the rearbody-mounted electronics pod during engine runs revealed that severe vibration generated by the vehicle's 2-cycle engine was being transferred to the pod. The vibration led to numerous component failures, which served to reinforce the decision to move the electronics pod to the forebody location.

Archytas uses the Aquila and AROD 26-horsepower engine for propulsion. The engine, coupled with a three-bladed ducted propeller, provides approximately 120 lbs of thrust to propel Archytas. To accomplish vertical take-off and landing, only 25 lbs of excess thrust are available. This limits the amount of equipment and payload the vehicle can carry. All of AROD's original fiber optic control equipment and surveillance systems were stripped from its fuselage, which then became the Archytas fuselage. Only the minimum equipment necessary for prototyping the concept was retained. A minimal fuel system is employed, again only for validation of the concept.

Future goals of the Archytas project are to optimize the tail-sitter VTOL configuration by adding state-of-the-art sensors, GPS receivers, and on-board microprocessors, allowing for fully autonomous flight guided through a MIMO controller. Uplinks and downlinks will provide continuous vehicle command and monitoring of flight parameters.

A general block diagram of the Archytas UAV control system developed in this thesis is shown in Figure 3. The following two chapters will detail the ground control equipment and on-board vehicle equipment shown in the diagram.

Chapter V then discusses the control vane guidance algorithms written to control the system. In general, the system works through sensors aboard the Archytas which sense vehicle motions and output analog signals. The sensor signals are conditioned aboard the vehicle to the proper voltage ranges, then are sent to the PC via the umbilical cord and control junction board. This information is used by a pilot, or a control algorithm, to guide the vehicle. Pilot inputs from two joysticks mounted on the

Archytas Vehicle

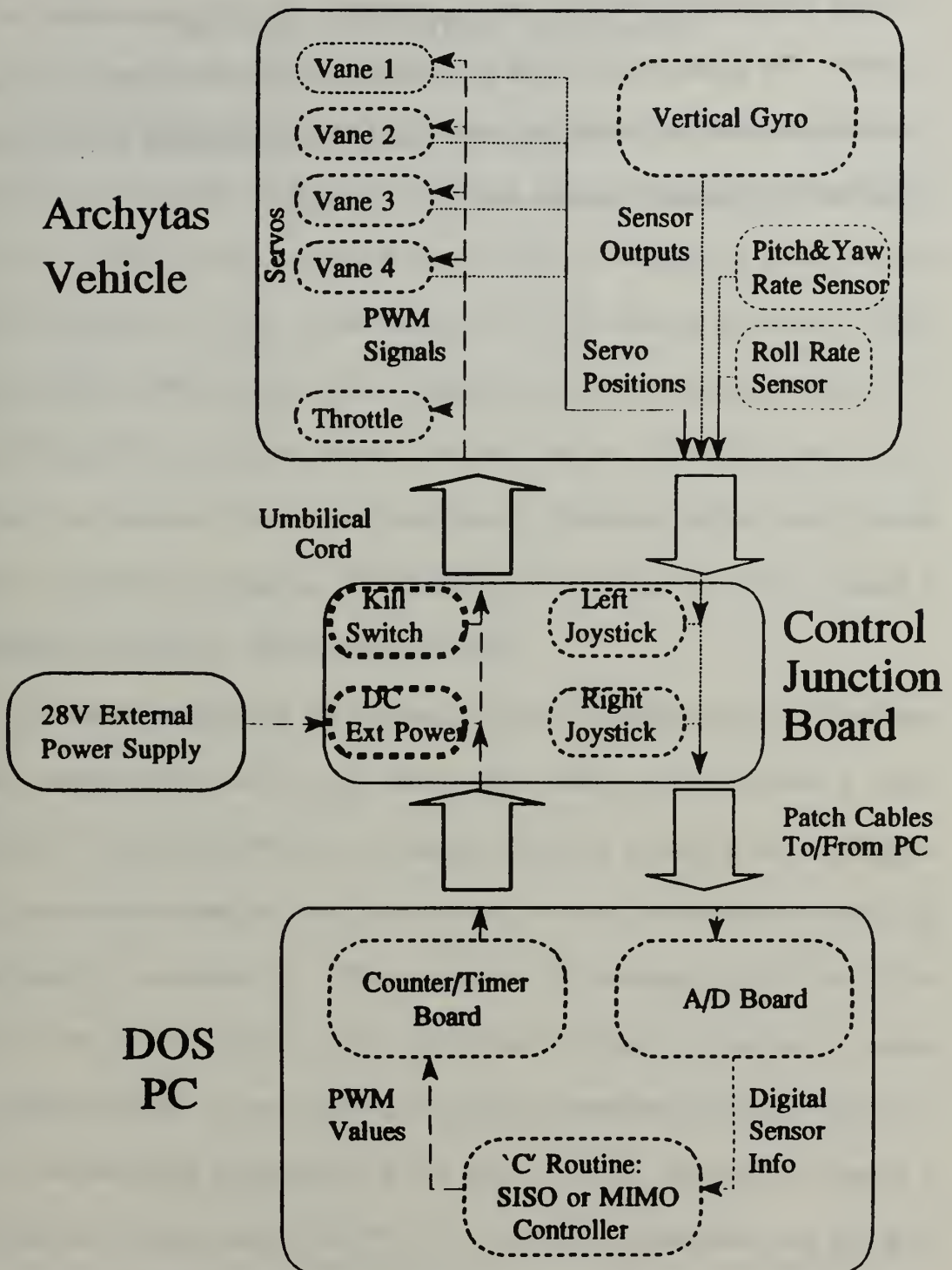


Figure 3 General Block Diagram of the Archytas UAV Control System

control junction board are converted from analog signals to digital numbers and are sent to the counter/timer boards in the PC, possibly via a control algorithm, to generate pulses. The pulses vary in width proportionally to the desired position of the servos. These pulses are then sent back to the vehicle via the umbilical cord to guide servos attached to the vehicle's control surfaces and throttle.

III. GROUND CONTROL EQUIPMENT

The ground equipment necessary to control Archytas in this phase of development is described in this chapter, as depicted in Figure 4. Much of the equipment was unique to this phase of the project, and will either be removed or relocated as the Archytas project progresses. For instance, the external PC which controls generation of pulse-width modulated (PWM) signals will be replaced in a future developmental phase by a 486 CPU aboard the vehicle to perform the same function. When this occurs, many umbilical cord functions will no longer be necessary. Commands will be passed between the pilot and vehicle by data link. It should be evident that many other changes in configuration will occur as the project progresses.

As described in Chapter I, the Archytas UAV will eventually have a self-contained stability augmentation system (SAS) aboard the vehicle centered around a micro-processor. To ease implementation and design of the SAS, it was felt that development should begin with an umbilical cord control system, with the micro-processor role being accomplished by an external PC. This would allow for developing the RF data link at the same time that the control system was being developed. A method of passing information to the PC via the umbilical cord, then transmitting commands back to the vehicle, was developed independently at this stage of design. Equipment necessary to accomplish this process included the PC's, the associated counter/timer and analog-to-digital boards, the control junction board which is the mounting location for two joysticks

Archytas Vehicle

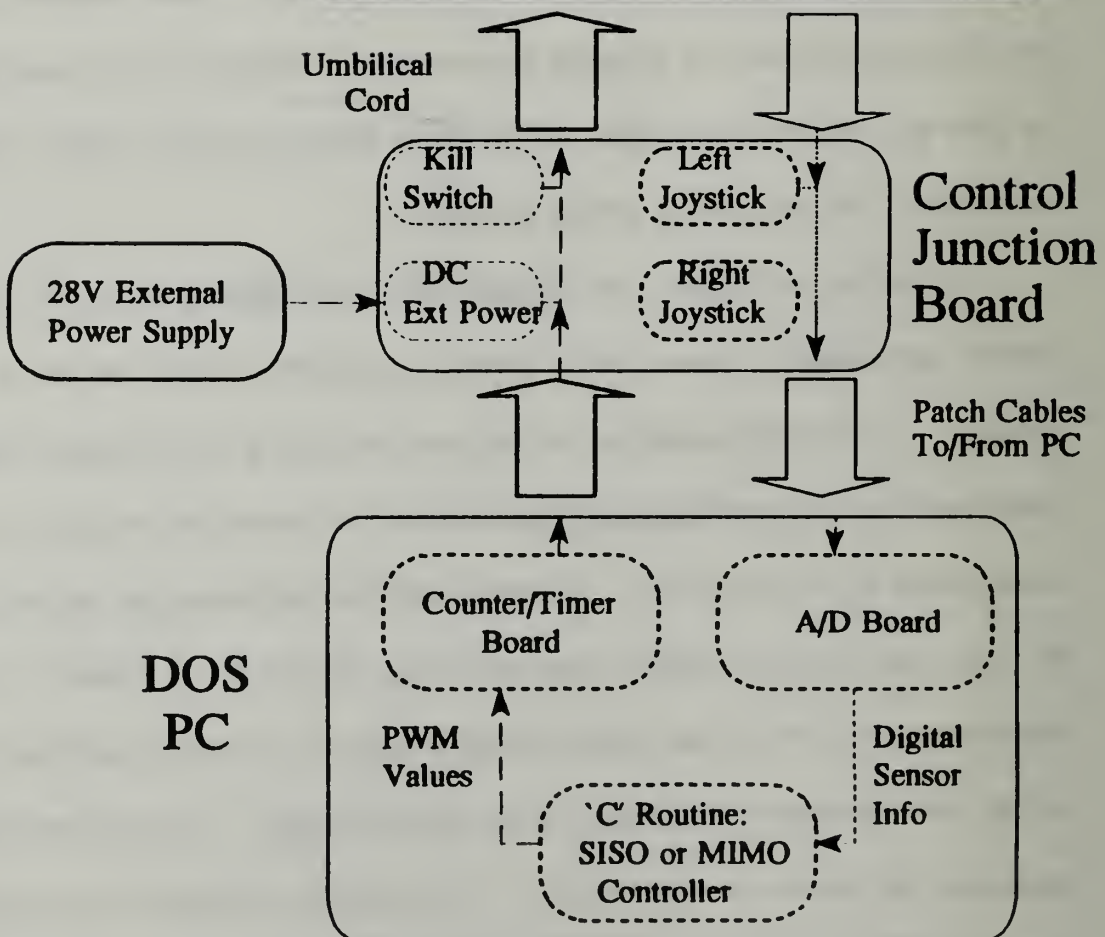
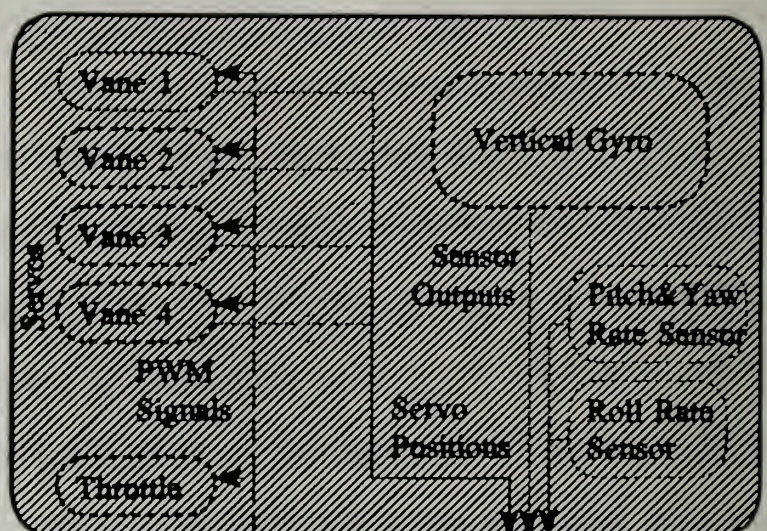


Figure 4 Archytas UAV Ground Equipment Block Diagram

and associated switches, and the umbilical itself. This equipment is described in this chapter.

A. COMPUTERS

The NPS UAV Lab operates two IBM-compatible PC's, a RAMPCOM 486DX 50 MHz and an IBM AT retrofitted with an OPTi 386DX 25 MHz motherboard. Both were used in development of 'C' routines written for Archytas using a Borland 'C' compiler. The 'C' programming language was used by Merz [Ref. 2] to develop initial PWM and A/D routines because it is relatively user-friendly and is widely used in engineering applications. Later phases of development necessarily follow the same 'C' conventions. Two peripheral boards, described in the next section, were used in each computer to control signals coming to and from the PC's through 'C' routines.

B. PC PERIPHERAL BOARDS

1. Counter/timers: 'Quartz' and 'CIO-CTR'

In order to develop PWM signals, a method of regulating the duration of each pulse was required. Two counter/timer boards, 'Quartz' made by Diamond Systems Corporation and 'CIO-CTR' made by Computerboards Inc., were used to generate PWM signals to control the aerodynamic control vane servos and the throttle servo. These boards were programmed to regulate pulses to a desired width and repetition rate. Specific register-level programming instructions for each board, as well as the A/D boards described in the following section, were well-documented by Merz [Ref. 2,

Chapters IV and V]. Both boards employ an Am 9513A counter/timer microchip as the heart of their circuitry. This compatibility allowed 'C' routines to be run interchangeably through either board in either computer. The Am 9513A chip has five individual counters, as well as a user-selectable frequency oscillator. The CIO-CTR board was configured with two Am 9513A chips, allowing the use of 10 counters, although this feature was not used since only five counters were necessary. The only difference operationally between the boards was their different connector plugs: Quartz used a 50-pin plug, while CIO-CTR used a 37-pin connector. This required the control junction board, which connected PC cables to the umbilical, to have adapters for both plug arrangements. The pin-out diagrams and necessary connections for each counter/timer are shown in Appendix B. Initial DIP switch settings for each board, which define the board's operating modes, are defined in Table 1.

TABLE 1: COUNTER/TIMER BOARD DIP SWITCH SETTINGS

| <u>Board</u> | <u>Base Address</u> | <u>Interrupt</u> | <u>Wait State</u> |
|--------------|---------------------|------------------|-------------------|
| Quartz | 220 Hex | 5 | N/A |
| CIO-CTR | 220 Hex | X (No IRQ) | On |

2. A/D Boards: 'CIO-AD16jr' and 'DAS-16'

An A/D board converts analog voltage signals to digital numbers, which can then be manipulated by software and the counter/timer boards to produce PWM signals. The A/D boards used were the 'CIO-AD16jr' made by Computerboards Inc., and 'DAS-16' made by the Metrabyte Corporation. Like the counter/timer boards, both A/D boards employed compatible microprocessors and timers, the Intel 8254 programmable interval timer, to complete the A/D conversion process. Again, the boards' compatibility allowed for 'C' routines to be run interchangeably on either computer. Both A/D boards used similar 37 pin plugs, but different pin arrangements. Fortunately, the pins used for Archytas were the same on both plug arrangements, easing interoperability. The pin-out diagrams for each A/D board and the necessary connections are shown in Appendix B. The initial DIP switch settings for each A/D board are shown in Table 2.

TABLE 2: A/D BOARD DIP SWITCH SETTINGS

| <u>Board</u> | <u>Base Address</u> | <u>Channel</u> | <u>Clock</u> | <u>DMA</u> | <u>Input Range</u> |
|--------------|---------------------|----------------|--------------|------------|--------------------|
| CIO-AD16jr | 300 Hex | 16 | 1 | 1 | Software-Driven |
| DAS-16 | 300 Hex | 16 | N/A | 1 | 1 1 0 0 0 |

C. CONTROL JUNCTION BOARD AND UMBILICAL CORD

Commands which guide Archytas' control vanes and throttle were made using two joysticks mounted on a control junction board. Earlier generation routines by Merz [Ref. 2] used input from only one joystick. The joysticks were arranged in a layout similar to that of a standard radio-control (RC) transmitter. The left joystick, taken from a surplus Futaba transmitter, controlled inputs to the rudder (left/right, spring-centered) and throttle (up/down, not spring-centered). The right joystick, taken from a surplus AROD ground control station, commanded ailerons (left/right, spring-centered) and elevator (up/down, spring-centered).

A photograph of the control junction board in its current configuration is shown in Figure 5. It shows the dual joysticks, umbilical cord connections, PC patch cables, kill switch, and DC external power connections.

A remote kill switch, which was a direct tap into the engine's ignition wire through the umbilical cord, was also mounted on the control junction board. The entire control junction board will eventually be replaced by an actual RC transmitter in a later project phase when the umbilical is no longer required.

Each joystick single degree-of-freedom had a different voltage range from its lower limit to upper limit. The left stick also was equipped with trim knobs for each degree-of-freedom. To prevent inadvertent movement of the trim knobs, the knobs were taped in the full down position for throttle, and centered position for rudder to ensure consistent voltage outputs. The analog voltage difference from each joystick output, when passed through the A/D board, translated to a range of digital values. The A/D board used a

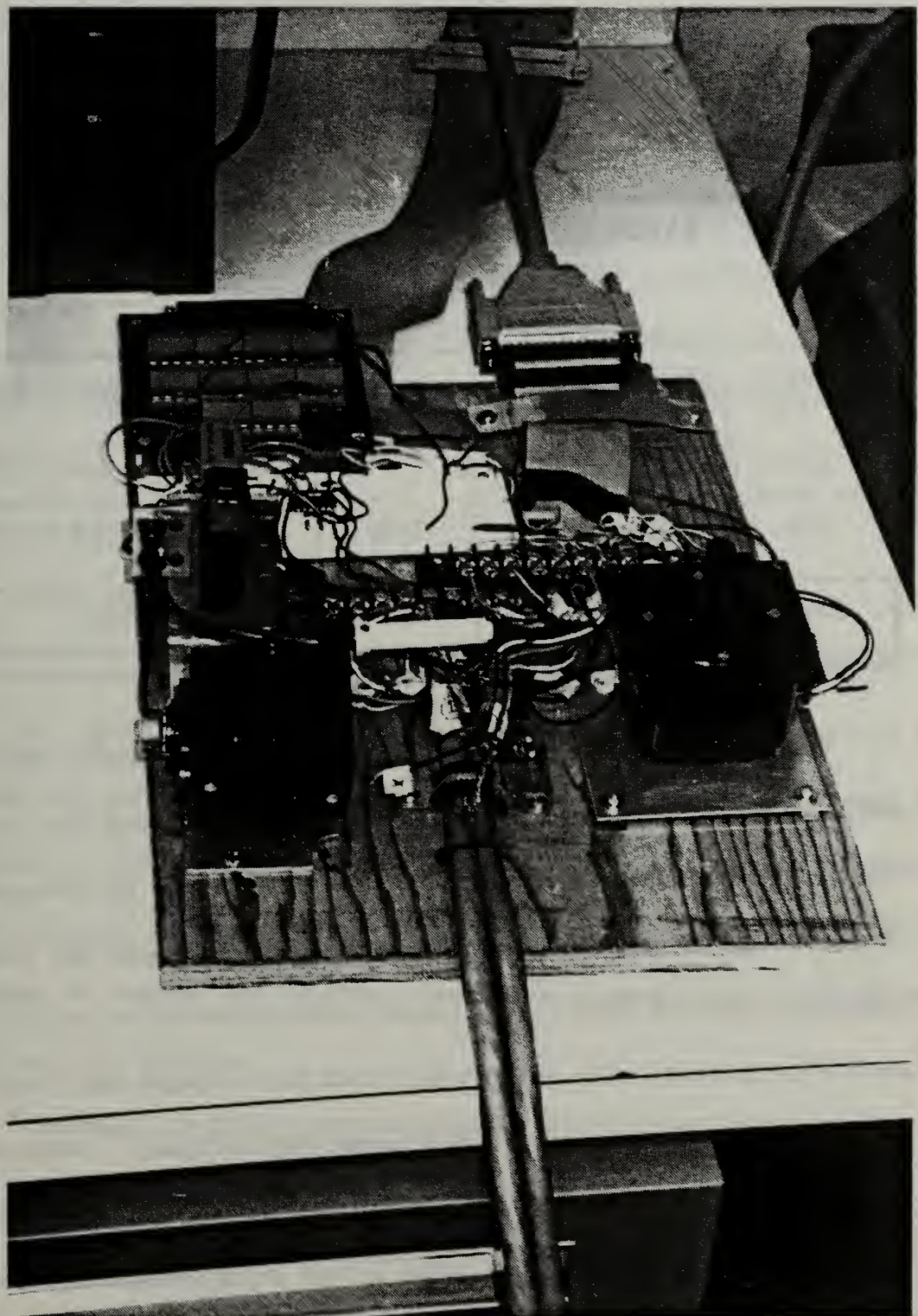


Figure 5 Control Junction Board Photograph

12-bit conversion, so that a 0 to 5 volt analog range translated to a 0 to 4096 digital range. Table 3 lists the minimum, center, and maximum digital units for each stick's two degrees-of-freedom. These values were recorded empirically.

TABLE 3: JOYSTICK DIGITAL UNIT RANGES
(AFTER A/D CONVERSION)

| <u>Joystick</u> | <u>Minimum</u> (Down) | <u>Center</u> | <u>Maximum</u> (Up) | <u>Minimum</u> (Left) | <u>Center</u> | <u>Maximum</u> (Right) |
|-----------------|--------------------------|---------------|------------------------|--------------------------|---------------|---------------------------|
| Left | 2490 | N/A | 3140 | 1600 | 1150 | 720 |
| Right | 1850 | 2260 | 2650 | 2470 | 2090 | 1680 |

The umbilical cord used consisted of shielded six-twisted-pair cable, obtained from surplus telephone cable. Since 21 signals needed to be transferred from the ground station to/from the vehicle, two cables were used side-by-side. The two cables were labelled '1' and '2' and tie-wrapped together for security. Signal flow through the umbilical is charted in Table 4. The vehicle's umbilical connection was at the lowest point of the rearbody. The endcap which would have normally been located at the bottom of the rearbody was replaced by a surplus forebody topcap. This arrangement allowed an easier and more secure method of mounting the umbilical cord to the vehicle. The Cannon plug connections at the vehicle end and wiring connections at the control junction board end of the umbilical cord are shown in Appendix B.

TABLE 4. UMBILICAL CORD SIGNAL FLOW

Total Wires: 21, plus shield & chassis ground. 23 of 24 Umbilical Pins Used.

| To Vehicle fm Control Junction Board | Fm Vehicle to Control Junction Board |
|---|---|
| 4 Vane Command Signals: Vanes 1, 2, 3, & 4 | 3 Rate Signals: Roll, Pitch & Yaw Rate 3 Control Positions: Aileron, Elevator & Rudder Position |
| 1 Throttle Command Signal | 2 Vertical Angles: Pitch & Yaw |
| 2 Kill Switch Leads to Ignition | 1 Tachometer Signal |
| External Power: 28V DC & Reference (2 of each) | 1 Common |

The control junction board also provided a convenient mounting location for external 28V DC power connections. External DC power was passed through the umbilical cord for use whenever the vehicle's engine-driven alternator was not supplying power. This also allowed operation of the vehicle engine with external electrical power supplying the vehicle. The alternator could then be disconnected for troubleshooting electrical system problems.

In summary, the ground control equipment described in this chapter includes:

- PC to perform micro-processor calculations via 'C' programming;
- Counter/timer board mounted within the PC to generate PWM signals;
- A/D board mounted within the PC to convert analog voltage signals from sensors and joysticks to digital values for PWM generation;

- Control junction board to serve as a connection point between the umbilical cord and PC counter/timer and A/D patch cables, and as a mounting location for two pilot joysticks and a remote kill switch.

In a later phase of the Archytas project, the external PC will be replaced by a 486 CPU aboard the vehicle. This will occur after all umbilical cord testing has been successfully accomplished and an RF data link has been developed. The control junction board's joysticks will be replaced by joysticks on an RC transmitter. The remote kill switch will be operated through a dedicated servo on the vehicle commanded from a switch on the RC transmitter. A receiver and antenna will be mounted on the vehicle to complete the RF data link for control and flight parameter information transmission.

IV. ON-BOARD VEHICLE EQUIPMENT

The Archytas UAV fuselage, as depicted in Figure 6, can be divided into three sections: the forebody, located on thin aluminum struts above the intake; the chassis, which is the main Archytas body made from the AROD fuselage; and the rearbody, which is below and inside of the chassis. Equipment related to this thesis was located in or on all three sections. A schematic diagram drawn for the AROD project was used extensively for forebody/chassis/rearbody wiring connections. The schematic is included in Appendix C in two diagrams titled "AROD-3 SCHEMATIC" and "SHEET 2 OF 2." Several full-size blueprint copies of the schematic are available in the NPS UAV Lab for closer inspection. Schematic diagrams of the Archytas control system are also included in Appendix C. A photograph of the Archytas forebody/chassis/rearbody assembly is shown in Figure 7.

A. FOREBODY

The forebody is a pod mounted on tubular aluminum struts above the engine intake. It houses the SAS sensors, signal conditioning circuit boards, and DC power distribution boards. A 28V fan mounted in the forward end, or top, circulates air within the pod for cooling. Electrical connections to the forebody are made through Cannon plugs located adjacent to the four strut mounting points. Connecting wire harnesses are guided down each strut and around the outside of the intake to the chassis. Individual components

Archytas Vehicle

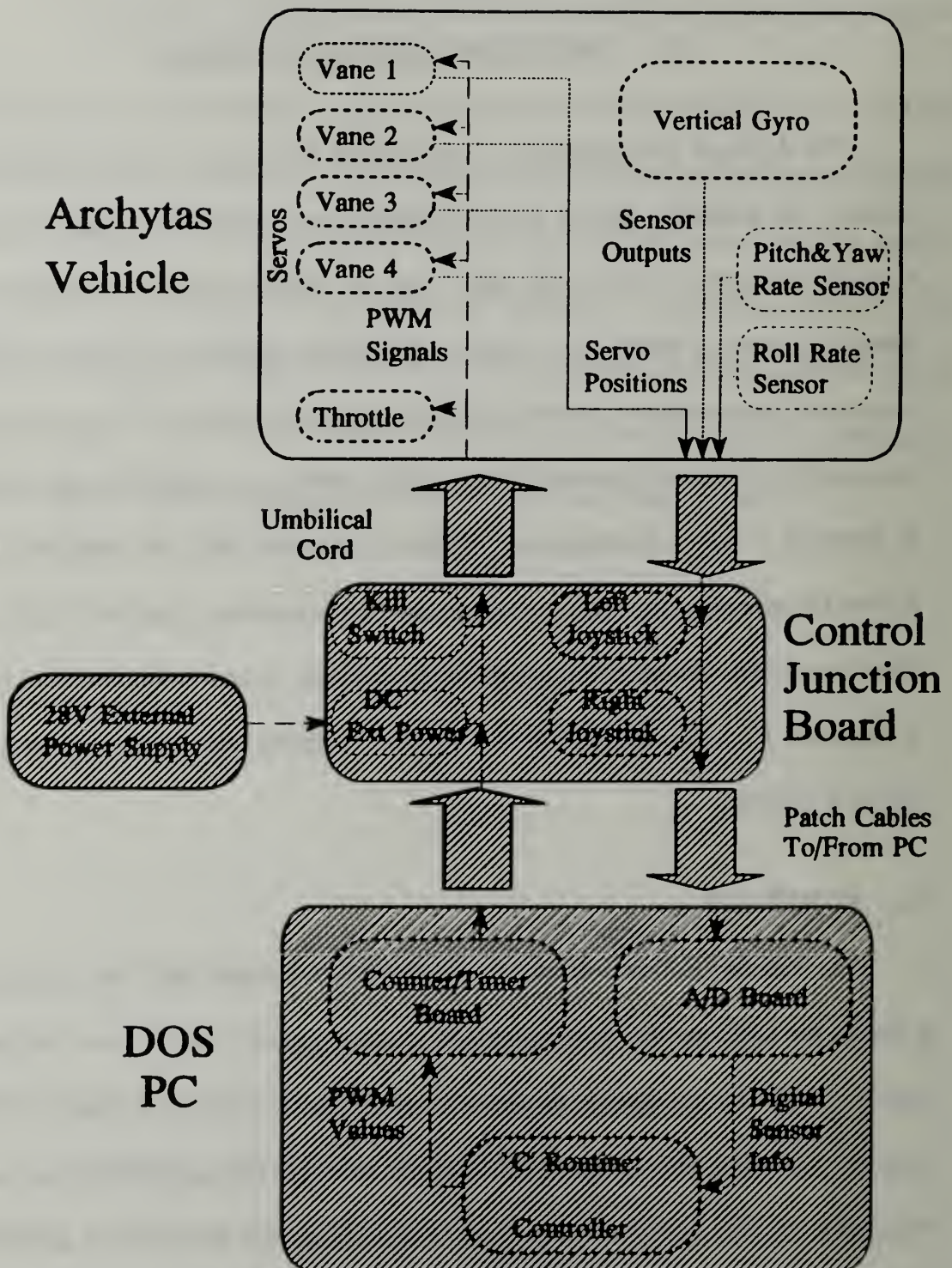


Figure 6 Archytas UAV On-Board Equipment Block Diagram

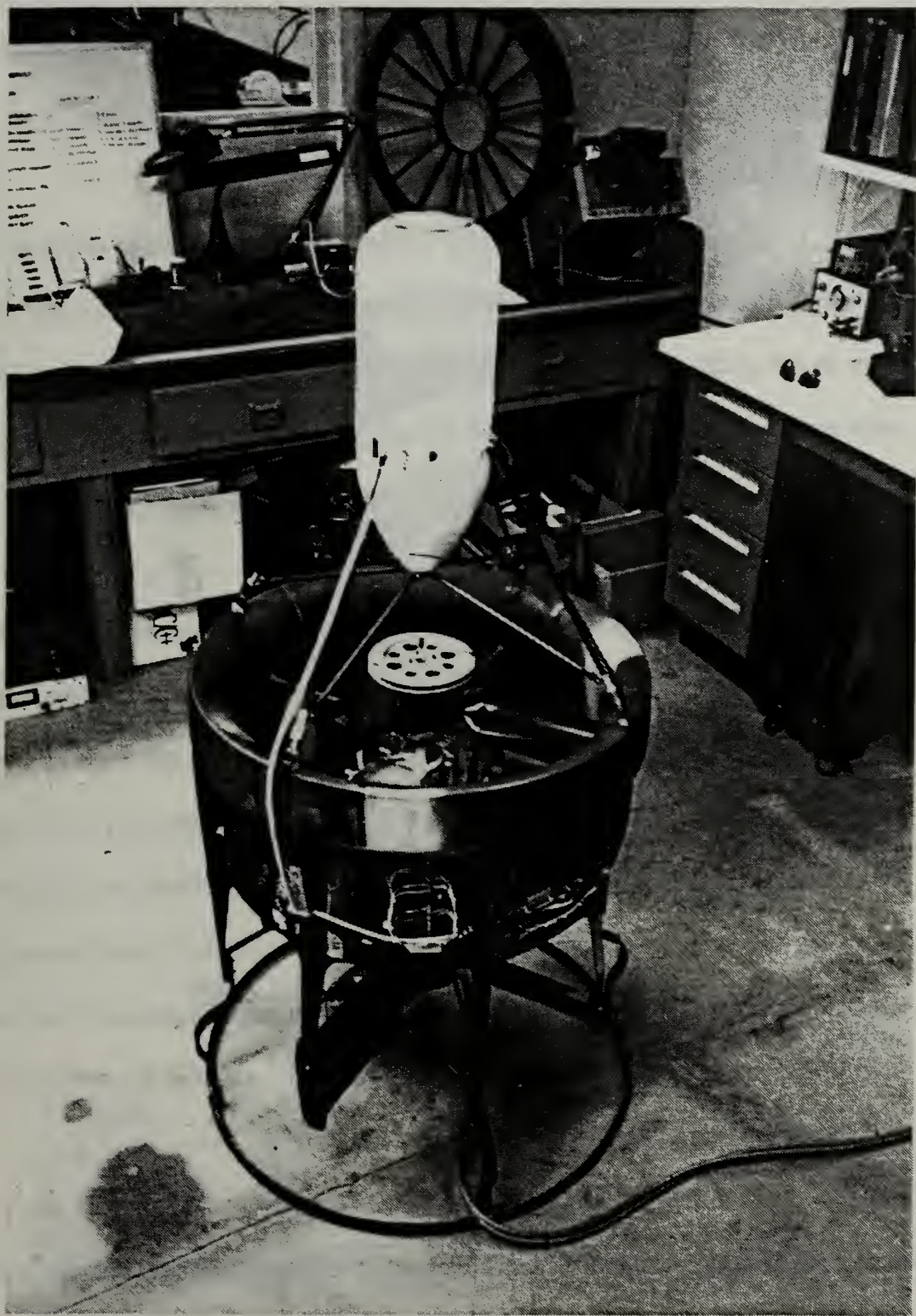


Figure 7 Photograph showing Archytas Forebody/Chassis/Rearbody Assembly

within the forebody are detailed in the following sections. A photograph depicting the sensors mounted in the lower portion of the forebody is shown in Figure 8.

1. SAS Sensors

The flight parameters which needed to be monitored and fed back for the A SAS to operate in a vertical hover flight mode were determined to be angular rotation rates in roll, pitch and yaw about each body axis x, y, and z, respectively, and vertical pitch and yaw angles about the y and z body axes, respectively [Ref. 1]. The sensors necessary to measure these parameters are three angular rate sensors and a vertical gyroscope.

Sandia Laboratory designers referenced AROD parameters using strut three as the ‘top’ of AROD. Strut three can be quickly distinguished from the other three struts by two small fuel tank vents located atop the intake next to the forebody connecting rod mounting point. There is one vent at struts two and four, and no vents at strut one. This convention led to labeling vane three, located below strut three, the ‘upper rudder’. Following the same convention, vane one is the ‘lower rudder’, vane four is the ‘left elevator’, and vane two is the ‘right elevator’. The natural body axes are then: x aligned with AROD’s vertical axis, with positive being forward, y positive toward strut two, and z positive toward strut one. [Ref. 8]

The same axes used for AROD were chosen for the Archytas UAV. This choice specified the attachment points for the UAV’s left and right wings. Angular rotation rates and angle measurements for Archytas are then: positive roll angle and rotation rate clockwise about the vertical x axis; positive pitch angle and rotation rate

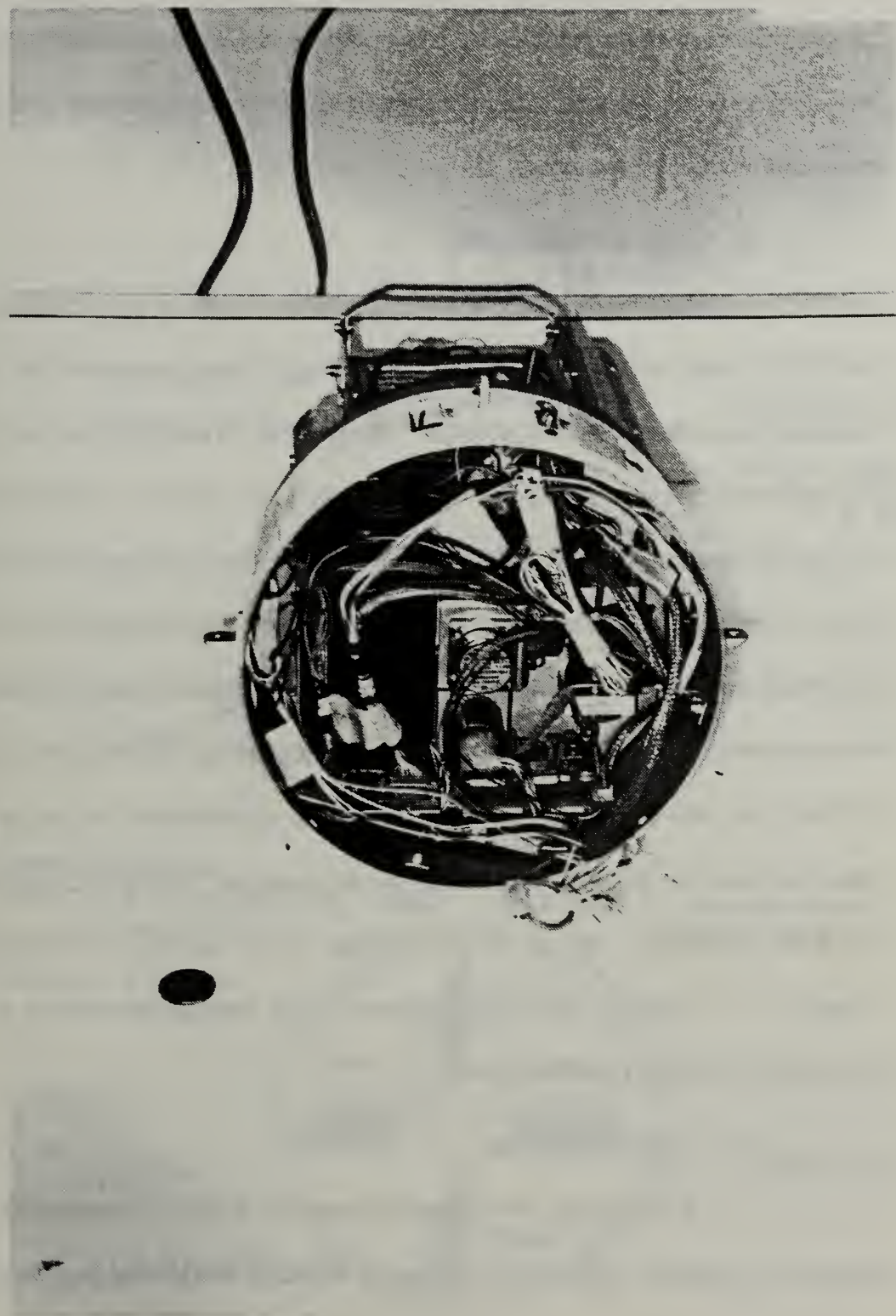


Figure 8 Photograph of SAS Sensors mounted in Forebody

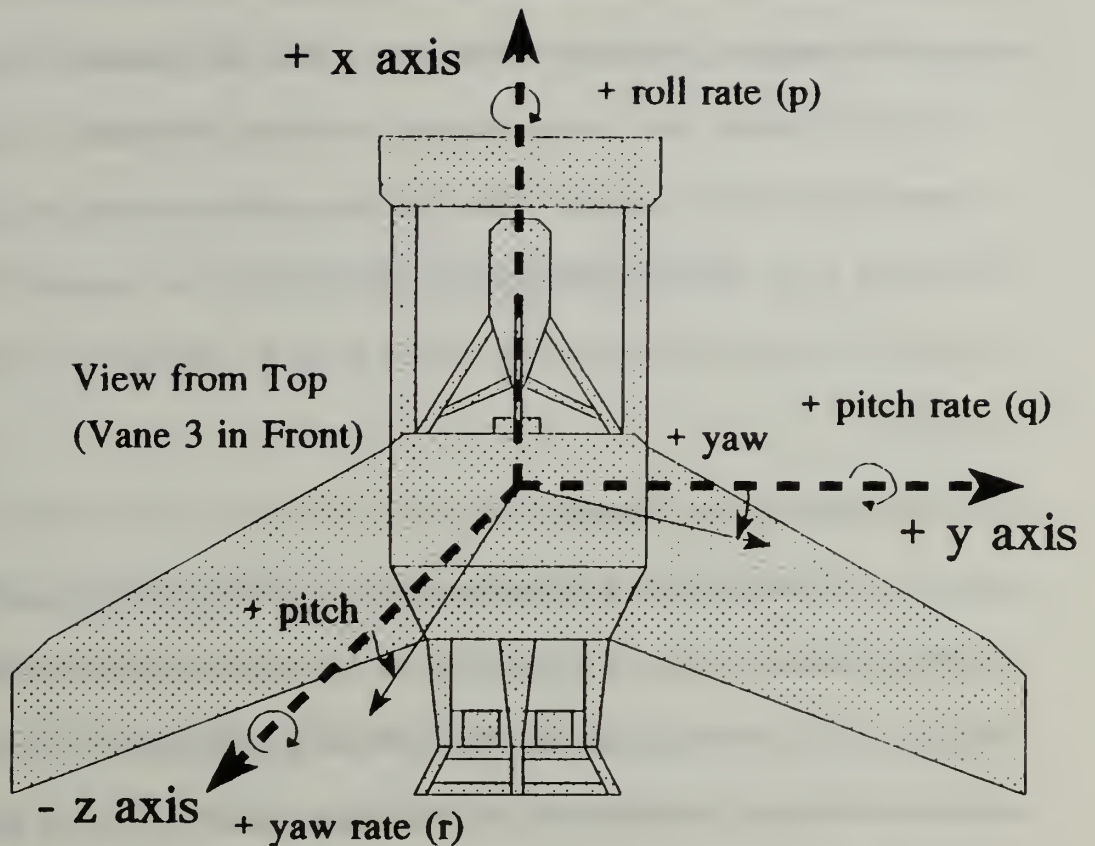
toward strut three and about the y axis; and positive yaw angle and rotation rate toward strut two and about the z axis. Figure 9 graphically depicts the axis and vane numbering conventions applied to Archytas.

a. Angular Rate Sensors

The angular rate sensors used aboard Archytas were Humphrey RT-01 and RT-09 single and dual rate sensors, respectively. Rate sensors are the "solid state functional equivalent of a rate gyroscope. They provide an output voltage that is linearly proportional to the angular rate of the sensor" [Ref. 10]. The RT-01 was used to sense roll rate about the x axis. The RT-09 measured pitch and yaw rates about the y and z axes. Appendix B contains diagrams of the electrical connections for the RT-01 and RT-09 angular rate sensors. Appendix B also contains manufacturer's specifications for both rate sensors, including maximum rates of 100°/sec for roll from the RT-01, and 100°/sec for pitch and yaw from the RT-09. The specifications call for at least one minute of warm-up before accurate rates can be measured. Electrical interconnections for both sensors are shown on the diagram titled "AROD-3 SCHEMATIC" in Appendix C. Forebody plug "P2" connects both rate sensor outputs to the A1 CHANNEL CONDITIONING BOARD.

b. Vertical Gyroscope

A Humphrey VG-34 vertical gyro was used to measure pitch and yaw angles from vertical. Appendix B includes an electrical connection diagram for the



Control Deflections:

Vanes 2 & 4 Trailing Edge (TE) Down:
Positive Elevator

All 4 Vanes TE Counterclockwise:
Positive Aileron

Vanes 1 & 3 TE Left:
Positive Rudder

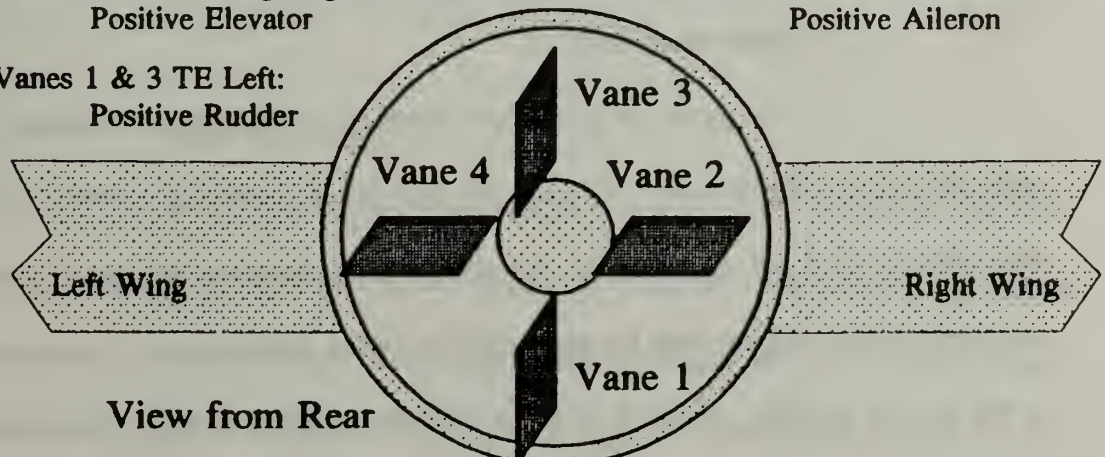


Figure 9 Axis and Vane Numbering Conventions for the Archytas UAV

VG-34. Appendix B also contains manufacturer's specifications for the VG-34, including a maximum angle of $\pm 60^\circ$ in pitch and $\pm 90^\circ$ in yaw, each accurate to $\pm 1^\circ$. As listed in the specifications sheet, a warm-up time of at least 5 minutes is required before accurate angles will be measured. Electrical interconnections for the vertical gyroscope are shown on the diagram titled "AROD-3 SCHEMATIC" in Appendix C. Forebody plug "P1" connects vertical gyroscope outputs to the A1 CHANNEL CONDITIONING BOARD.

2. SAS Sensor Modeling

A mathematical model of Archytas was developed in concurrent thesis work by Kuechenmeister [Ref. 12] in order to predict how the aircraft will actually perform in flight. Creation of the model involved representing each item of the Archytas control system as a dynamic element with its own characteristics within the larger, overall system. The vertical gyroscope and angular rate sensors, which react to vehicle motions, were represented using data derived from their manufacturers' specifications.

a. Angular Rate Sensors

A rate gyro is a gyroscope which reacts to angular rotational speeds in only one degree-of-freedom. Although the rate sensors used for Archytas were solid state devices, and not actual gyros, the theory of operation is the same. Rate gyros measure angular rotation rates by measuring the linear displacement of a spring attached to the gyro's gimbals, which is a direct measure of input speed. The measurement sensitivity of a given gyro is a function of the stiffness of the gyro's spring. The

spring's displacement is a reaction to torque developed by the momentum force due to the spinning gyroscope. The entire system for one degree-of-freedom can be expressed as a second-order transfer function:

$$V(s) = \left(\frac{\omega_n^2}{s^2 + 2s\zeta\omega_n + \omega_n^2} \right) \cdot (\omega_i(s) - D(s)) \quad (1)$$

where $V(s)$ is the LaPlace transform of the output voltage, $\omega_i(s)$ is the LaPlace transform of the input rotation rate, $D(s)$ is the error term, and ω_n and ζ are the natural frequency and damping ratio of the gyro, respectively [Ref. 11, pp. 9-11]. Manufacturer's specifications in Appendix B for both RT-01 and RT-09 sensors list ω_n as 25 Hz minimum and ζ as 0.7 typical. Assuming a zero error ($D(s)=0$), the LaPlace transform of the output voltage for each degree-of-freedom should be:

$$V(s) = \left(\frac{625}{s^2 + 875s + 625} \right) \cdot \omega_i(s) \quad (2)$$

b. Vertical Gyroscope

A vertical gyroscope is referenced to gravity in the downward direction. Therefore, it measures two angles in two degrees-of-freedom from vertical. Slaving to gravity is accomplished through closed-loop feedbacks within the gyro. Level sensors are mounted on gimbals, which are in turn coupled to slow-speed erection motors. The motors maintain the gimbals in a level condition in both degrees-of-freedom. In a

conventional aircraft application, each gimbal angle then would give an attitude angle, either pitch or roll, relative to local vertical [Ref. 11, pp. 11-12]. Since the Archytas axes were aligned with ‘x’ in the up or vertical direction, rather than the typical aircraft convention of ‘x’ in a forward direction, its vertical gyro measured pitch and yaw angles.

3. Forebody Interconnections

In order to bring each SAS sensor output to the standard voltage range of 0-5V, which was required by the A/D board, their outputs were conditioned by the A1 SIGNAL CONDITIONING BOARD and the anti-aliasing FILTER BOARD. The plug pin-outs for connections within the forebody to and from the A1 SIGNAL CONDITIONING BOARD and the FILTER BOARD are shown in Appendix B. Other plugs used in the forebody are described in Section E of this chapter, and listed in Table 5.

B. CHASSIS

AROD’s main chassis became the central fuselage chassis for Archytas. Equipment attached to the chassis and used for this phase of the project are detailed in following sections. In essence, from an electronics perspective, the chassis served only to provide attachment points for signal and electrical distribution buses. The only active component attached to the chassis was the diode rectifier board which translated alternator-produced AC power into necessary DC power for electronics. The Archytas UAV used no AC power directly.

1. Diode Rectifier Board

Electrical power used by Archytas is supplied by either of two sources. The primary source of power when the vehicle's engine is running is an engine-driven alternator, to be described in a later section. Alternatively, an external power connection to a 28V DC power supply is made through the umbilical cord.

The alternator provided 20-50V AC three-phase power, whose voltage varies proportionally with the engine's RPM. In order to allow either source of power to be supplied to the vehicle, a diode rectifier board was employed. The board is labeled "TSB5" on "SHEET 2 OF 2" of the AROD schematic in Appendix C. When external power was supplied, the diode circuit passed the DC power directly through, but the power supply was effectively isolated from return surge voltages by the diodes. With the engine running, the alternator's three-phase AC output is converted to 20-50V DC by the diode rectifier board. A 1000 μ f, 100V electrolytic power capacitor was used to smooth voltage ripples in the DC output.

The diode rectifier board is also equipped with a circuit which had been used by AROD as a path for charging the standby battery. This feature was not used in the Archytas configuration. A photo of the diode rectifier board is shown in Figure 10. A schematic of the diode rectifier board circuit is shown in Figure 11.

2. Signal Distribution Buses

All signal and electrical connections passing from forebody to rearbody were connected through distribution buses attached to the exterior of the chassis. A photo of

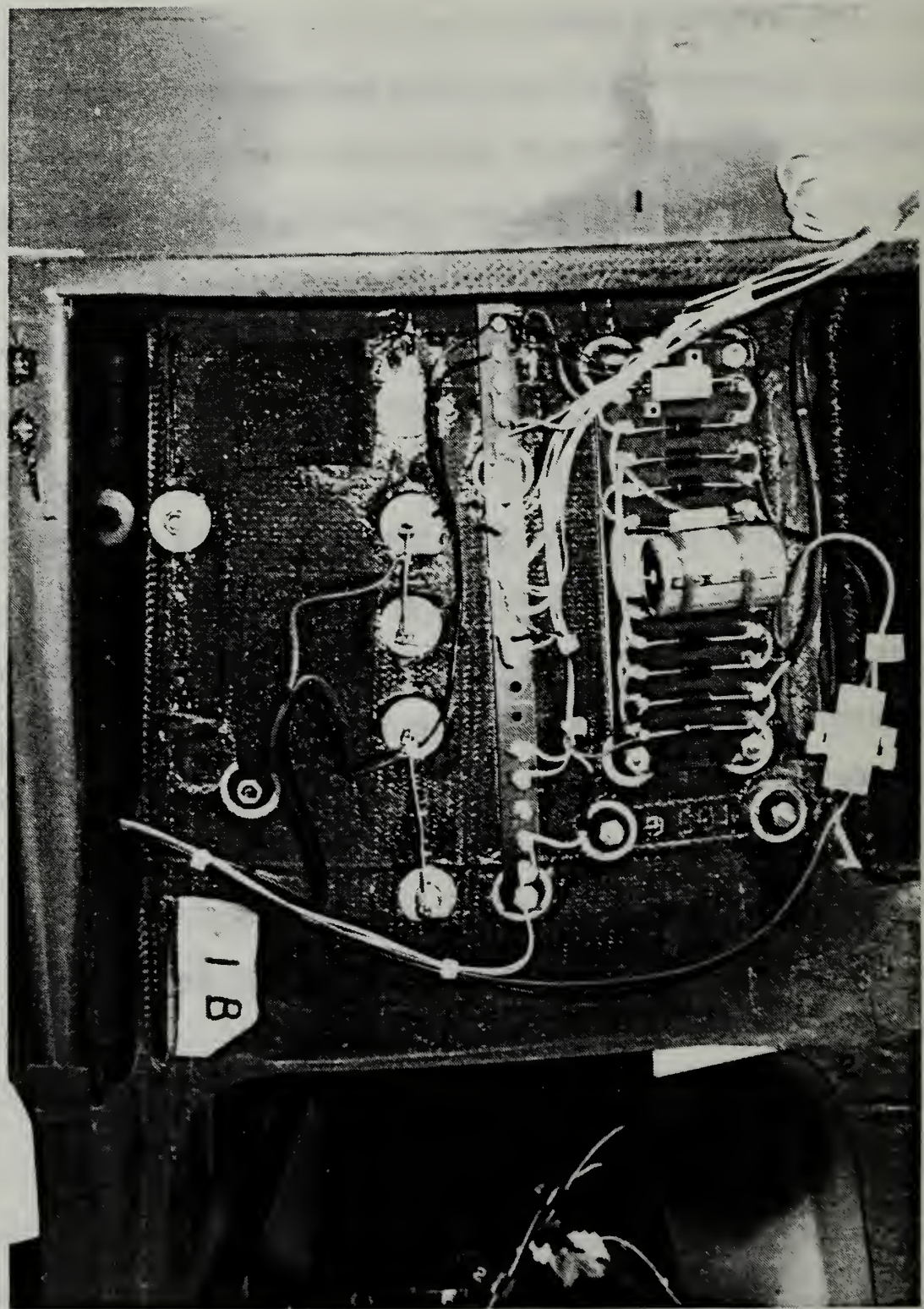


Figure 10 Photo of Chassis-mounted Diode Rectifier Board (TSB5)

Diode Rectifier Board (TSB5)

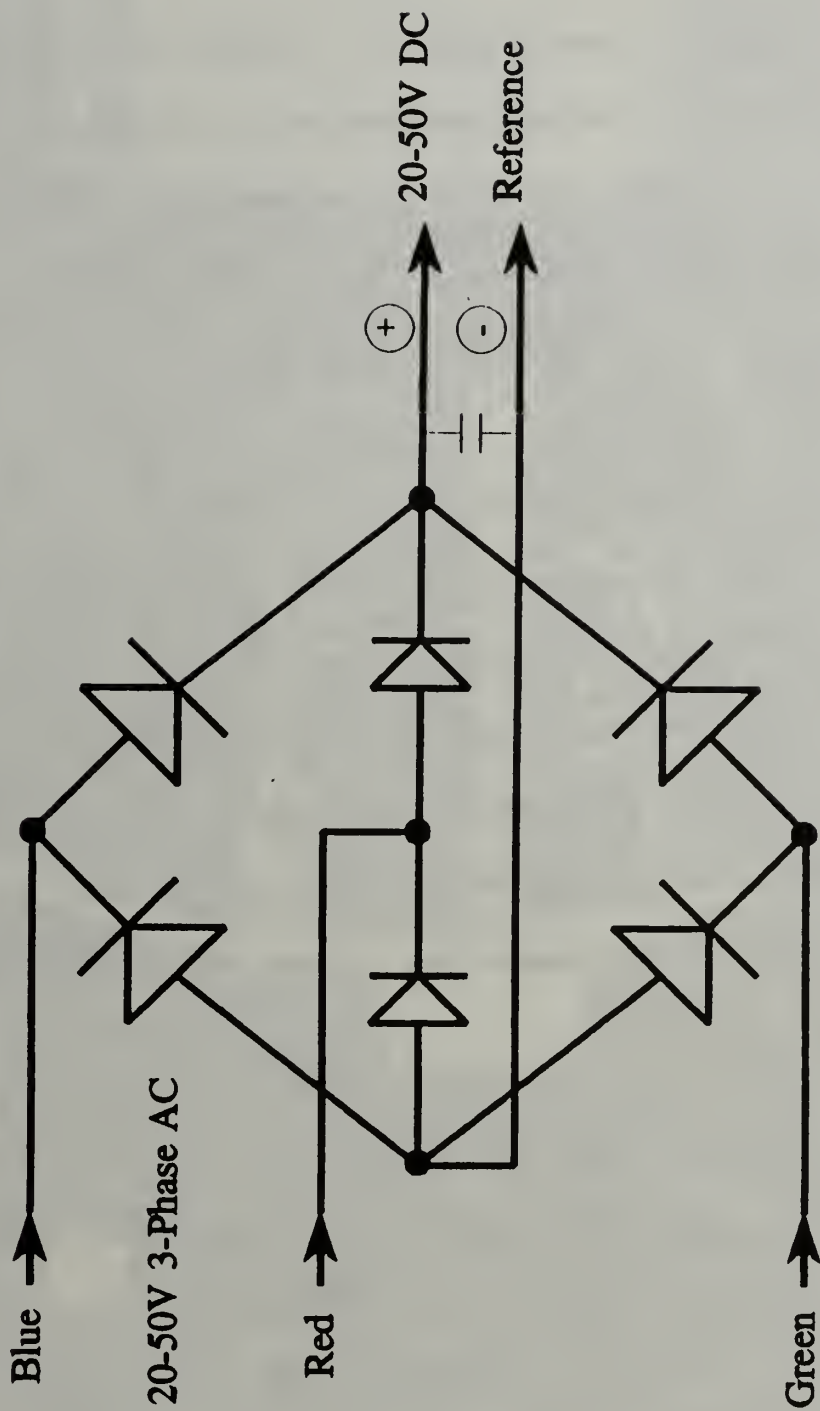


Figure 11 Schematic of Diode Rectifier Board (TSB5) with 3-Phase AC Input

a distribution bus is shown in Figure 12. The buses were labeled TSB# (for terminal strip board), where # indicates the nearest strut, i.e., TSB2 for the bus mounted next to strut two. The buses were useful for troubleshooting, as all important signals and voltages were accessible directly by simply removing the chassis outer shell, without requiring removal of forebody or rearbody hardware.

3. Engine

As previously mentioned, the Archytas UAV used a Herbrandson Dyad 280 2-cycle engine. The engine is supported by struts from the chassis interior to the rearbody, as well as by connecting rods running directly from the chassis interior to the engine. Engine starting was done with a detachable pull cord which wound around a starting pulley connected to the top of the engine drive shaft. A fuel mixture of 50:1 unleaded gasoline to oil was used. A safety checklist, shown in Appendix D, was developed for use during engine runs to ensure that proper safety precautions were followed.

C. REARBODY

The rearbody was supported by four radial support struts which connected to the chassis' interior. The aerodynamic control vanes were attached to the lower portion of the rearbody. The umbilical cord was connected to the endcap at the bottom of the rearbody. The normal endcap designed for use at the end of the rearbody was replaced by a spare forebody topcap to facilitate secure mounting of the umbilical cord. Figure 13

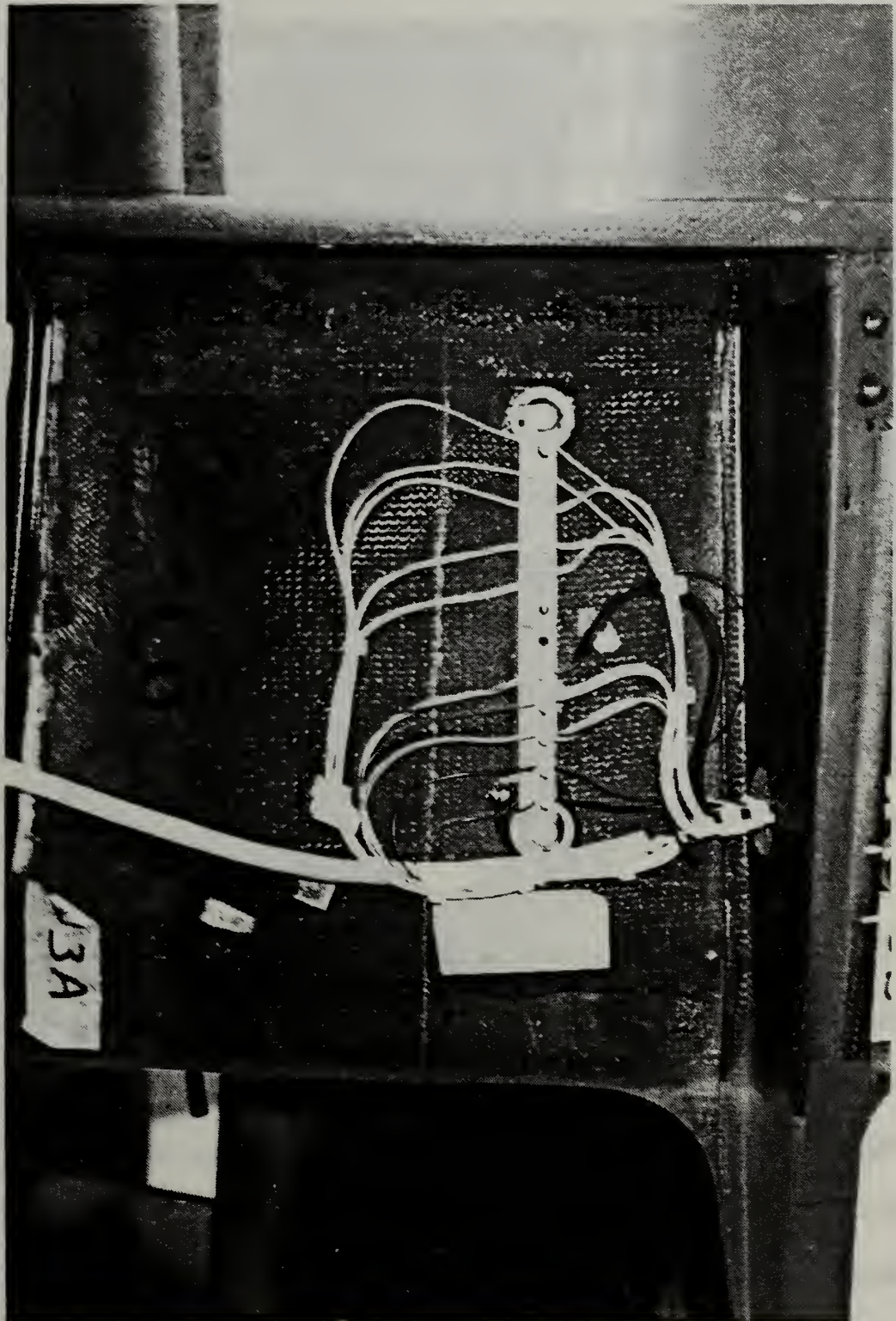


Figure 12 Photograph of Chassis Bus Board

shows the rearbody/chassis assembly, with the control vanes, servos, and umbilical connection visible in the foreground.

1. Control Vane and Throttle Servos

Standard RC modeling servos were used to control aerodynamic vane positions and throttle position. The servos were driven by varying the time width of a 0-5 volt pulse from a minimum of 1.0 ms to a maximum of 2.0 ms, with a nominal midrange of 1.5 ms. PWM servo control is described in *Section d*. They were powered by +5V from a power regulator in the forebody. The term ‘servo’ is short for servomechanism or servomotor, which Webster defines as a relatively small, low-powered device to control a much larger control force [Ref. 13]. In this application, the servos were small electrically-driven motors used to control position of the aircraft’s aerodynamic control vanes, which in turn created much larger aerodynamic forces and moments. Two different types of servos were used.

a. *Futaba Servos*

Sandia engineers used Futaba FP-S34 quarter-scale RC modeling servos for AROD’s control vanes. The FP-S34’s are constructed of mostly plastic parts, including the drive-train gears. The throttle servo used was a Futaba FP-S31S. Sandia engineers chose to obtain servo positions for SAS feedback for AROD by simply tapping into the servos’ internal single-wiper potentiometers [Ref. 8]. It was felt for the Archytas that such a method could cause interference with the internal feedback circuitry of the servo. The Futaba servos’ lack of ruggedness, coupled with their already being

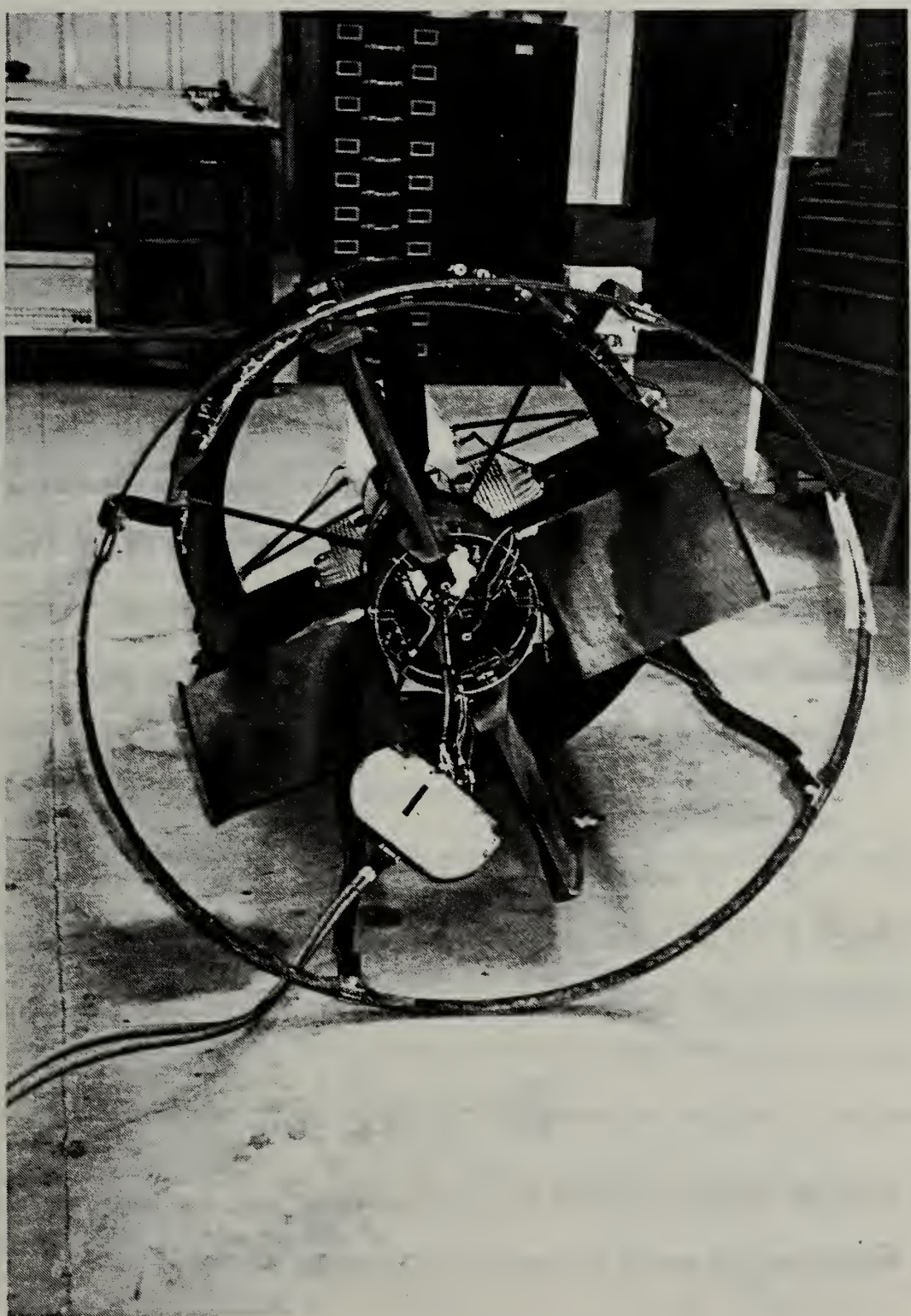


Figure 13 Photograph of Rearbody/Chassis Assembly

modified with position leads, led to a decision to use new servos for the Archytas control vanes.

b. Condor Servos

The servos chosen to replace the AROD's Futaba control vane servos were MS-747WB servos from Condor RC, Inc. The new servos are constructed with metal gears, are generally more durable, and provide 50% more torque (167 oz-in for the Condor MS-747WB versus 112.6 oz-in for the Futaba FP-S34). The MS-747WB servos are modified with dual-wiper potentiometers to allow for non-interfering electrical connections for incoming signals and feedback vane position signals. The original AROD Futaba FP-S31S throttle servo was retained for the Archytas. Throttle position is deemed not necessary for control feedback at this phase of the project, so no signal is taken from the servo's potentiometer.

c. Servo Modeling

A second-order Futaba FP-S34 servo model was developed by Merz [Ref. 2, p. 57] and Davis [Ref. 3, p. 116] by simulating a step input and observing the servo's response. Their model can be expressed as a second-order transfer function:

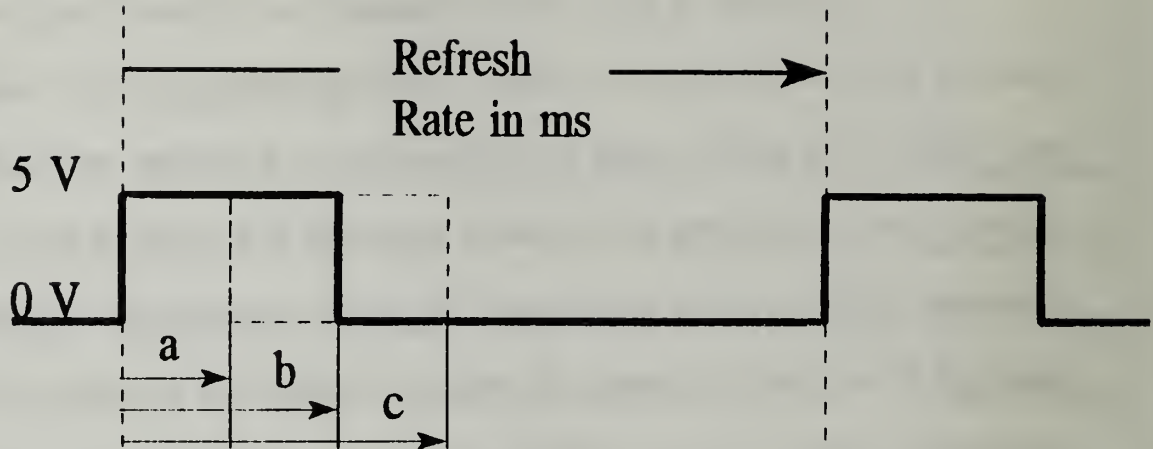
$$\frac{C(s)}{R(s)} = \frac{2745.8}{s^2 + 74.1s + 2745.8} \quad (3)$$

where the values of $\zeta=0.707$ and $\omega_n=52.4$ rad/sec were determined experimentally. Similar tests will need to be done for the Condor MS-747WB servos.

d. PWM Servo Control

Command of UAV servos is frequently accomplished through a system known as pulse-width modulation (PWM). PWM signals are comprised of rectangular pulse trains. The width of each pulse corresponds to a position command for its respective servo. The signal can be sent to the aircraft in a variety of ways, such as through an umbilical cord, as in this phase of the project. In the umbilical method, each signal has its own dedicated wire. This method of transmission is called parallel data transmission. Alternatively, the PWM signal may be sent serially by an RF transmitter, using a method known as time-division multiplexing. The signal may also be generated aboard the vehicle, as will be required for autonomous flight. Each servo has a circuit which compares its incoming PWM signal to a reference signal corresponding to its current position. If there is a difference between the two, the servo's internal motor is turned to try to drive the difference, or error, to zero.

The nominal, or midrange, pulse width for general purpose RC servos is 1.5 milliseconds. Full servo movement in one direction is commanded by a pulse width maximum of 2.0 ms, while full movement in the opposite direction corresponds to a pulse width minimum of 1.0 ms. Figure 14 shows a typical PWM signal waveform with all parameters labeled. The "refresh rate" determines how frequently a new pulse is sent and/or received. Standard RC servos operate at a refresh rate of about 20 ms (a frequency of 50 Hz). [Ref. 16]



- a: minimum pulse width - 1.0 ms
- b: nominal, centered pulse width - 1.5 ms
- c: maximum pulse width - 2.0 ms

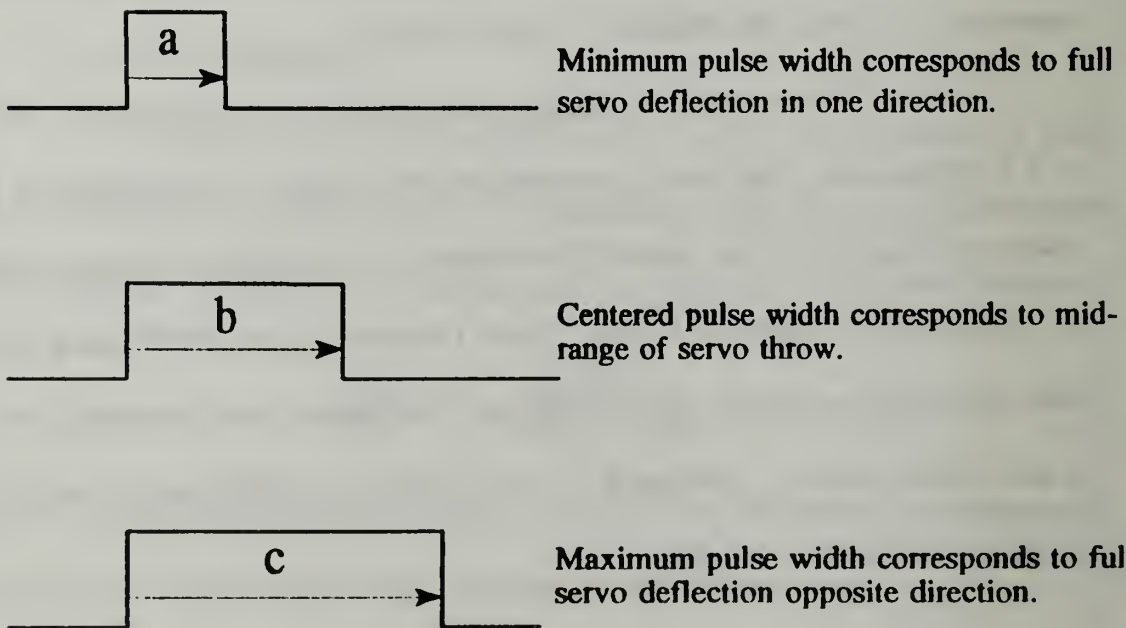


Figure 14 Typical PWM Waveform

2. Ignition and Tachometer

Engine ignition spark is provided to each cylinder's spark plug by the solid-state capacitor discharge ignition (CDI) system, which is housed in the rearbody below the alternator. A 28V DC-DC converter located in the forebody provided power to the CDI system. Also, a kill switch mounted on the control junction board is connected via the umbilical cord directly to the ignition leads. The connection is made on chassis bus board TSB2N.

A tachometer signal is provided within the CDI circuitry which could be monitored during engine operation and displayed on an oscilloscope. The tachometer signal is generated by a magnetic pickup mounted adjacent to the engine drive shaft which is exposed to plate spinning with the shaft. The plate has notches in its perimeter which caused a spike in the pickup's magnetic field as the plate spun past the pickup, which in turn produces observable pulses on the oscilloscope. The gap from pulse to pulse represented ms per revolution, so the conversion from ms/rev to RPM is:

$$\text{RPM} = \left(\frac{\text{ms}}{\text{rev}} \times \frac{\text{sec}}{1000\text{ms}} \times \frac{\text{min}}{60\text{sec}} \right)^{-1} \quad (4)$$

3. Alternator

The engine-driven 20-50V three-phase AC alternator is also mounted with the rearbody. It connected to the engine drive shaft through a bulkhead separating the rearbody from the chassis. The alternator's three-phase output harness is fed through the bulkhead and out through a support strut to the outer chassis. There it connected directly

to the diode rectifier board (TSB5) and was rectified to DC for distribution to the rest of the vehicle.

D. VEHICLE INTERCONNECTIONS

Wiring harnesses connected the forebody to the chassis and the chassis to the rearbody. Surplus AROD harnesses were used wherever possible, as many of the connections required are the same as had been implemented on the AROD system. The only new connections not remaining from AROD were those involving the umbilical cord. The two AROD schematics, which can be found in Appendix C, detail many more connections than were used on Archytas at this phase of the project. Also included in Appendix C are schematics showing only those connections which were used in the Archytas application for this phase of the project. Table 5 defines the connections used for this thesis referenced to the AROD and Archytas schematics. Plug numbering was the same as for the AROD system in most cases, as all cables, plugs and sockets on surplus AROD equipment are well marked and labeled. Differences from the AROD system are noted in Table 5 as "new", or existing labels have an "N" suffix added to them. For instance, the new plug for strut three is labeled "P103N".

In summary, the three sections of the Archytas vehicle each contained hardware utilized in this thesis. The forebody contains the three sensors, two rate sensors and a vertical gyro, plus their associated signal conditioning circuits. The chassis is the mounting location for bus boards which connect signals and voltage supplies from

forebody to rearbody. The rearbody houses the alternator, CDI, and servos, and is the mounting location for the umbilical cord.

Most connecting wiring harnesses were derived from existing surplus AROD harnesses. New harnesses and bus boards, labeled with an "N", were built to connect the necessary signals and voltages to the umbilical cord. New plugs and bus boards which were developed for this work, P21N, P103N, TSB3N, and TSB2N, have pin diagrams enclosed in Appendix B. Their physical locations are described in Table 5.

TABLE 5: FOREBODY/CHASSIS/REARBODY CONNECTIONS

Reference: AROD-3 SCHEMATIC, PAGES 1 & 2, Appendix B

Forebody:

Intraconnections:

Plug P1- VERTICAL GYRO to A1 CHANNEL CONDITIONING BOARD

Plug P2- RATE SENSORS to A1 CHANNEL CONDITIONING BOARD

Plug P5- Sensor Outputs and Servo Position Feedbacks (via P102) to
A1 CHANNEL CONDITIONING BOARD

Plug P6- A1 CHANNEL CONDITIONING BOARD to Filter Board and
Power Supplies

Plug P13- Fan to 28V DC-DC CONVERTER PS7

Plug P17- FILTER BOARD to Exterior Plug P103N (N=new)

8 Sensor Outputs plus Common

Exterior Connections:

Plug P101- Strut 1 Harness to Chassis Bus Board TSB1

Plug P102- Strut 2 Harness to Chassis Bus Board TSB2

Plug P103N- Strut 3 Harness to New Chassis Bus Board TSB3N (N=new)

Chassis:

All Chassis Connections were to/from Forebody & Rearbody via Bus Boards

TSB1, TSB2, TSB2N, & TSB3N described above and below with the exception of direct connections (no plugs) from Diode Rectifier Board TSB5 to TSB1 (20-50V DC). An additional plug was installed in the harness from the AC alternator output to the diode rectifier board (TSB5) for troubleshooting electrical system problems.

Rearbody:

Intraconnections:

Five Servo Signal/Power and Feedback Plugs

Umbilical Inner Plug (New)

Exterior Connections:

Plug P200/P202- 5V/Common to Servos and 20-50V 3-Phase AC from Alternator directly to Diode Rectifier Board TSB5 (AC) and TSB1 (5V)

Plug P201- Signals to/from Servos and Electrical Power to CDI Ignition from Chassis Bus Boards TSB2 and TSB2N (N=new)

Plug P21N- New 21-pin Connector connect TSB2N and TSB3N to Internal Umbilical 24-pin Cannon Plug Connector (N=new)

Umbilical Cord Exterior 24-pin Cannon Connector (New)

V. CONTROL VANE GUIDANCE ‘C’ ROUTINES

Implementation of control laws to guide the Archytas UAV’s control vanes was accomplished through ‘C’ routines which controlled the counter/timer and A/D boards. The evolutionary process which lead up to a routine for hovering flight began with several simpler intermediate steps. Each new generation of ‘C’ routine advanced the system to meet the next requirement. Initially, a system to generate a servo control signal using PWM was implemented. Then, a method of quickly and reliably commanding inputs was needed and a joystick was added. Next, a way of providing a simple feedback using a sensor aboard the vehicle in order to control the vehicle in one degree-of-freedom was needed, and a roll rate sensor with an uncoupled SISO controller was added. When the simple SISO feedback system was successfully implemented the system was advanced to three-axis control. Command inputs for three axes from dual joysticks were added. To accomplish hovering flight control, more sensory data was needed, so three-axis rate sensors and a vertical gyro were added to provide data for a MIMO controller. This introduction describes the current state of the Archytas control system.

As an introduction, the two routines written by Merz [Ref. 2, Appendices A and B] to generate PWM signals and control them through an A/D process are summarized in Section A. Then, Davis’ reduced-order SISO controller for roll [Ref. 2, pp. 62-3] was incorporated via discretized equations. This was done in a routine called *roll.c*, which

is described in Section B. The routine is listed in Appendix A. The final routine, *ai_el_ru.c*, took input from two joysticks, mixed the commands, then sent separate, independent signals to each vane. This improvement allowed command of three aerodynamic surfaces, aileron, elevator, and rudder, through a varying combination of four control vanes. Section C of this chapter describes how *ai_el_ru.c* differs from previous routines, while the routine listing can be found in Appendix A.

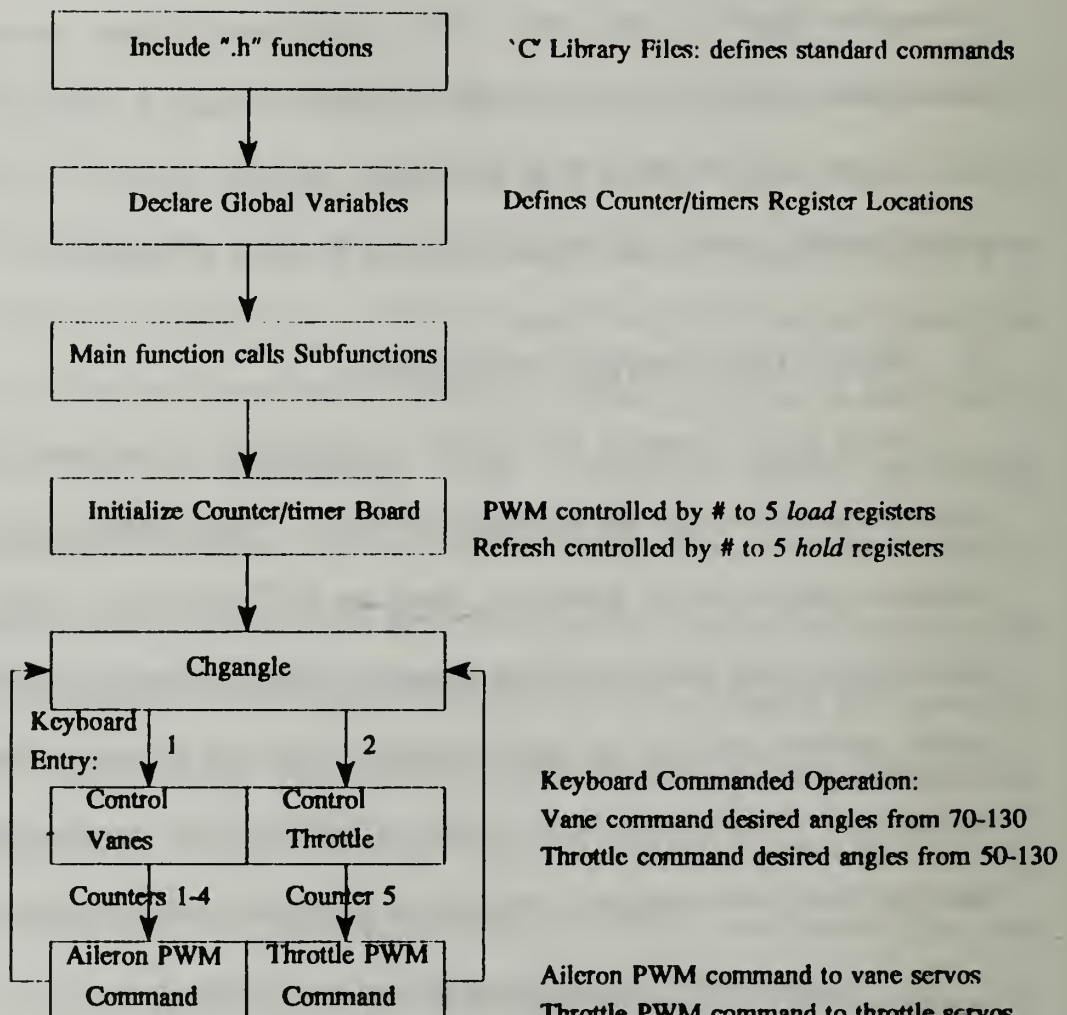
A. PWM VANE CONTROL ROUTINES

PWM signal generation was initially accomplished by Merz with a routine called *pwm.c*, which used only the counter/timer board. Vane positions were selected by numeric inputs on the PC keyboard. Next, the A/D process was added in a routine called *atod.c*, which took inputs from a single joystick to control the vanes collectively, so that all four moved in the same direction. This was effectively commanding an aileron input.- Two routines, both written by Merz [Ref. 2], are summarized. Flow charts for both *pwm.c* and *atod.c* routines are shown in Figures 15 and 16.

1. Basic PWM Control Using Counter/timer Board

The first Merz routine, *pwm.c*, uses a counter/timer to generate the pulses of the PWM signal, controlling both the pulse width and refresh rate. This was done by loading numbers into the counter/timer's five counters' *load* and *hold* registers, respectively. The registers are storage locations within the counter/timer's circuitry which are the heart of the device's operation. The value entered into each counter's *load* register controls the pulse width, while the value entered into the *hold* register controls

pwm.c Flowchart

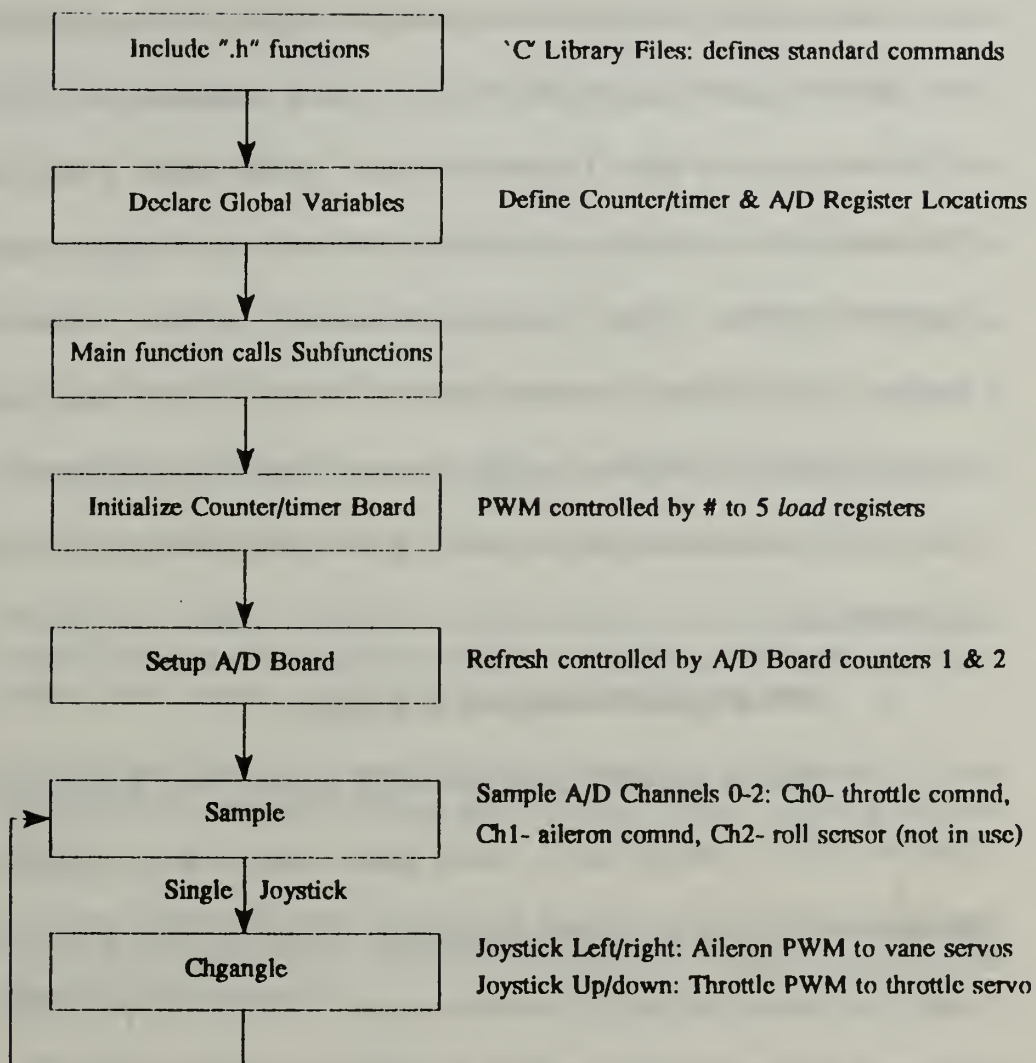


Reference: Quartz and CIO-CTR Counter/timer Manuals

(Written by Paul Merz, Ref. 2, Appendix A)

Figure 15 Flow Chart for *pwm.c* Routine

atod.c Flowchart



Reference: CIO-AD16jr and DAS-16 A/D Board Manuals

Reference: CIO-CTR and Quartz Board Manuals

(Written by Paul Merz, Ref. 2, Appendix B)

Figure 16 Flow Chart for *atod.c* Routine

the interval between pulses. Counters one through four control pulses sent to the four respective vanes, while counter five controls throttle pulses. Desired commands to the servos are entered by numerical input from a PC keyboard. Vane commands range from an "effective joystick angle" of 70 to 130, which represented a -30° to $+30^\circ$ vane deflection, a span of 60° . The term "effective joystick angle" is used since these vane command values represent actual angles of the stick with respect to horizontal in each degree-of-freedom. When the vanes are properly adjusted in the servo mounting brackets, a 100 keyboard command achieves a centered or 0° vane position. Throttle commands from the keyboard ranged from an effective joystick throttle angle of 50 at idle to 130 at maximum power, a total span of 80° on the actual joystick. [Ref. 2, Appendix A]

2. PWM Signal Control Via A/D Board

The use of effective joystick angles in *pwm.c* was in anticipation of the next generation Merz routine, *atod.c*, which added sampled actual joystick analog inputs through the A/D board. Besides the addition of joystick input, a basic difference from *pwm.c* was the use of the A/D board's counters to control the PWM refresh rate. The necessary refresh rate was calculated by Davis to be 10 ms [Ref. 3, p. 55]. This was implemented through trial and error input of values to the A/D counters until the proper refresh rate was achieved as observed on an oscilloscope display. The 12-bit A/D board measured analog inputs from 0 to 5 volts and translated them to a digital value between 0 and 4096 [Ref. 2, Appendix B]. The two degrees-of-freedom available from the joystick represented throttle inputs (up/down) and aileron commands (left/right).

B. SISO ROLL CONTROLLER ROUTINE

Implementation of the reduced-order SISO roll controller model developed by Davis [Ref. 3, pp. 62-3] consisted of adding the discretized control equations to *atod.c*. Also, the necessary adjustments were made to sample another A/D channel for the roll rate sensor in addition to the two already being sampled for throttle and roll command. The sampled data were then scaled to a true scale by subtracting the digital value of the sensor's initial bias voltage. The resulting routine, *roll.c*, includes the equations developed by Davis [Ref. 3, pp. 62-3]. A flow chart of the routine is shown in Figure 17. Appendix A contains the routine listing for *roll.c*, including explanatory comments. Modifications to Merz' *atod.c* routine which are included in *roll.c* are:

- Within the "sample" function, control of the A/D conversion process is passed from external-triggering to software-triggering during the continuous loop to allow for the sequential sampling of multiple channels;
- The "sample" function includes discretized equations for the reduced-order control model, utilizing a lookup table to assign proper values to the vane servos;
- Software limiting is used in the "sample" function to prevent vane angles past 30°, which would result in vane stall, by assigning a constant vane command when the vanes reach 30°;
- A "senbias" function samples the roll rate sensor input 10 times, then averages, before initiation of routine loop; calculated average bias is then subtracted from every roll rate sample.

C. MIXED CONTROL SURFACE GUIDANCE ROUTINE

The use of two joysticks is required for control of all three aerodynamic control surfaces and throttle. Commands to the four vanes needed to be mixed so that the three control functions could be achieved using the same four vanes. As previously mentioned

roll.c Flowchart

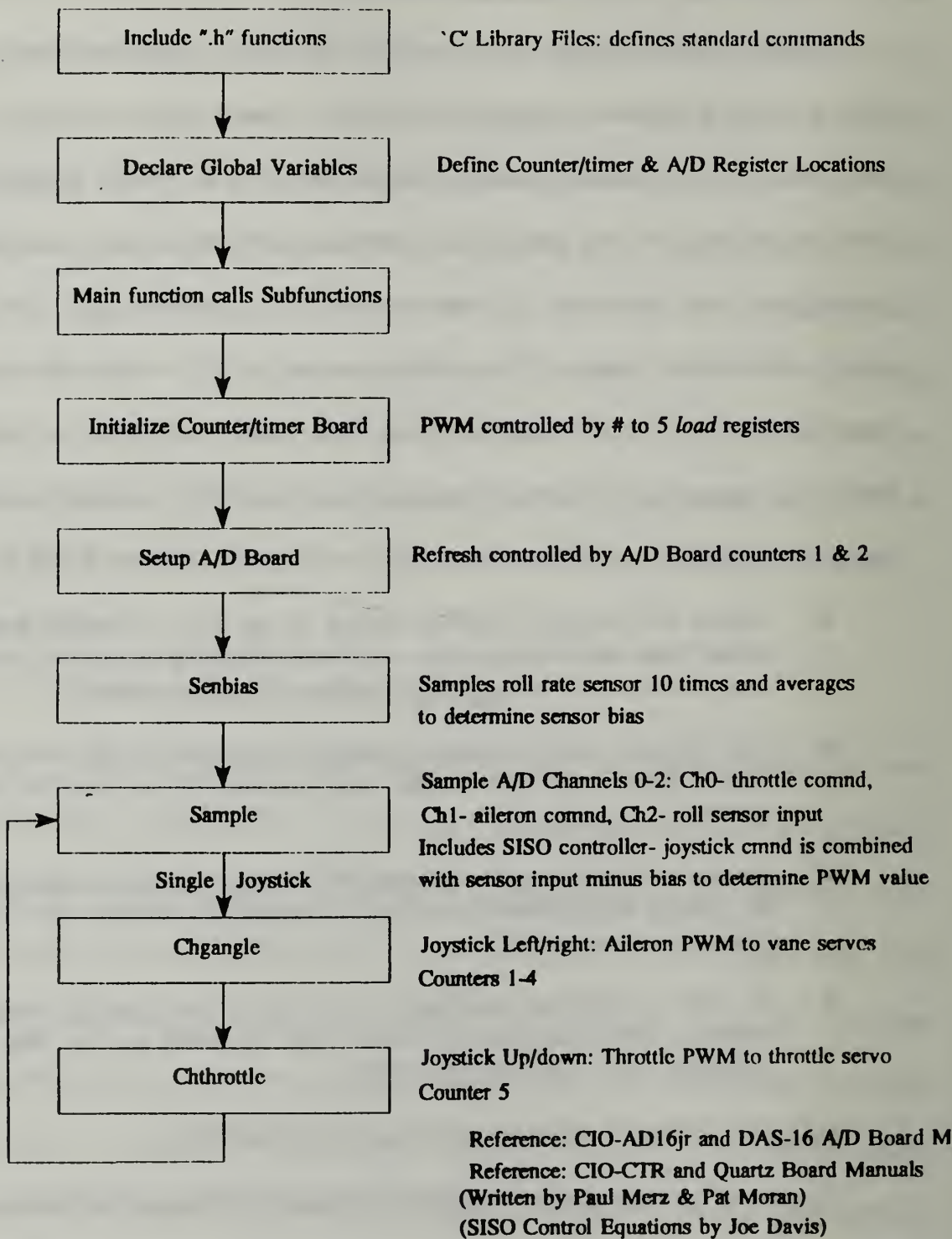


Figure 17 Flow Chart for *roll.c* Routine

in Chapter III, vanes one and three represent the upper and lower rudder, vanes two and four the left and right elevator, and a combination of all four vanes represent the aileron.

The equations to translate three joystick degrees-of-freedom into four vane commands is:

$$\begin{aligned}
 \text{vane 1} &= \left(\frac{\text{aileron}}{4} + \frac{\text{rudder}}{2} \right) \\
 \text{vane 2} &= \left(\frac{\text{aileron}}{4} + \frac{\text{elevator}}{2} \right) \\
 \text{vane 3} &= \left(\frac{\text{aileron}}{4} - \frac{\text{rudder}}{2} \right) \\
 \text{vane 4} &= \left(\frac{\text{aileron}}{4} - \frac{\text{elevator}}{2} \right)
 \end{aligned} \tag{5}$$

where *vanes 1-4* represent the values sent to the counter/timer to determine each vane servo's pulse width, and *aileron*, *rudder*, and *elevator* represent the commands input through each of the three respective joystick degrees-of-freedom. The factors of $\frac{1}{2}$ and $\frac{1}{4}$ arise from the fact that elevator and rudder commands are split between two vanes each, while aileron commands must be split among all four vanes. This algorithm, developed by Kaltenberger [Ref. 14], accomplished the necessary mixing of aileron, elevator, and rudder inputs to allow four independent vane positions to be commanded. Several trial and error loops were required to determine proper multiplicative and additive factors to apply to the A/D digitized values to achieve the proper vane deflection angles for a given joystick input while keeping the vane servos properly aligned. The factors applied to each channel, from the *sample* function in *ai_el_ru.c*, are:

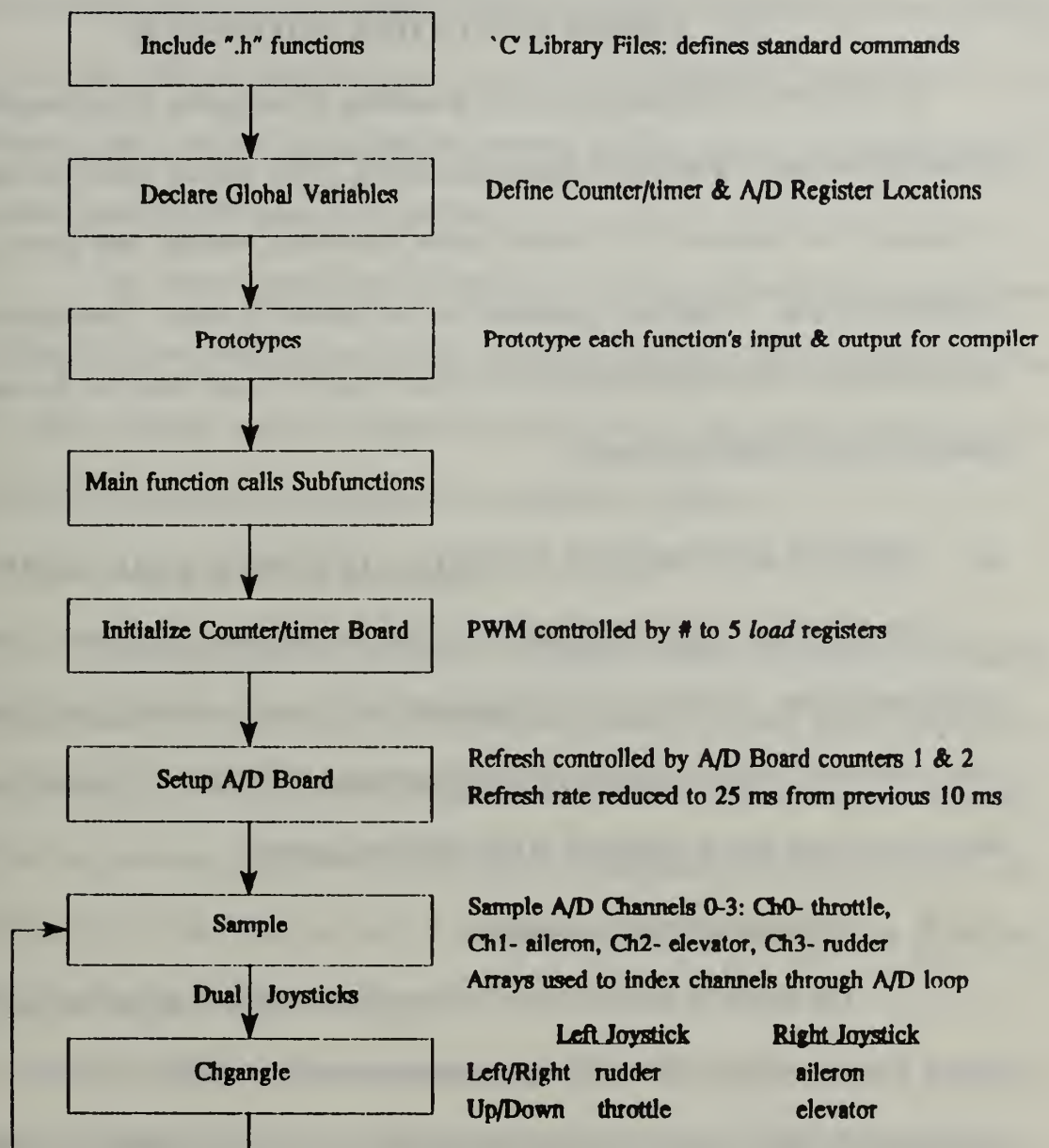
$$\begin{aligned}
 \text{throttle} &= (\text{channel0} - 2714) \cdot 0.12 + 80 \\
 \text{aileron} &= (\text{channel1} - 1600) \cdot 0.4 + 200 \\
 \text{elevator} &= (\text{channel2} - 1850) \cdot 0.2 - 80 \\
 \text{rudder} &= (\text{channel3} - 720) \cdot 0.2 - 80
 \end{aligned} \tag{6}$$

This system was implemented in *ai_el_ru.c* which is listed in Appendix A. A flow chart of *ai_el_ru.c* is shown in Figure 18. Improvements written into *ai_el_ru.c* over previous generation routines include:

- The use of ‘C’ language “prototypes” to pass variables from function to function, and to specify to the compiler what each function expects as inputs and outputs. [Ref. 18]
- Use of arrays to minimize repetition of similar sequences and improve speed. Arrays in ‘C’ are indexed starting at ‘0’, which agreed with the A/D board’s convention of numbering channels starting with Channel 0. [Ref. 18]
- Reduced sampling period from the 10 ms rate used in previous routines to 25 ms, in anticipation of additional computing time necessary for the more calculation-intensive MIMO control law implementation. This was done by increasing the numbers assigned to the A/D board’s counters in the “setup” function, as commented in the routine listing in Appendix A.

In summary, two routines have been written to accomplish specific tasks which built upon each other. These routines were based upon PWM and A/D routines written by Merz [Ref. 2]. The first routine (*roll.c*) used PWM signals commanded from a single joystick and a SISO controller to control single-axis roll. The second is a routine (*ai_el_ru.c*) to command the PWM signal using dual joysticks to blend three joystick inputs into four independent vane commands.

ai_el_ru.c Flowchart



Reference: CIO-AD16jr and DAS-16 A/D Board Manuals

Reference: CIO-CTR and Quartz Board Manuals

(Written by Pat Moran, Basic PWM & A/D Sampling by Paul Metz)

Figure 18 Flow Chart for `ai_el_ru.c` Routine

VI. SYSTEM EVALUATION AND RESULTS

As with any developmental system, evaluation of the system is not complete until the design has been validated by appropriate testing. This chapter details the tests done to evaluate the Archytas UAV control system algorithms, vehicle, and ground control hardware designs. Results are presented for each phase of work. Conclusions drawn from the results and recommendations for improving the system based on the results are presented in the following chapter.

A. VEHICLE AND GROUND CONTROL EQUIPMENT EVALUATION

The hardware results of this thesis fall into the categories of ground control and vehicle equipment. Ground Control Equipment development is described in Chapter III, while On-board Vehicle Equipment design is discussed in Chapter IV. Evaluation of the hardware in each area is described in the following sections.

1. Ground Control Equipment

The design of ground control equipment consisted of expanding the existing system to accommodate the additional requirements of the MIMO controller, which required more signal capacity through the umbilical cord for the additional sensors. A new umbilical cord was required and was added to the control junction board with an additional connection bus. The control junction board was modified to provide for dual joystick pilot command, and to allow for remote connection of the external DC power supply. The A/D board connections were expanded to allow for the sampling of the 12

channels necessary for MIMO control. When all wiring connections were accomplished, each signal line was checked to ensure electrical continuity. The joysticks were verified to work over their full range, as given in Table 3 in Chapter III. A new 486 PC was configured and used for generation of routines and lab testing of control systems, providing dual-site PC operating capability.

The counter/timer and A/D boards were tested using software provided from their manufacturers which exercised their circuitry to determine proper installation in the PC. Their operation was also validated by observation of the expected PWM outputs from PWM routines when displayed on an oscilloscope display.

2. On-board Vehicle Equipment

Accomplishments in the area of On-board Vehicle Equipment consisted of reconfiguration of the sensor pod from its previous rearbody location to the AROD-style forebody location. Surplus AROD harnesses were installed for the dual-axis rate sensor, the vertical gyroscope, and three-axis accelerometers (although not yet used in this phase of the project). The wiring of new A1 Channel Conditioning Board, Filter Board and signal output plugs was also completed.

The chassis was reconfigured using AROD bus boards and new umbilical chassis bus boards. The AC power supply diode rectifier board was relocated from the sensor pod to the chassis exterior. New wiring harnesses to and from the umbilical were constructed. The rearbody AROD servo wiring harness was used in its entirety. Additional rearbody umbilical-related harnesses and plugs were constructed.

Again, when all vehicle wiring connections had been accomplished, all signal wires were checked for proper electrical continuity from the vehicle to the control junction board through the umbilical cord. The use of chassis bus boards, which were accessible easily on the exterior of the chassis, greatly improved the ease with which signal flow could be traced.

While conducting engine runs to determine vehicle characteristics, the +5V voltage regulators mounted in the forebody which supply 5V servo power were tested. On two occasions, the 5V regulators burned out. It is believed that high engine RPM during testing drove a higher than expected voltage output from the alternator, which in turn supplied too high a voltage to the regulator. Since excess voltage to the regulator is dissipated through heat discharge, if more voltage is supplied than can be dissipated, the regulator fails. A temporary fix was installed, which consisted of adding resistors in series with the input to the +5V regulator to reduce the voltage potential being supplied to the regulator. The resistors also failed later during engine runs. Subsequent testing was done only on external power. Recommendations in Chapter IV include resolving this problem.

The alternator and ignition systems were tested during engine runs. The vehicle operated normally when the external DC power supply was removed, indicating proper operation of the alternator. No specific observations were made of the three-phase output from the AC alternator, such as voltage for a given engine RPM. The ignition system operated adequately for engine operation, but was also not specifically observed. The CDI tachometer output was used to determine engine RPM, as given by

Equation 4 in Chapter IV. Tachometer speeds were verified using a Futaba transmitter's RPM meter, which measured engine RPM through a photo-optic sensor which sensed propeller speed.

Severe vehicle vibration was apparent during all engine operations with the sensor pod mounted in the rearbody position, causing numerous component failures. The engine was not run after the sensor pod was relocated to the forebody position. To prevent future vibration-related problems, rubber grommets were used in hardware connections whenever possible to dampen vibrations. All electrical connections were converted to sturdy plugs held together by nuts and bolts to prevent vibration-induced disconnections.

The sensor outputs from the vertical gyroscope and two rate sensors were tested in the lab using Personal VISSIM, Version 2, a software program capable of displaying analog signals in real time through another A/D board mounted in the 486 computer. Digitized graphs of the analog sensor outputs, resembling oscilloscope displays, were used to simultaneously observe all five sensor outputs at once. Simulated vehicle movements were achieved by holding the forebody sensor pod independent of the vehicle and moving it in the desired direction. Both vertical angle signals varied linearly with the angle of inclination of the sensor pod as it was inclined in each axis. Roll, pitch, and yaw rate signals varied in magnitude with the rate at which the pod was rotated in each respective axis. Sensor outputs through the forebody A1 Channel Conditioning and Filter Boards were verified by observing the proper 0-5V ranges from each sensor output with a voltmeter.

The servos which guide the control vanes and throttle were observed to exhibit noticeable chatter when operated at the 10 ms refresh rate used by Merz and Davis. Reducing the refresh rate to 25 ms reduced the chatter significantly. The use of commercially available noise suppressors also helped minimize chatter. The noise suppressors operate through an 74LS04N hex inverter microchip, which inverts each PWM signal, then reinverts the signal. The original PWM signal is retained, but noise is suppressed by the double inversion process.

B. CONTROL ROUTINE EVALUATION

Evaluation of the PWM and A/D vane control system consisted of commanding inputs to the control vanes via joysticks and observing the deflection responses of the vanes and throttle to ensure that they remained within the vane stall limits of 30° for the vanes and within the engine throttle linkage limit for the throttle. This was done first with a single joystick, commanding throttle and ailerons, then with dual joysticks commanding throttle, ailerons, elevator, and rudder. SISO control law implementations were tested by simulating vehicle motions, thereby upsetting the installed sensors, and observing the vane counteraction responses. MIMO control laws were written into a routine, with testing accomplished and documented by Kaltenberger [Ref. 14].

Merz' basic PWM and A/D conversion programs [Ref. 2] were tested in the lab on a stationary vehicle. The next step in complexity, implemented in *roll.c*, involved addition of the SISO roll control. This led to testing with the engine running. A roll disturbance was simulated by upsetting the vehicle with a rolling force. The vane

deflection response observations were purely qualitative in that the vanes responded in the proper direction to counter the disturbance. However, no analysis was conducted to determine if the amount of vane deflection was appropriate for the given disturbance.

Implementation of the dual joystick vane control program, *ai_el_ru.c*, was again tested primarily in the lab. Evaluation involved observation of vane deflection responses from commanded inputs from both joysticks. Again, the vane deflections and the throttle linkage remained within linear limits.

1. Implementation of SISO Controller

The simplified roll rate controller developed by Davis [Ref. 3] was tested with the vehicle engine running while mounted in a rigid test stand. The system satisfactorily commanded the proper direction aileron vane deflections to counteract simulated roll disturbances, although the tests were only qualitative and not fully conclusive since no analytical data on the degree of deflection for a given disturbance could be obtained due to the limits of the test stand. Joystick roll command was operable allowing input of a slow operator-commanded rolling motions within the limits of the test stand (about one full turn of the vehicle).

A problem which arose during testing of the roll controller implementation was the inability of the controller to recognize when the vanes had reached their aerodynamic effective limit of 30° deflection. A simple solution was added which stopped the aileron vane deflection when it reached 30° , which is the limit of deflection where stall is expected to occur, even if the joystick continued to command an increasing roll. This was done by freezing the PWM command to the vanes when the limit was

reached. The controller, however, continued to integrate the difference between the joystick command and the roll rate sensor input, thereby calculating an increasingly greater deflection command. The effect is known as *controller windup*. It can be resolved by adding an *antiwindup* algorithm to the controller to limit the controller from calculating commands larger than the limit of the device it is controlling. [Ref. 19]

2. Dual Joystick Control Vane Guidance

Control of the four vanes using mixed input from dual joysticks was accomplished. Vane deflections were controllable from both joysticks throughout the $\pm 30^\circ$ range of each vane, providing a full range of control for each aerodynamic control surface. The equations used to implement vane mixing and the factors applied to each digitized channel are provided in Equations (5) and (6) in Chapter V. Slowing the refresh rate from 10 ms to 25 ms in *ai_el_ru.c* improved the steadiness of the servo responses. Through discussions with a Futaba representative, it was determined that the faster refresh rate was driving the servos faster than they were designed to react. Futaba FP-S34 servos are designed to operate on a 20 ms refresh rate. [Ref. 15]

C. SUMMARY OF RESULTS

Ground control equipment was expanded from the previous design to allow for the greater signal capacity required by the MIMO controller. The vehicle was redesigned to a forebody-mounted sensor pod, due primarily to excessive vibration observed during engine runs. Center of gravity requirements for forward flight stability also were improved by moving the pod forward. Voltage regulators failed during engine runs,

which resulted in loss of power to the servos. A temporary solution was installed, but it too was ineffective.

Implementation of the SISO controller was accomplished and tested in conjunction with the work of Merz and Davis. The SISO controller reached a limit when the vanes were commanded by joystick to their maximum angle, which resulted in vane position being fixed at that position until the controller was commanded back into its region of authority. This problem may be rectified by adding an *antiwindup* algorithm to the controller, as discussed previously.

Dual joystick-commanded control of three aerodynamic control surfaces through four control vanes was achieved. Array indexing and ‘C’ language prototypes were implemented to improve software efficiency. Servo chatter was reduced by slowing the PWM signal refresh rate from 10 ms to 25 ms.

VII. CONCLUSIONS AND RECOMMENDATIONS

This thesis began under the assumption that the rear-mounted sensor pod design previously implemented by Merz [Ref. 2] would be suitable for the Archytas UAV. However, it became obvious, after several engine runs during testing to acquire aerodynamic data about the vehicle, that the vibration generated by the vehicle's two-stroke engine was more than the rear-mounted sensor pod design could withstand. This, combined with further stability calculations by Stoney [Ref. 9], led to a decision to move the sensor pod to the forebody location. The focus of this thesis became reconfiguration of the ground control equipment including the umbilical cord and associated control junction board, and redesign of the vehicle to a forebody-mounted sensor pod.

Much awareness was gained in the area of real-world electrical system design. The impact of such things as floating grounds, noise interference, and signal crosstalk became apparent when they impacted system design and testing. What at first seemed to be a simple requirement to "move the pod forward", became a much larger requirement to resurrect surplus AROD harnesses and reverse-engineer the AROD system design. A frequent question became "Why did they do that?", which usually lead to more research through old AROD documentation and schematics. Also, unexpected airframe design considerations impacted the design of several electrical components involved with this thesis, such as wiring harness paths which had to be moved to allow for mounting of the wing spars.

An "antiwindup" scheme should be added within the controller equation loop, which would prevent the integral controller from continuing to integrate the errors after the 30° vane software limit has been reached. This would prevent the controller from continuing to calculate corrections after the vanes had reached their aerodynamic stall limits. [Ref. 19]

All equipment should be mounted using vibration damping techniques and fixtures. Before actual flight test of the vehicle, all hardware should be secured using LokTite, or a similar product which will prevent screws and nuts from backing off due to vibration.

The three-phase output of the AC alternator should be measured during engine operation to determine AC voltage ranges and volts/RPM. Investigation should be done toward the replacement of the AC alternator system with DC battery power, which could lead to a reduction in vehicle weight, as suggested by Hoffman [Ref. 17]. A full power budget will be required to determine complete present and future system power requirements.

The forebody +5V DC power regulators which supply servo power should be redesigned so that they will not fail when the engine runs at high speeds. This problem could be rectified by replacement of the engine-driven AC alternator with DC batteries.

The hovering flight MIMO control equations developed by Kaltenberger [Ref. 14] were formatted for computer implementation. The MIMO program design needs to be completed, then tested using a simulated model of the Archytas UAV fed by feedback of model outputs.

APPENDIX A: 'C' PROGRAMS DEVELOPED FOR THE ARCHYTAS UAV

```
*****
/* ROLL.C */
*****
/* Written by Paul Merz & Pat Moran, Oct 92 */  
/* Uses Counter/timer & A/D boards */  
/* Implements Roll rate control using Joe Davis' simplified controller. */  
/* Input comes from joystick or roll sensor to guide 4 vanes together. */  
/* Throttle controlled from joystick. PM 4/27/93 */  
  
#include <dos.h>  
#include <stdio.h>  
#include <time.h>  
  
int datreg = 544; /* Ctr/timer board, base address */  
int conreg = 545; /* Ctr/timer board, base addr +1 */  
int basaddr=768; /* A/D board, base address */  
int basepl1=769; /* A/D board, base addr +1 */  
int mux=770; /* A/D board, base addr +2 */  
int statreg=776; /* A/D board, base addr +8 */  
int intcont=777; /* A/D board, base addr +9 */  
int pclock=778; /* A/D board, base addr +10 */  
int inrange=779; /* A/D board, base addr +11 */  
int cntrl=781; /* A/D board, base addr +13 */  
int cntr2=782; /* A/D board, base addr +14 */  
int cntrcon=783; /* A/D board, base addr +15 */  
float ts = .010;  
float ki = .004376; /* # controls rate of response to stick mvmnt, */  
float k1 = -.2027; /* .004376 gives slow roll, .04 gives quick roll */  
int lookup[70],newangle,throttle,bias; /* Global variables */  
  
main()  
{  
    initialize();  
    setup();  
    throttle = 51;  
    chthrottle();
```

```

senbias();
sample();
}

initialize() /* This function is thoroughly commented
               by Merz [Ref. 2, Appendix A] */
{
    int cmnd,i;
    cmnd=255;           /* reset all board functions      */
    outportb(conreg,cmnd);
    cmnd=23;            /* select master mode register   */
    outportb(conreg,cmnd);
    cmnd=176;           /* low byte enables fout        */
    outportb(datreg,cmnd);
    cmnd=65;
    outportb(datreg,cmnd);
    cmnd=249;
    outportb(conreg,cmnd);
    for (i=1;i<=5;i++)
    {
        cmnd=i;          /* Select group 1-5             */
        outportb(conreg,cmnd);
        cmnd=2;            /* Low byte set ctr 1-5 mode in CMR */
        outportb(datreg,cmnd);
        cmnd=27;           /* High byte: no gating for ctr 1-5 */
        outportb(datreg,cmnd);
    }
    for (i=25;i<=29;i++)
    {
        cmnd=i;          /* Load hold register for refresh rate */
        outportb(conreg,cmnd);
        cmnd=0;
        outportb(datreg,cmnd);
        cmnd=10;
        outportb(datreg,cmnd);
    }
    for (i=9;i<=13;i++)
    {
        cmnd=i;          /* Select load register for pulse width */
        outportb(conreg,cmnd);
        cmnd=110;          /* Load low byte into load register */
        outportb(datreg,cmnd);
        cmnd=5;
    }
}

```

```

    outportb(datreg,cmnd);
}
for (i=233;i<=237;i++)
{
    cmnd=i;
    outportb(conreg,cmnd);
}
cmnd=127;           /* Load and arm ctr 1-5 */ *
outportb(conreg,cmnd);
for (i=1;i<=70;i++) lookup[i]=50+i;
printf("COMPLETED INITIALIZATION OF SERVOS\n");
}

setup()           /* This function is thoroughly commented
                   by Merz [Ref. 2, Appendix A] */
{
    int cmnd;
    cmnd=0;           /* Set the mux to read channels 0-2 */ *
    outportb(mux,cmnd);
    cmnd=2;           /* Set up pacer clock for clock driven-sampling */ /
    outportb(pclock,cmnd);
    cmnd=5;           /* Set up for correct input & type of voltage */ /
    outportb(inrange,cmnd);
    cmnd=118;          /* This selects control reg for mode & ctr 1 */ /
    outportb(cntrcon,cmnd);
    cmnd=100;          /* Load up counter one of pacer clock */ /
    outportb(cntr1,cmnd);
    cmnd=0;
    outportb(cntr1,cmnd);
    cmnd=182;          /* Selects control reg for mode & ctr 2 */ /
    outportb(cntrcon,cmnd);
    cmnd=100;          /* Load ctr 2 of pacer clock */ /
    outportb(cntr2,cmnd);
    cmnd=0;
    outportb(cntr2,cmnd);
    printf("COMPLETED CARD INITIALIZATION\n");
}

```

```

senbias()          /* This function samples the roll rate sensor
                   input 10 times to determine an average sensor
                   bias prior to entering the A/D sampling loop. */

{
    int x,lsb,msb,tsb,sreg;
    x=0; bias=0;           /* Set counter and initial bias to 0 */
    while (x<=10)         /* Count 10 times through bias loop */
    {
        sreg=inportb(statreg); /* Check int bit of status reg for high */
        sreg=sreg & 16;       /* indicating start of new refresh cycle. */
        if (sreg==16)
        {
            lsb=inportb(basaddr); /* Read in lobyte */
            msb=inportb(basepl1); /* Read in hibyte */
            lsb=lsb >> 4;       /* Roll lower 4 bits right */
            msb=msb << 4;       /* Roll upper 4 bits left */
            tsb=msb|lsb;         /* Bitwise 'OR' */
            bias=tsb + bias;     /* Maintain cumulative sum */
            x=x+1;               /* Increment loop counter */
        }
    }
    bias = bias / x;        /* Average bias by # of times thru loop */
    bias = 2048 - bias;     /* 2048 is center of A/D range, so bias */
    printf(" bias = %d \n",bias); /* will be above or below center */
    printf("hit any key to start: "); /* Wait for operator start */
    scanf(" %d",&x);        /* Read in start (any #) */
}

```

```

sample()
{
    int x,cmnd,lsb,lsb1,lsb2,lsb3,sreg;
    float x1k,epink1,epink,epk,u1k,pk;
    x=1; epink = 0;           /* Set loop counter to 0; Set initial values */
    pk=0;                  /* of error increment & roll increment =0 */
    while (x==1)             /* Infinite loop */
    {
        sreg=inportb(statreg); /* Check int bit of status reg for hi, indicating */
        sreg=sreg & 16;       /* pacer clock has triggered new refresh cycle */
        if (sreg==16)          /* When int=hi, enter A/D loop */
        {
            cmnd=32;           /* Set mux to count Ch 0-2 */
            outportb(mux,cmnd);
            cmnd=0;

```

```

outportb(intcont,cmnd);
outportb(basaddr,cmnd);
lsb = inportb(basaddr);
lsb1 = inportb(basepl1);
lsb = lsb >> 4;
lsb1 = lsb1 << 4;
lsb1 = lsb1 | lsb;
outportb(basaddr,cmnd);
lsb = inportb(basaddr);
lsb2 = inportb(basepl1);
lsb = lsb >> 4;
lsb2 = lsb2 << 4;
lsb2 = lsb2 | lsb;
outportb(basaddr,cmnd);
lsb = inportb(basaddr);
lsb3 = inportb(basepl1);
lsb = lsb >> 4;
lsb3 = lsb3 << 4;
lsb3 = lsb3 | lsb;
cmnd=2;
outportb(intcont,cmnd);
cmnd=inportb(statreg);
outportb(statreg,cmnd);
x1k = ((lsb1+bias)-2048) * .048828; /* Convrstion fm dig to rad of 'pcommand'*/
pk = (lsb3-1033) * .0351; /* Read in current value of 'p' or roll rate */
epk = pk - x1k; /* Tracking Error= 'p' - 'pcommand' */
epink1 = epink + epk; /* Sum cumulative errors */
u1k = ((-1 * ki) * epink1) - (k1 * x1k); /* Davis' Eqn. 4.19, Ref. 3, p. 63 */
epink = epink1; /* Increment Error term */
newangle=(int)(u1k + 35); /* Truncate command, add normalizing factor */
if (newangle < 1) newangle = 1; /* Software limit to keep total */
if (newangle > 69) newangle = 69; /* vane deflectn below +/-30 deg */
newangle=lookup[newangle]; /* Keeps vane deflctn in +/-30 range */
chgangle(); /* Call change angle routine */
throttle = (int)((lsb2-2714) * .15 + 65); /* Throttle cmnd normalizing */
chthrottle(); /* Call change throttle routine */
}

}

}

chgangle() /* CHANGES VANES VIA CONTROL EQNS, CALLED FM sample()*/
{
int i,hibyte,lobyte,angle,cmnd;

```

```

angle=((1900/206)*newangle+600); /* Algorithm to convrt fm deg to dig # */
hibyte=(angle/256); /* Hibyte formed, residue remaining for lobyte */
lobyte=(angle-hibyte*256); /* Lobyte fromed from remaining residue */
cmnd=207; /* Disarms ctrs 1-4 for loading */
outportb(conreg,cmnd); /* Sends to control reg */
for (i = 9; i <= 12;i++) /* Selects load reg for pulse width of ctrs 1-4 */
{
    outportb(conreg,i); /* Loads lobyte, then hibyte into each ctr */
    outportb(datreg,lobyte);
    outportb(datreg,hibyte);
}
for (i = 233;i <= 236;i++) outportb(conreg,i); /* Sets toggle high for ctr 1-4 */
cmnd=111; /* Load and arm ctrs 1-4 */
outportb(conreg,cmnd);
}

chthrottle() /* CHANGES THROTTLE, CALLED FROM sample() */
{
int i, hibyte, lobyte, angle, cmnd; /* This routine is same as CHGANGLE */
cmnd=208; /* except it changes only ctr 5 */
outportb(conreg,cmnd); /* for throttle */
angle=((1900/206)*throttle+600);
hibyte=(angle/256);
lobyte=(angle-hibyte*256);
cmnd=13;
outportb(conreg,cmnd);
outportb(datreg,lobyte);
outportb(datreg,hibyte);
cmnd=237;
outportb(conreg,cmnd);
cmnd=112;
outportb(conreg,cmnd);
}

```

```
*****
/* AI_EL_RU.C, ARCHYTAS UAV PROJECT, NPS MONTEREY */
*****
/* Written by LCDR Pat Moran      5/14/93      */
/* Basic PWM routine by LT Paul Merz [Ref. 2, App A & B]      */
/* Demo to move aileron, rudder, elevator, & throttle      */
/* from 2 joysticks. Blends 3 degrees-of-freedom into      */
/* 4 independent vane commands.      */
/* With assistance from Chris Miller NPS EE Dept; Isaac      */
/* Kaminer/Burke Kaltenberger for mixing algorithm.      */
*****
```

```
#include <dos.h>
#include <stdio.h>
#include <conio.h>      /* Only used by 'clrscr' command      */

int datreg = 544;          /* Ctr/timer board, base address      */
int conreg = 545;          /* Ctr/timer board, base addr +1      */
int basaddr=768;          /* A/D board, base address      */
int basepl1=769;          /* A/D board, base addr +1      */
int mux=770;              /* A/D board, base addr +2      */
int statreg=776;          /* A/D board, base addr +8      */
int intcont=777;          /* A/D board, base addr +9      */
int pclock=778;           /* A/D board, base addr +10      */
int inrange=779;          /* A/D board, base addr +11      */
int cntr1=781;             /* A/D board, base addr +13      */
int cntr2=782;             /* A/D board, base addr +14      */
int cntrcon=783;           /* A/D board, base addr +15      */

void main(void);          /* Prototypes:      */
void initialize(void);     /* prototyping functions- tells compiler      */
void setup(void);          /* what goes into and out of each function      */
void sample(void);         /* i.e. int sample(void) means integer input      */
void chgangle(int,int,int,int); /* and no or 'void' output      */

void main(void)
{
    initialize();
    setup();          /* Main function calls all others      */
    sample();
}
```

```

void initialize(void) /* Initializes cntr/timer board */ {
{
    int i;
    clrscr(); /* Clears screen for display */
    outportb(conreg,255); /* Reset all board functions */
    outportb(conreg,23); /* Select master mode register */
    outportb(datreg,176); /* Lobyte enables FOUT, F1 source */
    outportb(datreg,65); /* Hibyte selects binary division
                           /* disable incr, 8bit bus, FOUT on
                           /* divide by 1. */
    outportb(conreg,249); /* Disable prefetch for write ops */
    for (i=1;i<=5;i++)
    {
        outportb(conreg,i); /* Select ctrs 1-5 */
        outportb(datreg,2); /* Lobyte: set modes ctrs 1-5 in CMR */
        outportb(datreg,27); /* Hibyte: no gating for ctrs 1-5 */
    }
    for (i=25;i<=29;i++)
    {
        outportb(conreg,i); /* Load hold registers for refresh rate */
        outportb(datreg,0); /* Ctrl reg+Ctrl2 reg = Refresh Rate */
        outportb(datreg,10); /* This combo = 25 ms rate (40 Hz) */
    }
    for (i=9;i<=13;i++)
    {
        outportb(conreg,i); /* Select load registers for pulse width */
        outportb(datreg,110); /* Sets time for next pulse */
        outportb(datreg,5);
    }
    for (i=233;i<=237;i++) outportb(conreg,i);
    outportb(conreg,127); /* Load & arm ctrs 1-5 */
    printf("\n\n\n *** COMPLETED COUNTER/TIMER INITIALIZATION ***\n");
}

void setup(void) /* Initializes A/D board */
{
    outportb(mux,48); /* Sets mux to read chan 0-3 */
    outportb(intcont,2); /* Sets pacer for clock-driven sampling */
    outportb(inrange,5); /* Sets for input voltage range: 0-5V */
    /* Fm data sheet: SC-01, RW-11, M-011, BCD-0 */
    outportb(cntrcon,118); /* Ctr 1, READ/WR 1sbyte 1ST, mode 3, binary */
    outportb(cntr1,100); /* Load ctr 1 lower byte */
    outportb(cntr1,0); /* Load ctr 1 upper byte */
}

```

```

/* Fm data sheet: SC-10, RW-11, M-011, BCD-0 */  

outportb(cntrcon,182); /* Ctr 2, READ/WR 1sbyte 1ST, mode 3, binary */  

outportb(cntr2,250); /* Load ctr 2 lower byte */  

outportb(cntr2,0); /* Load ctr 2 upper byte */  

/* Ctrs 1&2 combo sets sampling period: 25ms */  

printf(" *** COMPLETED A/D BOARD INITIALIZATION ***\n");  

}  
  

void sample(void) /* Samples channels via A/D board */  

{  

    int x,i,cmnd,lsb,msb,sreg,elev,rud,ail,thr,ch[4];  

    x=1;  

    while (x==1) /* Endless loop */  

    {  

        sreg=inportb(statreg);/* Read stat reg to check intrpt bit */  

        sreg=sreg&16; /* 'AND' with 16 to get only 5th bit */  

        if (sreg==16) /* If intrpt (5th) hi, pulse rcvd */  

        {  

            outportb(mux,48); /* Read Channels 0-3 */  

            outportb(intcont,0); /* Software triggered A/D only */  

            for (i=0;i<=3;i++) /* Read Ch0-3 for thr,ail,elev,rud */  

            {  

                outportb(basaddr,0); /* Immediate A/D conversion */  

                lsb = inportb(basaddr); /* Read lobyte, MSB-8 to LSB + Chan */  

                msb = inportb(basepl1); /* Read hibyte, MSB to MSB-7 */  

                lsb = lsb >> 4; /* Roll lobyte right 4 bits */  

                msb = msb << 4; /* Roll hibyte left 4 bits */  

                ch[i] = msb | lsb; /* 'OR' to get 12 bit info */  

            }  

            outportb(intcont,2); /* Return to pacer clock-driven sampling */  

            cmnd=inportb(statreg); /* Read status reg, then write back to */  

            outportb(statreg,cmnd); /* status reg: resets Pin25 flip-flop */  

            thr = (int)((ch[0]-2714)*.12+80); /* Input fm throttle up/down */  

            ail = (int)((ch[1]-1600)*.4+200); /* Input fm aileron lt/rt */  

            elev = (int)((ch[2]-1850)*.2-80); /* Input fm elevator up/down */  

            rud = (int)((ch[3]-720)*.2-80); /* Input fm rudder lt/rt */  

            chgangle(thr, ail, elev, rud); /* Call chgangle function */  

        }  

    }  

}

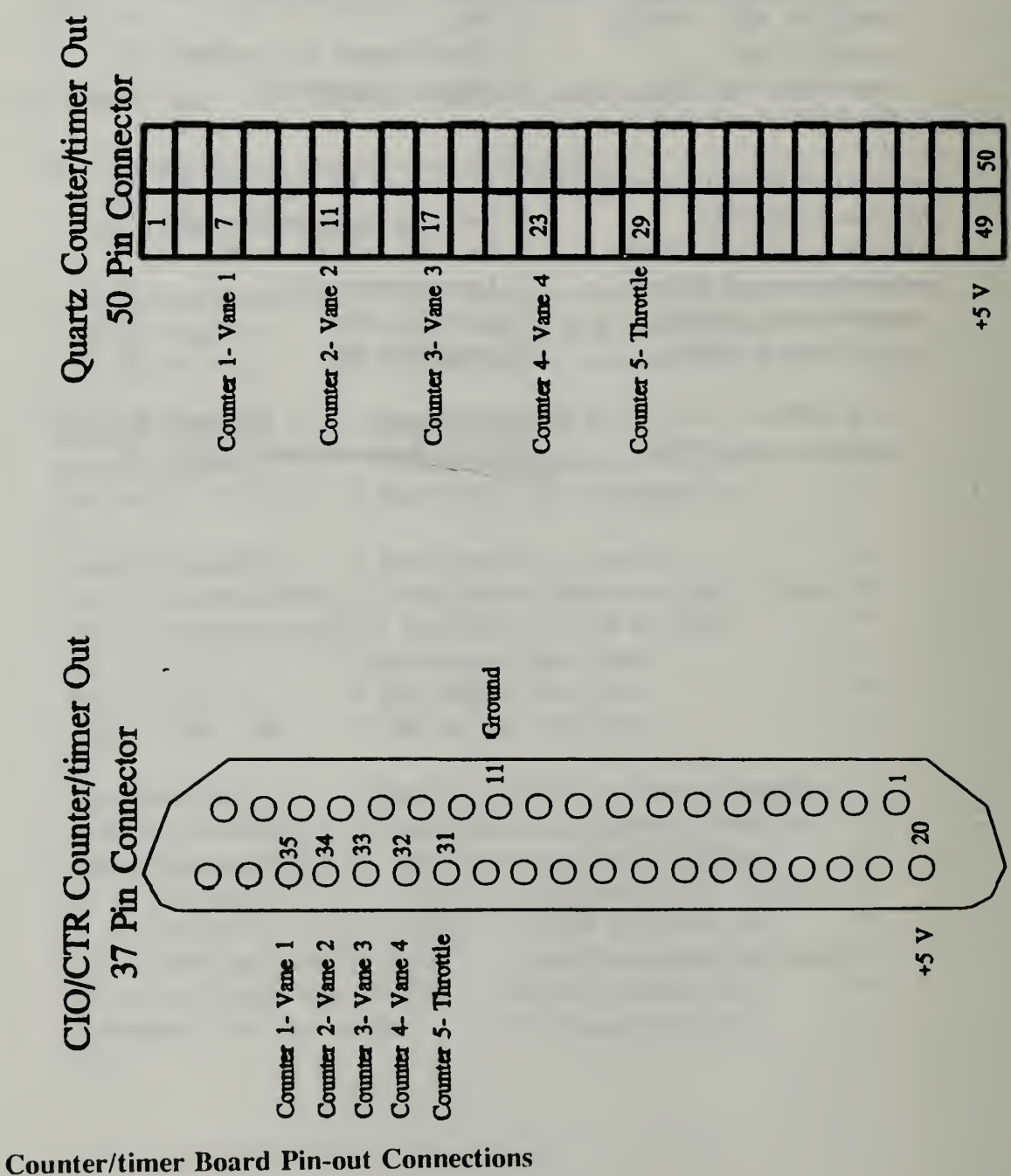
```

```

void chgangle(thr, ail, elev, rud) /* Uses counter/timer to calculate */
{                                /* each pulse width */ 
    int i,hibyte,lobyte,angle,vane[5];
    vane[0] = ail/4 + rud/2;      /* V1; Translation algorithm fm 3 */
    vane[1] = ail/4 + elev/2;    /* V2; control surfaces to 4 vanes */
    vane[2] = ail/4 - rud/2;    /* V3; */
    vane[3] = ail/4 - elev/2;   /* V4; */
    vane[4] = thr;              /* Throttle needs no conversion */
    outportb(conreg,223);       /* Disarm counters 1-5 */
    for (i=0;i<=4;i++)
    {
        angle=((1900/206)*(vane[i])+600); /* Convert fm deg to dig #
        hibyte=(angle/256);                /* Calc high byte, residue left */
        lobyte=(angle-hibyte*256);         /* Calc low byte fm residue */
        outportb(conreg,(i+9));           /* Load counters 1-5 */
        outportb(datreg,lobyte);          /* Load low byte */
        outportb(datreg,hibyte);          /* Load high byte */
    }
    for (i=233;i<=237;i++) outportb(conreg,i); /* Set toggle hi 1-5 */
    outportb(conreg,127);             /* Load & arm counters 1-5 */
}

```

APPENDIX B: HARDWARE SPECIFICATIONS

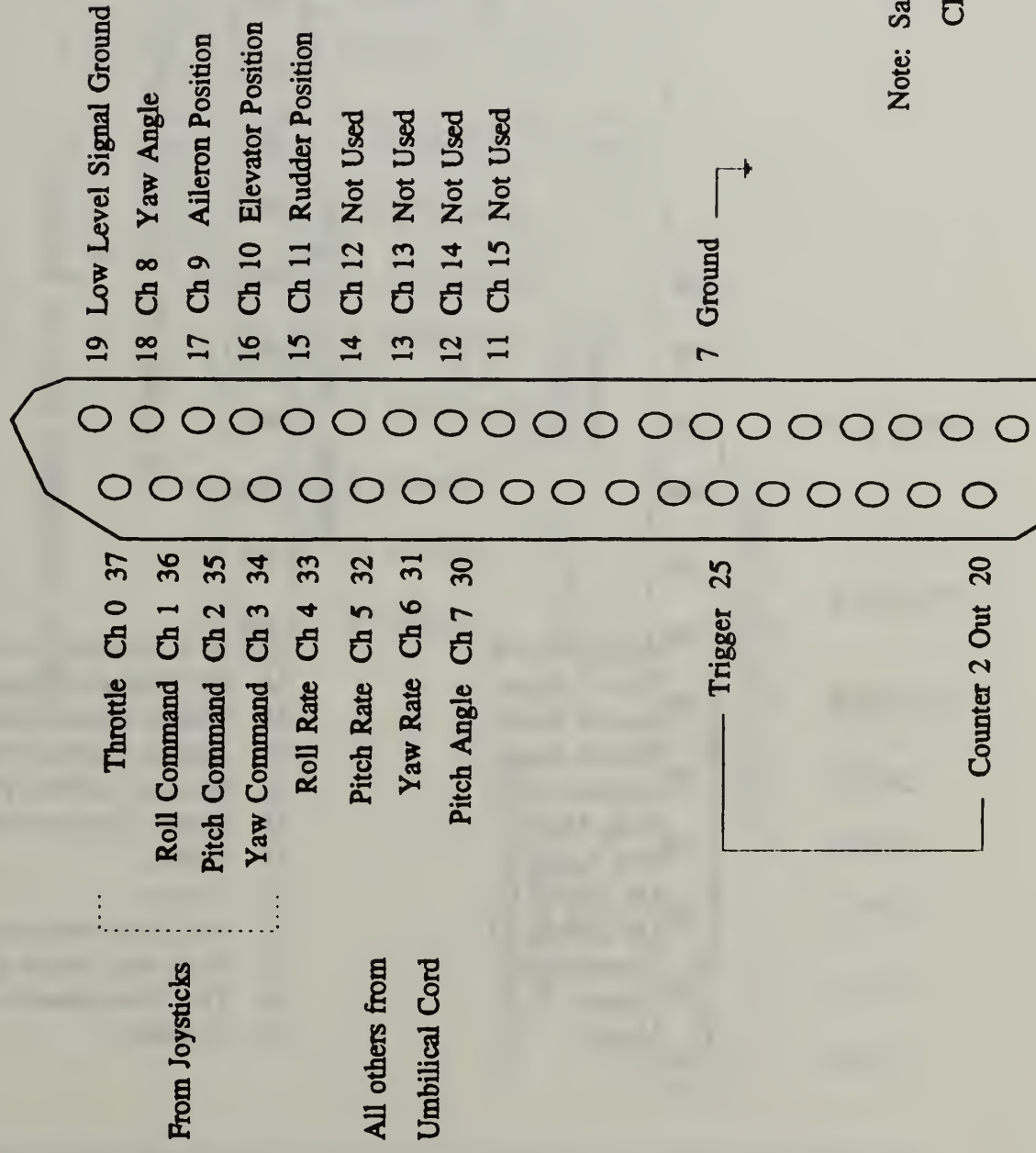


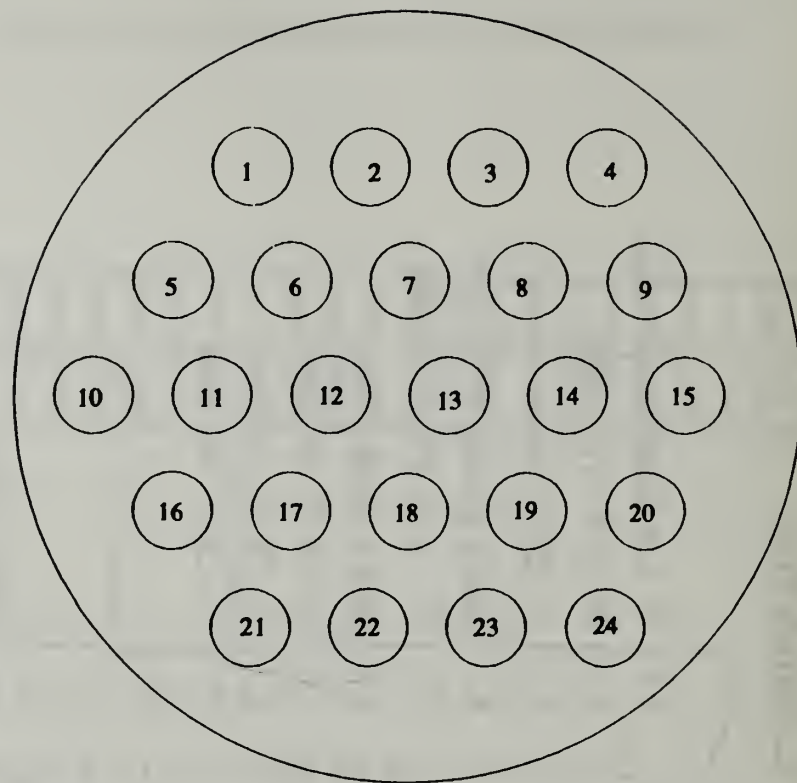
Counter/timer Board Pin-out Connections

Analog-to-Digital (A/D) In

37 Pin Connector

A/D Board Pin-out Connections



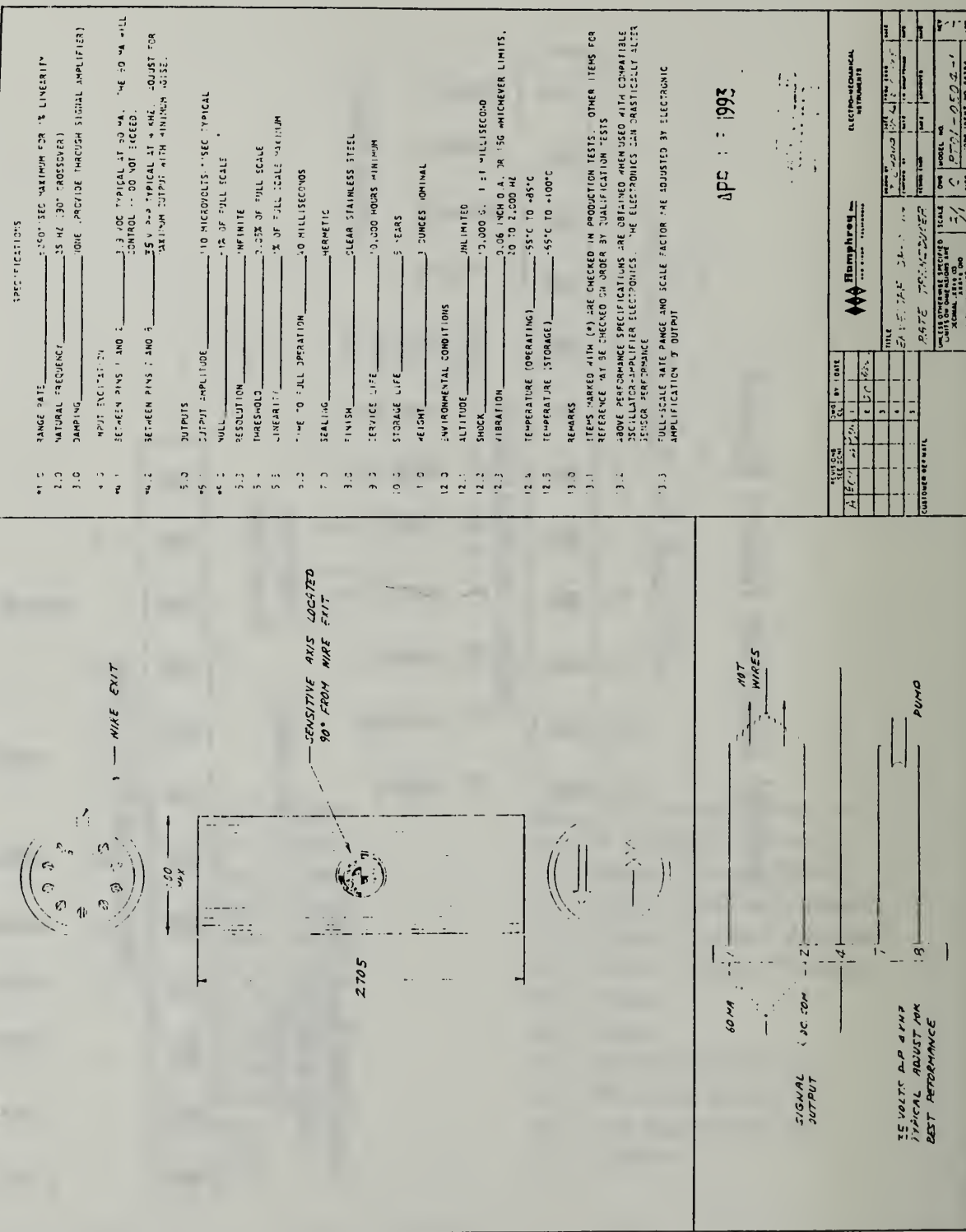


- | | |
|--------------------|--------------------------------|
| 1. Vane 1 Signal | 13. 28 V External Power (+) |
| 2. Vane 2 Signal | 14. 28 V External Power (-) |
| 3. Vane 3 Signal | 15. Chassis Ground (Shield) |
| 4. Vane 4 Signal | 16. Aileron Position Feedback |
| 5. Throttle Signal | 17. Elevator Position Feedback |
| 6. Pitch Angle | 18. Rudder Position Feedback |
| 7. Yaw Angle | 19. Vacant |
| 8. Kill Switch (+) | 20. Vacant |
| 9. Kill Switch (-) | 21. Roll Rate Sensor (p) |
| 10. Tachometer | 22. Pitch Rate Sensor (q) |
| 11. Vacant | 23. Yaw Rate Sensor (r) |
| 12. Vacant | 24. Common |

Umbilical Cord Cannon Plug Pin-numbering Convention

Control Junction Board Busses

Umbilical Cord Connections at Control Junction Board



Roll Rate Sensor (RT-01) Wiring Connections

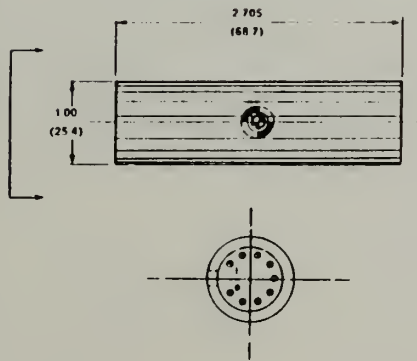


RT01-0504-1

Single-axis sensor. This typifies the RT01 series. It is a cylinder one inch in diameter and its length is inversely proportional to the rate range. It is hermetically sealed, weighs only three ounces, and is controlled by an optional miniature electronic package.

SPECIFICATIONS

| | |
|-------------------|--------------------------|
| Rate range | 1 to 250 /second maximum |
| Natural frequency | 25 Hz minimum |
| Damping | 0.7 typical |
| Output | 25 millivolts nominal |
| Linearity | +1% of full scale |
| Resolution | Infinite |
| Hysteresis | None |
| Null signal | 5 /second |
| Threshold | Virtually zero |
| Noise | 0.1% of full scale |
| Sensor excitation | 3.6 volts at 60 mA DC |
| Pump drive | 18 volts peak at 4K Hz |
| Altitude | Unlimited |
| Shock | 10,000 G |
| Temperature | -55 to +85 C |
| Life | 5 years |
| Weight | 3 ounces |



Humphrey RT-01 Single Rate Sensor Specifications

| SPECIFICATIONS | |
|----------------|--|
| 0.0 | RANGE RATE AXIS "A" |
| 0.1 | -15°/SEC |
| 0.2 | 100°/SEC |
| 0.3 | NATURAL FREQUENCY |
| 0.4 | 25 Hz (90° CROSSOVER) |
| 0.5 | DAMPING |
| 0.6 | HOME (PROVIDE THROUGH SIGNAL AMPLIFIER) |
| 1.0 | INPUT EXCITATION |
| 1.1 | BETWEEN PINS 1 AND 2 _____ 50 MHZ THRU HOT WIRES |
| 1.2 | BETWEEN PINS 5 AND 6 _____ 50 MHZ THRU HOT WIRES |
| 1.3 | BETWEEN PINS 7 AND 8 _____ 35V D.C. OPTICAL AT 4 MHZ. ADJUST FOR MAXIMUM OUTPUT WITH MINIMUM NOISE |
| 2.0 | OUTPUTS |
| 2.1 | AXIS "A" _____ 100 MICROSEC. SEC TYPICAL AXIS "B" _____ 100 MICROSEC. SEC TYPICAL |
| 2.2 | NULL |
| 2.3 | RESOLUTION |
| 2.4 | INFINITE |
| 2.5 | THRESHOLD |
| 2.6 | 3 DEG. OF FULL SCALE |
| 2.7 | LINEARITY |
| 2.8 | 1% OF FULL SCALE MAX |
| 3.0 | TIME TO FULL OPERATION _____ 40 MILLISECONDS |
| 3.1 | SEALING |
| 3.2 | MERMETIC |
| 3.5 | FINISH |
| 3.6 | STAINLESS STEEL |
| 4.0 | SERVICE LIFE _____ 10,000 HOURS MINIMUM |
| 4.1 | STORAGE LIFE _____ 6 YEARS |
| 4.2 | WEIGHT _____ 3 OUNCES NOMINAL |
| 5.0 | ENVIRONMENTAL CONDITIONS |
| 5.1 | ALTITUDE _____ UNLIMITED |
| 5.2 | SHOCK _____ 10,000 G'S 1±1 MILLISECOND |
| 5.3 | VIBRATION _____ 0.06 INCH C.L. OR 15G WHICH EVER LIMITS. 20 TO 2000 Hz |
| 5.4 | TEMPERATURE (OPERATING) _____ -55°C TO +65°C |
| 5.5 | TEMPERATURE (STORAGE) _____ -55°C TO +100°C |
| 6.0 | REMARKS |
| 6.1 | ITEMS MARKED WITH (*) ARE CHECKED IN PRODUCTION TESTS. OTHER ITEMS FOR REFERENCE MAY BE CHECKED ON ORDER BY QUALIFICATION TESTS. |
| 6.2 | ABOVE PERFORMANCE SPECIFICATIONS ARE OBTAINED WITH USE OF ALT. COMPATIBLE OSCILLATOR/AMPLIFIER ELECTRONICS |
| 7.0 | VIEW A-A SCALE 1/2 |
| 7.1 | VIEW B-B SCALE 1/2 |
| 7.2 | VIEW C-C SCALE 1/2 |
| 7.3 | VIEW D-D SCALE 1/2 |
| 7.4 | VIEW E-E SCALE 1/2 |
| 7.5 | VIEW F-F SCALE 1/2 |
| 7.6 | VIEW G-G SCALE 1/2 |
| 7.7 | VIEW H-H SCALE 1/2 |
| 7.8 | VIEW I-I SCALE 1/2 |
| 7.9 | VIEW J-J SCALE 1/2 |
| 7.10 | VIEW K-K SCALE 1/2 |
| 7.11 | VIEW L-L SCALE 1/2 |
| 7.12 | VIEW M-M SCALE 1/2 |
| 7.13 | VIEW N-N SCALE 1/2 |
| 7.14 | VIEW O-O SCALE 1/2 |
| 7.15 | VIEW P-P SCALE 1/2 |
| 7.16 | VIEW Q-Q SCALE 1/2 |
| 7.17 | VIEW R-R SCALE 1/2 |
| 7.18 | VIEW S-S SCALE 1/2 |
| 7.19 | VIEW T-T SCALE 1/2 |
| 7.20 | VIEW U-U SCALE 1/2 |
| 7.21 | VIEW V-V SCALE 1/2 |
| 7.22 | VIEW W-W SCALE 1/2 |
| 7.23 | VIEW X-X SCALE 1/2 |
| 7.24 | VIEW Y-Y SCALE 1/2 |
| 7.25 | VIEW Z-Z SCALE 1/2 |
| 7.26 | VIEW AA-AA SCALE 1/2 |
| 7.27 | VIEW BB-BB SCALE 1/2 |
| 7.28 | VIEW CC-CC SCALE 1/2 |
| 7.29 | VIEW DD-DD SCALE 1/2 |
| 7.30 | VIEW EE-EE SCALE 1/2 |
| 7.31 | VIEW FF-FF SCALE 1/2 |
| 7.32 | VIEW GG-GG SCALE 1/2 |
| 7.33 | VIEW HH-HH SCALE 1/2 |
| 7.34 | VIEW II-II SCALE 1/2 |
| 7.35 | VIEW JJ-JJ SCALE 1/2 |
| 7.36 | VIEW KK-KK SCALE 1/2 |
| 7.37 | VIEW LL-LL SCALE 1/2 |
| 7.38 | VIEW MM-MM SCALE 1/2 |
| 7.39 | VIEW NN-NN SCALE 1/2 |
| 7.40 | VIEW OO-OO SCALE 1/2 |
| 7.41 | VIEW PP-PP SCALE 1/2 |
| 7.42 | VIEW QQ-QQ SCALE 1/2 |
| 7.43 | VIEW RR-RR SCALE 1/2 |
| 7.44 | VIEW SS-SS SCALE 1/2 |
| 7.45 | VIEW TT-TT SCALE 1/2 |
| 7.46 | VIEW UU-UU SCALE 1/2 |
| 7.47 | VIEW VV-VV SCALE 1/2 |
| 7.48 | VIEW WW-WW SCALE 1/2 |
| 7.49 | VIEW XX-XX SCALE 1/2 |
| 7.50 | VIEW YY-YY SCALE 1/2 |
| 7.51 | VIEW ZZ-ZZ SCALE 1/2 |
| 7.52 | VIEW AA-AA SCALE 1/2 |
| 7.53 | VIEW BB-BB SCALE 1/2 |
| 7.54 | VIEW CC-CC SCALE 1/2 |
| 7.55 | VIEW DD-DD SCALE 1/2 |
| 7.56 | VIEW EE-EE SCALE 1/2 |
| 7.57 | VIEW FF-FF SCALE 1/2 |
| 7.58 | VIEW GG-GG SCALE 1/2 |
| 7.59 | VIEW HH-HH SCALE 1/2 |
| 7.60 | VIEW II-II SCALE 1/2 |
| 7.61 | VIEW JJ-JJ SCALE 1/2 |
| 7.62 | VIEW KK-KK SCALE 1/2 |
| 7.63 | VIEW LL-LL SCALE 1/2 |
| 7.64 | VIEW MM-MM SCALE 1/2 |
| 7.65 | VIEW NN-NN SCALE 1/2 |
| 7.66 | VIEW OO-OO SCALE 1/2 |
| 7.67 | VIEW PP-PP SCALE 1/2 |
| 7.68 | VIEW QQ-QQ SCALE 1/2 |
| 7.69 | VIEW RR-RR SCALE 1/2 |
| 7.70 | VIEW SS-SS SCALE 1/2 |
| 7.71 | VIEW TT-TT SCALE 1/2 |
| 7.72 | VIEW UU-UU SCALE 1/2 |
| 7.73 | VIEW VV-VV SCALE 1/2 |
| 7.74 | VIEW WW-WW SCALE 1/2 |
| 7.75 | VIEW XX-XX SCALE 1/2 |
| 7.76 | VIEW YY-YY SCALE 1/2 |
| 7.77 | VIEW ZZ-ZZ SCALE 1/2 |
| 7.78 | VIEW AA-AA SCALE 1/2 |
| 7.79 | VIEW BB-BB SCALE 1/2 |
| 7.80 | VIEW CC-CC SCALE 1/2 |
| 7.81 | VIEW DD-DD SCALE 1/2 |
| 7.82 | VIEW EE-EE SCALE 1/2 |
| 7.83 | VIEW FF-FF SCALE 1/2 |
| 7.84 | VIEW GG-GG SCALE 1/2 |
| 7.85 | VIEW HH-HH SCALE 1/2 |
| 7.86 | VIEW II-II SCALE 1/2 |
| 7.87 | VIEW JJ-JJ SCALE 1/2 |
| 7.88 | VIEW KK-KK SCALE 1/2 |
| 7.89 | VIEW LL-LL SCALE 1/2 |
| 7.90 | VIEW MM-MM SCALE 1/2 |
| 7.91 | VIEW NN-NN SCALE 1/2 |
| 7.92 | VIEW OO-OO SCALE 1/2 |
| 7.93 | VIEW PP-PP SCALE 1/2 |
| 7.94 | VIEW QQ-QQ SCALE 1/2 |
| 7.95 | VIEW RR-RR SCALE 1/2 |
| 7.96 | VIEW SS-SS SCALE 1/2 |
| 7.97 | VIEW TT-TT SCALE 1/2 |
| 7.98 | VIEW UU-UU SCALE 1/2 |
| 7.99 | VIEW VV-VV SCALE 1/2 |
| 7.100 | VIEW WW-WW SCALE 1/2 |
| 7.101 | VIEW XX-XX SCALE 1/2 |
| 7.102 | VIEW YY-YY SCALE 1/2 |
| 7.103 | VIEW ZZ-ZZ SCALE 1/2 |
| 7.104 | VIEW AA-AA SCALE 1/2 |
| 7.105 | VIEW BB-BB SCALE 1/2 |
| 7.106 | VIEW CC-CC SCALE 1/2 |
| 7.107 | VIEW DD-DD SCALE 1/2 |
| 7.108 | VIEW EE-EE SCALE 1/2 |
| 7.109 | VIEW FF-FF SCALE 1/2 |
| 7.110 | VIEW GG-GG SCALE 1/2 |
| 7.111 | VIEW HH-HH SCALE 1/2 |
| 7.112 | VIEW II-II SCALE 1/2 |
| 7.113 | VIEW JJ-JJ SCALE 1/2 |
| 7.114 | VIEW KK-KK SCALE 1/2 |
| 7.115 | VIEW LL-LL SCALE 1/2 |
| 7.116 | VIEW MM-MM SCALE 1/2 |
| 7.117 | VIEW NN-NN SCALE 1/2 |
| 7.118 | VIEW OO-OO SCALE 1/2 |
| 7.119 | VIEW PP-PP SCALE 1/2 |
| 7.120 | VIEW QQ-QQ SCALE 1/2 |
| 7.121 | VIEW RR-RR SCALE 1/2 |
| 7.122 | VIEW SS-SS SCALE 1/2 |
| 7.123 | VIEW TT-TT SCALE 1/2 |
| 7.124 | VIEW UU-UU SCALE 1/2 |
| 7.125 | VIEW VV-VV SCALE 1/2 |
| 7.126 | VIEW WW-WW SCALE 1/2 |
| 7.127 | VIEW XX-XX SCALE 1/2 |
| 7.128 | VIEW YY-YY SCALE 1/2 |
| 7.129 | VIEW ZZ-ZZ SCALE 1/2 |
| 7.130 | VIEW AA-AA SCALE 1/2 |
| 7.131 | VIEW BB-BB SCALE 1/2 |
| 7.132 | VIEW CC-CC SCALE 1/2 |
| 7.133 | VIEW DD-DD SCALE 1/2 |
| 7.134 | VIEW EE-EE SCALE 1/2 |
| 7.135 | VIEW FF-FF SCALE 1/2 |
| 7.136 | VIEW GG-GG SCALE 1/2 |
| 7.137 | VIEW HH-HH SCALE 1/2 |
| 7.138 | VIEW II-II SCALE 1/2 |
| 7.139 | VIEW JJ-JJ SCALE 1/2 |
| 7.140 | VIEW KK-KK SCALE 1/2 |
| 7.141 | VIEW LL-LL SCALE 1/2 |
| 7.142 | VIEW MM-MM SCALE 1/2 |
| 7.143 | VIEW NN-NN SCALE 1/2 |
| 7.144 | VIEW OO-OO SCALE 1/2 |
| 7.145 | VIEW PP-PP SCALE 1/2 |
| 7.146 | VIEW QQ-QQ SCALE 1/2 |
| 7.147 | VIEW RR-RR SCALE 1/2 |
| 7.148 | VIEW SS-SS SCALE 1/2 |
| 7.149 | VIEW TT-TT SCALE 1/2 |
| 7.150 | VIEW UU-UU SCALE 1/2 |
| 7.151 | VIEW VV-VV SCALE 1/2 |
| 7.152 | VIEW WW-WW SCALE 1/2 |
| 7.153 | VIEW XX-XX SCALE 1/2 |
| 7.154 | VIEW YY-YY SCALE 1/2 |
| 7.155 | VIEW ZZ-ZZ SCALE 1/2 |
| 7.156 | VIEW AA-AA SCALE 1/2 |
| 7.157 | VIEW BB-BB SCALE 1/2 |
| 7.158 | VIEW CC-CC SCALE 1/2 |
| 7.159 | VIEW DD-DD SCALE 1/2 |
| 7.160 | VIEW EE-EE SCALE 1/2 |
| 7.161 | VIEW FF-FF SCALE 1/2 |
| 7.162 | VIEW GG-GG SCALE 1/2 |
| 7.163 | VIEW HH-HH SCALE 1/2 |
| 7.164 | VIEW II-II SCALE 1/2 |
| 7.165 | VIEW JJ-JJ SCALE 1/2 |
| 7.166 | VIEW KK-KK SCALE 1/2 |
| 7.167 | VIEW LL-LL SCALE 1/2 |
| 7.168 | VIEW MM-MM SCALE 1/2 |
| 7.169 | VIEW NN-NN SCALE 1/2 |
| 7.170 | VIEW OO-OO SCALE 1/2 |
| 7.171 | VIEW PP-PP SCALE 1/2 |
| 7.172 | VIEW QQ-QQ SCALE 1/2 |
| 7.173 | VIEW RR-RR SCALE 1/2 |
| 7.174 | VIEW SS-SS SCALE 1/2 |
| 7.175 | VIEW TT-TT SCALE 1/2 |
| 7.176 | VIEW UU-UU SCALE 1/2 |
| 7.177 | VIEW VV-VV SCALE 1/2 |
| 7.178 | VIEW WW-WW SCALE 1/2 |
| 7.179 | VIEW XX-XX SCALE 1/2 |
| 7.180 | VIEW YY-YY SCALE 1/2 |
| 7.181 | VIEW ZZ-ZZ SCALE 1/2 |
| 7.182 | VIEW AA-AA SCALE 1/2 |
| 7.183 | VIEW BB-BB SCALE 1/2 |
| 7.184 | VIEW CC-CC SCALE 1/2 |
| 7.185 | VIEW DD-DD SCALE 1/2 |
| 7.186 | VIEW EE-EE SCALE 1/2 |
| 7.187 | VIEW FF-FF SCALE 1/2 |
| 7.188 | VIEW GG-GG SCALE 1/2 |
| 7.189 | VIEW HH-HH SCALE 1/2 |
| 7.190 | VIEW II-II SCALE 1/2 |
| 7.191 | VIEW JJ-JJ SCALE 1/2 |
| 7.192 | VIEW KK-KK SCALE 1/2 |
| 7.193 | VIEW LL-LL SCALE 1/2 |
| 7.194 | VIEW MM-MM SCALE 1/2 |
| 7.195 | VIEW NN-NN SCALE 1/2 |
| 7.196 | VIEW OO-OO SCALE 1/2 |
| 7.197 | VIEW PP-PP SCALE 1/2 |
| 7.198 | VIEW QQ-QQ SCALE 1/2 |
| 7.199 | VIEW RR-RR SCALE 1/2 |
| 7.200 | VIEW SS-SS SCALE 1/2 |
| 7.201 | VIEW TT-TT SCALE 1/2 |
| 7.202 | VIEW UU-UU SCALE 1/2 |
| 7.203 | VIEW VV-VV SCALE 1/2 |
| 7.204 | VIEW WW-WW SCALE 1/2 |
| 7.205 | VIEW XX-XX SCALE 1/2 |
| 7.206 | VIEW YY-YY SCALE 1/2 |
| 7.207 | VIEW ZZ-ZZ SCALE 1/2 |
| 7.208 | VIEW AA-AA SCALE 1/2 |
| 7.209 | VIEW BB-BB SCALE 1/2 |
| 7.210 | VIEW CC-CC SCALE 1/2 |
| 7.211 | VIEW DD-DD SCALE 1/2 |
| 7.212 | VIEW EE-EE SCALE 1/2 |
| 7.213 | VIEW FF-FF SCALE 1/2 |
| 7.214 | VIEW GG-GG SCALE 1/2 |
| 7.215 | VIEW HH-HH SCALE 1/2 |
| 7.216 | VIEW II-II SCALE 1/2 |
| 7.217 | VIEW JJ-JJ SCALE 1/2 |
| 7.218 | VIEW KK-KK SCALE 1/2 |
| 7.219 | VIEW LL-LL SCALE 1/2 |
| 7.220 | VIEW MM-MM SCALE 1/2 |
| 7.221 | VIEW NN-NN SCALE 1/2 |
| 7.222 | VIEW OO-OO SCALE 1/2 |
| 7.223 | VIEW PP-PP SCALE 1/2 |
| 7.224 | VIEW QQ-QQ SCALE 1/2 |
| 7.225 | VIEW RR-RR SCALE 1/2 |
| 7.226 | VIEW SS-SS SCALE 1/2 |
| 7.227 | VIEW TT-TT SCALE 1/2 |
| 7.228 | VIEW UU-UU SCALE 1/2 |
| 7.229 | VIEW VV-VV SCALE 1/2 |
| 7.230 | VIEW WW-WW SCALE 1/2 |
| 7.231 | VIEW XX-XX SCALE 1/2 |
| 7.232 | VIEW YY-YY SCALE 1/2 |
| 7.233 | VIEW ZZ-ZZ SCALE 1/2 |
| 7.234 | VIEW AA-AA SCALE 1/2 |
| 7.235 | VIEW BB-BB SCALE 1/2 |
| 7.236 | VIEW CC-CC SCALE 1/2 |
| 7.237 | VIEW DD-DD SCALE 1/2 |
| 7.238 | VIEW EE-EE SCALE 1/2 |
| 7.239 | VIEW FF-FF SCALE 1/2 |
| 7.240 | VIEW GG-GG SCALE 1/2 |
| 7.241 | VIEW HH-HH SCALE 1/2 |
| 7.242 | VIEW II-II SCALE 1/2 |
| 7.243 | VIEW JJ-JJ SCALE 1/2 |
| 7.244 | VIEW KK-KK SCALE 1/2 |
| 7.245 | VIEW LL-LL SCALE 1/2 |
| 7.246 | VIEW MM-MM SCALE 1/2 |
| 7.247 | VIEW NN-NN SCALE 1/2 |
| 7.248 | VIEW OO-OO SCALE 1/2 |
| 7.249 | VIEW PP-PP SCALE 1/2 |
| 7.250 | VIEW QQ-QQ SCALE 1/2 |
| 7.251 | VIEW RR-RR SCALE 1/2 |
| 7.252 | VIEW SS-SS SCALE 1/2 |
| 7.253 | VIEW TT-TT SCALE 1/2 |
| 7.254 | VIEW UU-UU SCALE 1/2 |
| 7.255 | VIEW VV-VV SCALE 1/2 |
| 7.256 | VIEW WW-WW SCALE 1/2 |
| 7.257 | VIEW XX-XX SCALE 1/2 |
| 7.258 | VIEW YY-YY SCALE 1/2 |
| 7.259 | VIEW ZZ-ZZ SCALE 1/2 |
| 7.260 | VIEW AA-AA SCALE 1/2 |
| 7.261 | VIEW BB-BB SCALE 1/2 |
| 7.262 | VIEW CC-CC SCALE 1/2 |
| 7.263 | VIEW DD-DD SCALE 1/2 |
| 7.264 | VIEW EE-EE SCALE 1/2 |
| 7.265 | VIEW FF-FF SCALE 1/2 |
| 7.266 | VIEW GG-GG SCALE 1/2 |
| 7.267 | VIEW HH-HH SCALE 1/2 |
| 7.268 | VIEW II-II SCALE 1/2 |
| 7.269 | VIEW JJ-JJ SCALE 1/2 |
| 7.270 | VIEW KK-KK SCALE 1/2 |
| 7.271 | VIEW LL-LL SCALE 1/2 |
| 7.272 | VIEW MM-MM SCALE 1/2 |
| 7.273 | VIEW NN-NN SCALE 1/2 |
| 7.274 | VIEW OO-OO SCALE 1/2 |
| 7.275 | VIEW PP-PP SCALE 1/2 |
| 7.276 | VIEW QQ-QQ SCALE 1/2 |
| 7.277 | VIEW RR-RR SCALE 1/2 |
| 7.278 | VIEW SS-SS SCALE 1/2 |
| 7.279 | VIEW TT-TT SCALE 1/2 |
| 7.280 | VIEW UU-UU SCALE 1/2 |
| 7.281 | VIEW VV-VV SCALE 1/2 |
| 7.282 | VIEW WW-WW SCALE 1/2 |
| 7.283 | VIEW XX-XX SCALE 1/2 |
| 7.284 | VIEW YY-YY SCALE 1/2 |
| 7.285 | VIEW ZZ-ZZ SCALE 1/2 |
| 7.286 | VIEW AA-AA SCALE 1/2 |
| 7.287 | VIEW BB-BB SCALE 1/2 |
| 7.288 | VIEW CC-CC SCALE 1/2 |
| 7.289 | VIEW DD-DD SCALE 1/2 |
| 7.290 | VIEW EE-EE SCALE 1/2 |
| 7.291 | VIEW FF-FF SCALE 1/2 |
| 7.292 | VIEW GG-GG SCALE 1/2 |
| 7.293 | VIEW HH-HH SCALE 1/2 |
| 7.294 | VIEW II-II SCALE 1/2 |
| 7.295 | VIEW JJ-JJ SCALE 1/2 |
| 7.296 | VIEW KK-KK SCALE 1/2 |
| 7.297 | VIEW LL-LL SCALE 1/2 |
| 7.298 | VIEW MM-MM SCALE 1/2 |
| 7.299 | VIEW NN-NN SCALE 1/2 |
| 7.300 | VIEW OO-OO SCALE 1/2 |
| 7.301 | VIEW PP-PP SCALE 1/2 |
| 7.302 | VIEW QQ-QQ SCALE 1/2 |
| 7.303 | VIEW RR-RR SCALE 1/2 |
| 7.304 | VIEW SS-SS SCALE 1/2 |
| 7.305 | VIEW TT-TT SCALE 1/2 |
| 7.306 | VIEW UU-UU SCALE 1/2 |
| 7.307 | VIEW VV-VV SCALE 1/2 |
| 7.308 | VIEW WW-WW SCALE 1/2 |
| 7.309 | VIEW XX-XX SCALE 1/2 |
| 7.310 | VIEW YY-YY SCALE 1/2 |
| 7.311 | VIEW ZZ-ZZ SCALE 1/2 |
| 7.312 | VIEW AA-AA SCALE 1/2 |
| 7.313 | VIEW BB-BB SCALE 1/2 |
| 7.314 | VIEW CC-CC SCALE 1/2 |
| 7.315 | VIEW DD-DD SCALE 1/2 |
| 7.316 | VIEW EE-EE SCALE 1/2 |
| 7.317 | VIEW FF-FF SCALE 1/2 |
| 7.318 | VIEW GG-GG SCALE 1/2 |
| 7.319 | VIEW HH-HH SCALE 1/2 |
| 7.320 | VIEW II-II SCALE 1/2 |
| 7.321 | VIEW JJ-JJ SCALE 1/2 |
| 7.322 | VIEW KK-KK SCALE 1/2 |
| 7.323 | VIEW LL-LL SCALE 1/2 |
| 7.324 | VIEW MM-MM SCALE 1/2 |
| 7.325 | VIEW NN-NN SCALE 1/2 |
| 7.326 | VIEW OO-OO SCALE 1/2 |
| 7.327 | VIEW PP-PP SCALE 1/2 |
| 7.328 | VIEW QQ-QQ SCALE 1/2 |
| 7.329 | VIEW RR-RR SCALE 1/2 |
| 7.330 | VIEW SS-SS SCALE 1/2 |
| 7.331 | VIEW TT-TT SCALE 1/2 |
| 7.332 | VIEW UU-UU SCALE 1/2 |
| 7.333 | VIEW VV-VV SCALE 1/2 |
| 7.334 | VIEW WW-WW SCALE 1/2 |
| 7.335 | VIEW XX-XX SCALE 1/2 |
| 7.336 | VIEW YY-YY SCALE 1/2 |
| 7.337 | VIEW ZZ-ZZ SCALE 1/2 |
| 7.338 | VIEW AA-AA SCALE 1/2 |
| 7.339 | VIEW BB-BB SCALE 1/2 |
| 7.340 | VIEW CC-CC SCALE 1/2 |
| 7.341 | VIEW DD-DD SCALE 1/2 |
| 7.342 | VIEW EE-EE SCALE 1/2 |
| 7.343 | VIEW FF-FF SCALE 1/2 |
| 7.344 | VIEW GG-GG SCALE 1/2 |
| 7.345 | VIEW HH-HH SCALE 1/2 |
| 7.346 | VIEW II-II SCALE 1/2 |
| 7.347 | VIEW JJ-JJ SCALE 1/2 |
| 7.348 | VIEW KK-KK SCALE 1/2 |
| 7.349 | VIEW LL-LL SCALE 1/2 |
| 7.350 | VIEW MM-MM SCALE 1/2 |
| 7.351 | VIEW NN-NN SCALE 1/2 |
| 7.352 | VIEW OO-OO SCALE 1/2 |
| 7.353 | VIEW PP-PP SCALE 1/2 |
| 7.354 | VIEW QQ-QQ SCALE 1/2 |
| 7.355 | VIEW RR-RR SCALE 1/2 |
| 7.356 | VIEW SS-SS SCALE 1/2 |
| 7.357 | VIEW TT-TT SCALE 1/2 |
| 7.358 | VIEW UU-UU SCALE 1/2 |
| 7.359 | VIEW VV-VV SCALE 1/2 |
| 7.360 | VIEW WW-WW SCALE 1/2 |
| 7.361 | VIEW XX-XX SCALE 1/2 |
| 7.362 | |

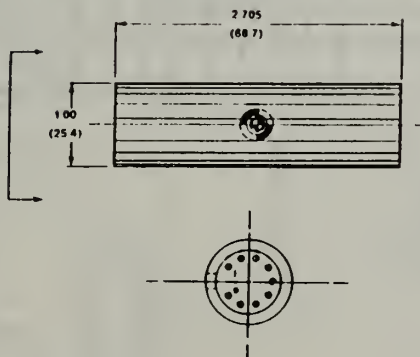


RT09-0103-1

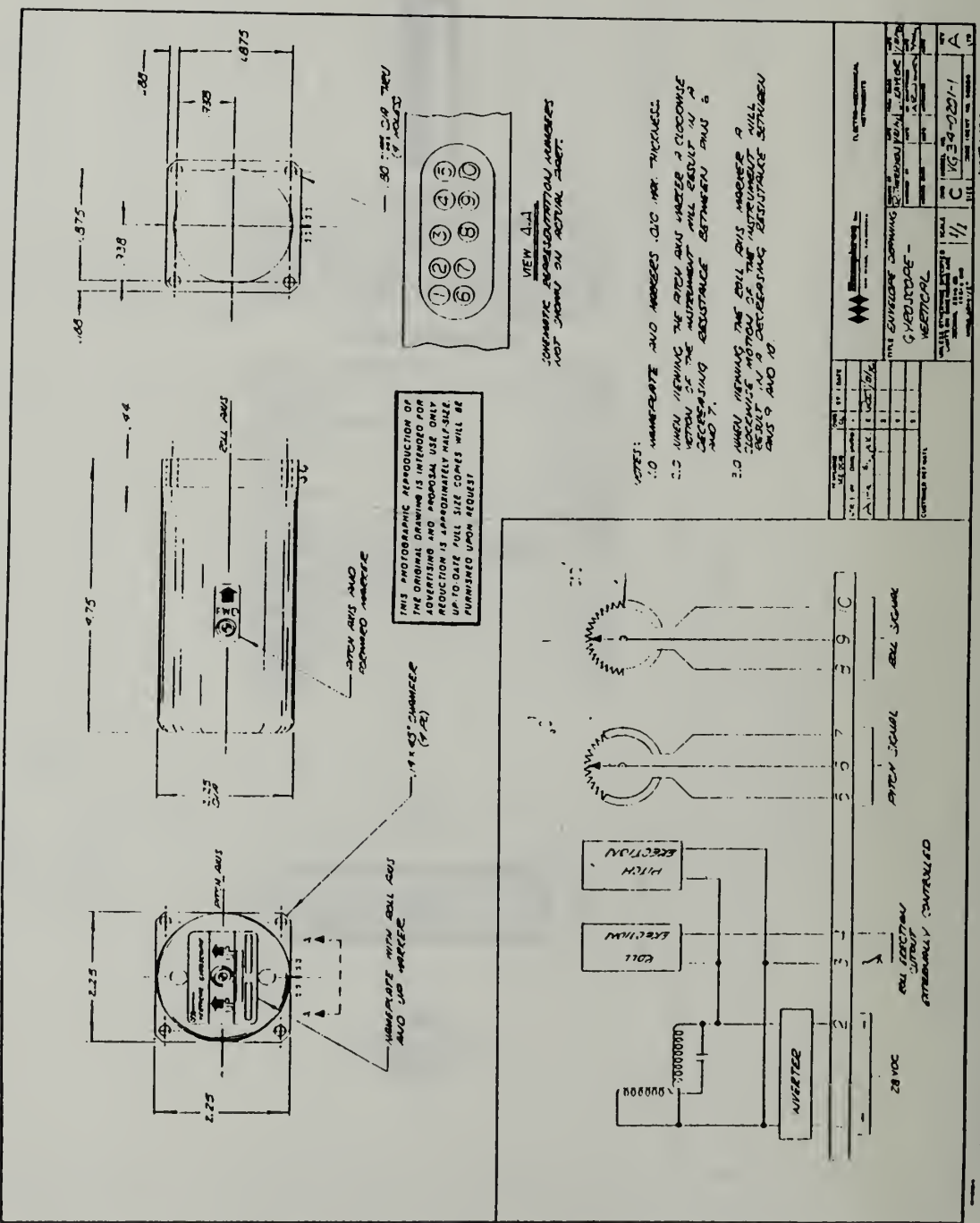
Dual-axis sensor. The RT09 series incorporates two sets of sensor wires, orthogonally mounted, in one package to give dual-axis operation. Externally, units are physically identical with the RT01 series and operation is essentially identical.

SPECIFICATIONS

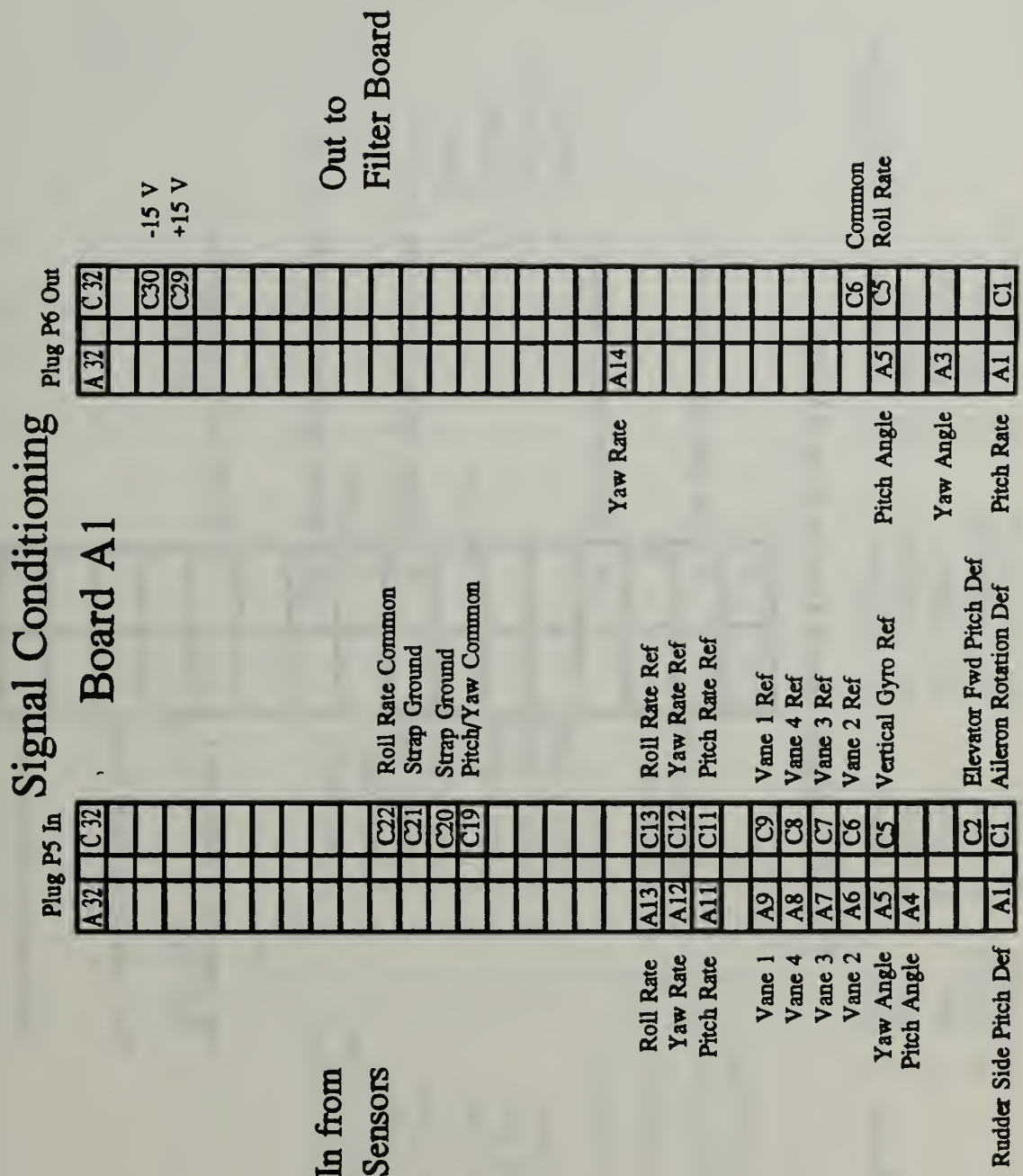
| | |
|-----------------------------|---|
| Range rate | 100%/second each axis |
| Natural frequency | 25 Hz minimum |
| Damping | 0.7 typical |
| Output | +10 millivolts nominal |
| Linearity | < 1% of full scale |
| Resolution | Infinite |
| Hysteresis | None |
| Null signal | 12 /sec |
| Threshold | Virtually zero |
| Noise | 0.1% of full scale |
| Sensor excitation | 60 MA DC current thru two pairs of wires |
| Pump drive | 18 volts peak at 4K Hz |
| Altitude | Unlimited |
| Shock | 10,000 G |
| Temperature | -55 to +85 C |
| Life | 5 years |
| Weight | .3 ounces |



Humphrey RT-09 Dual Rate Sensor Specifications



Vertical Gyroscope (VG-34) Wiring Connections

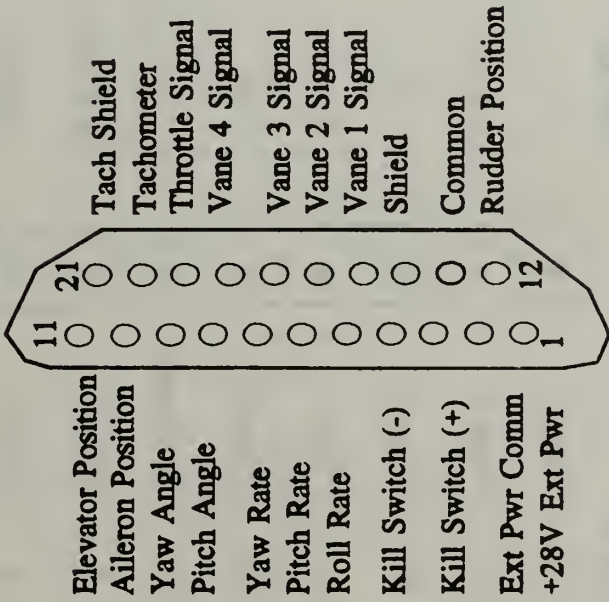


Forebody A1 Channel Conditioning Board Connections

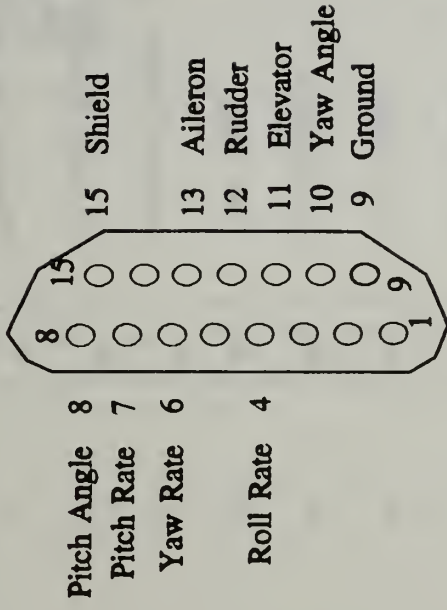
Plug P17: Filter Board Out to Plug P103N

Forebody Filter Board Connections

P21N



P103N



| | | | | |
|-------------|-----------|-----------|---------------|------------------|
| In general: | 1- Black | 6- Green | 11- Wh/Black | 16- Wh/Green |
| | 2- Brown | 7- Blue | 12- Wh/Brown | 17- Wh/Blue |
| | 3- Red | 8- Violet | 13- Wh/Red | 18- Wh/Violet |
| | 4- Orange | 9- Gray | 14- Wh/Orange | 19- Wh/Gray |
| | 5- Yellow | 10- White | 15- Wh/Yellow | 20- Wh/Blk/Brown |
| | | | | 21-Wh/Blk/Red |

New Plug P21N and P103N Pin-out Diagrams

| TSB2N | | TSB3N | |
|------------------|----------|--------------|----------------------|
| P21N In | P201 Out | P103N In | P21N Out |
| 15 Vane 1 | 14 | 4 | 5 |
| 16 Vane 2 | 17 | 7 | Pitch Rate 6 |
| 17 Vane 3 | 18 | 6 | Yaw Rate 7 |
| 18 Vane 4 | 15 | 8 | Pitch Angle 8 |
| 19 Throttle | 16 | 10 | Yaw Angle 9 |
| 20 Tachometer | ● 5 | 13 | Aileron Position 10 |
| 3 Kill (+) | ● 6 | 11 | Elevator Position 11 |
| 4 Kill (-) | ● 7 | 12 | Rudder Position 12 |
| 1 +28V Ext Power | ● 8 | ● 8 | Common 13 |
| 2 Ext Power Com | ● 9 | To TSB5 - 9 | Shield 14 |
| | ● 10 | To TSB5 - 11 | ● 9 |
| | | To TSB5 - 15 | ● 10 |
| In general: | | 6- Green | 16- Wh/Green |
| 1- Black | | 7- Blue | 17- Wh/Blue |
| 2- Brown | | 8- Violet | 18- Wh/Violet |
| 3- Red | | 9- Gray | 19- Wh/Gray |
| 4- Orange | | 10- White | 20- Wh/Blk/Brown |

New Chassis Bus Boards TSB2N and TSB3N Diagrams

Futaba

FP-S134 FP-S34

For J. M. SG. MAGNUM, and CHALLENGER Series
For E. F. G. H. L. Series

Large high torque watertight and dustproof servos

The FP-S134 and FP-S34 are large high torque and light weight servos. They are built with Futaba's unique features. They are perfect for large servo applications where high torque is required.

GENERAL

- Large torque is up to 112.6oz-in (8.8kg-cm) and is perfect for large models. It is also capable of high torque.
- Other unique design features include improved insulation and shock absorption, and the use of multiple precision bearings.
- Ball bearing power system (BPS) provides high starting torque, instant dead band, and excellent linearity.
- Thermoplastic reinforced PTFE polybutylene (except that the injection molded cover) is mechanically strong and insusceptible to play tool.
- Nylon polyimide wire protection set, a gear operated clutch, and pin lock pins for durability and durability no backlash.
- Thick film gold plated connector has chromate finish contact and improves reliability against shock and vibration. The S134 has a reverse insertion prevention mechanism.
- Special gear type potentiometer is mounted on mounting carry and has an excellent self-braking effect.
- Six adjustable capture horns are available.

FEATURES

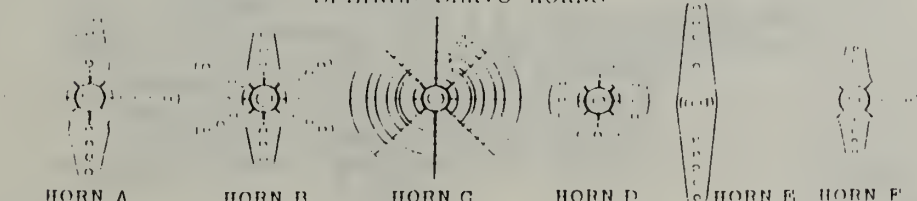
| | |
|-------------------|--|
| Control system | radio width control (FUTABA standard S134) FM/AM standard (S34) |
| Operating angle | Rotary Type one side 160° from the bottom line (from 0° to 180°) |
| Power supply | 4.8V to 6.0V (shared with receiver) |
| Power consumption | 6.0V 8mA (at idle) |
| Output torque | 112.6oz-in (8.8kg-cm) |
| Operating speed | 0.19sec/60° |
| Dimensions | 2.32" x 1.14" x 1.02" in (59.0 x 29.0 x 25.5mm) |
| Weight | 2.2oz (64g) |

ATTACHMENTS

- Use the S134 with Futaba J. M. SG. MAGNUM and CHALLENGER Series sets and the S34 with E. F. G. H. and L. Series sets. These servos cannot be used with other RC sets.
- Install the servo so that the rod adjuster, flexible wire, hinges, and other parts operate smoothly. Be especially careful when the travel is large.
- When using screws, install the servo through a bushing and tighten the screws so that the bushing is slightly crushed. If the screws are too tight, the cushioning oil out of the bushing will be lost.
- A spare servo horn is provided. Use it as needed.

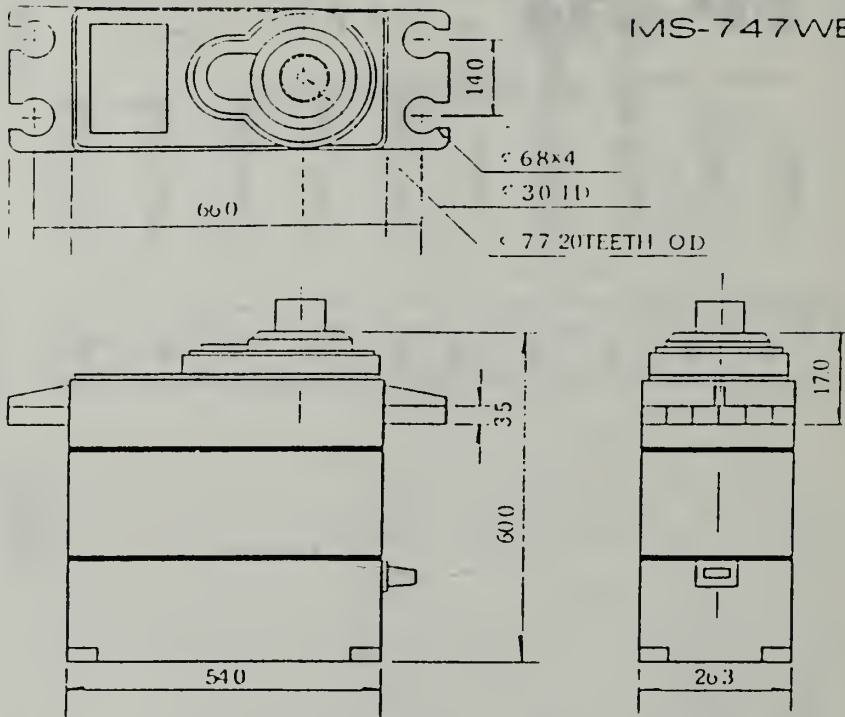
(Ratings and specifications are subject to change without notice.)

SPLINED SERVO HORNS



Futaba FP-S34 Quarter-scale Servo Specifications

MS-747WB



SPECIFICATIONS

SIZE: $2\frac{1}{2} \times 3\frac{1}{2} \times 1\frac{1}{8}$ [54.0x60.0x26.3mm]

WEIGHT: 3.9 OZ (110 g)

SPEED: 0.26 SEC/60 DEGREES

TORQUE: 167 OZ/IN (12 KG/CM)

INPUT VOLTAGE: 4.8-6.0 V DC

INPUT SIGNAL: CONVENTIONAL R/C POSITIVE PULSE
WIDTH MODULATION WITH 1.5MS ± 0.5
US NEUTRAL

CURRENT CONSUMPTION: IDLE 25MA

NO LOAD 300MA

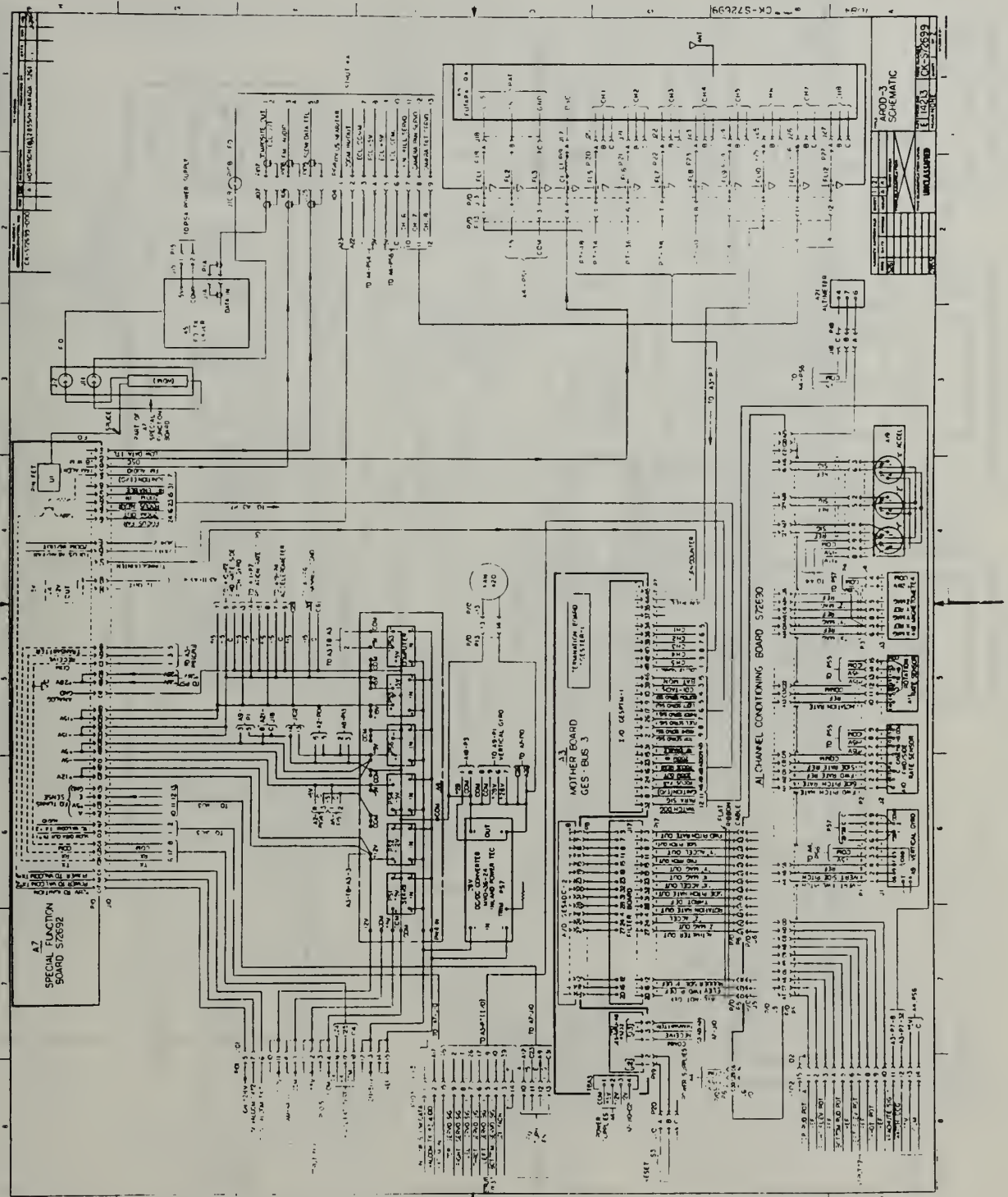
MAX. 1400MA

OUTPUT ROTATION: 90 & 180 DEGREES, TWO TYPES

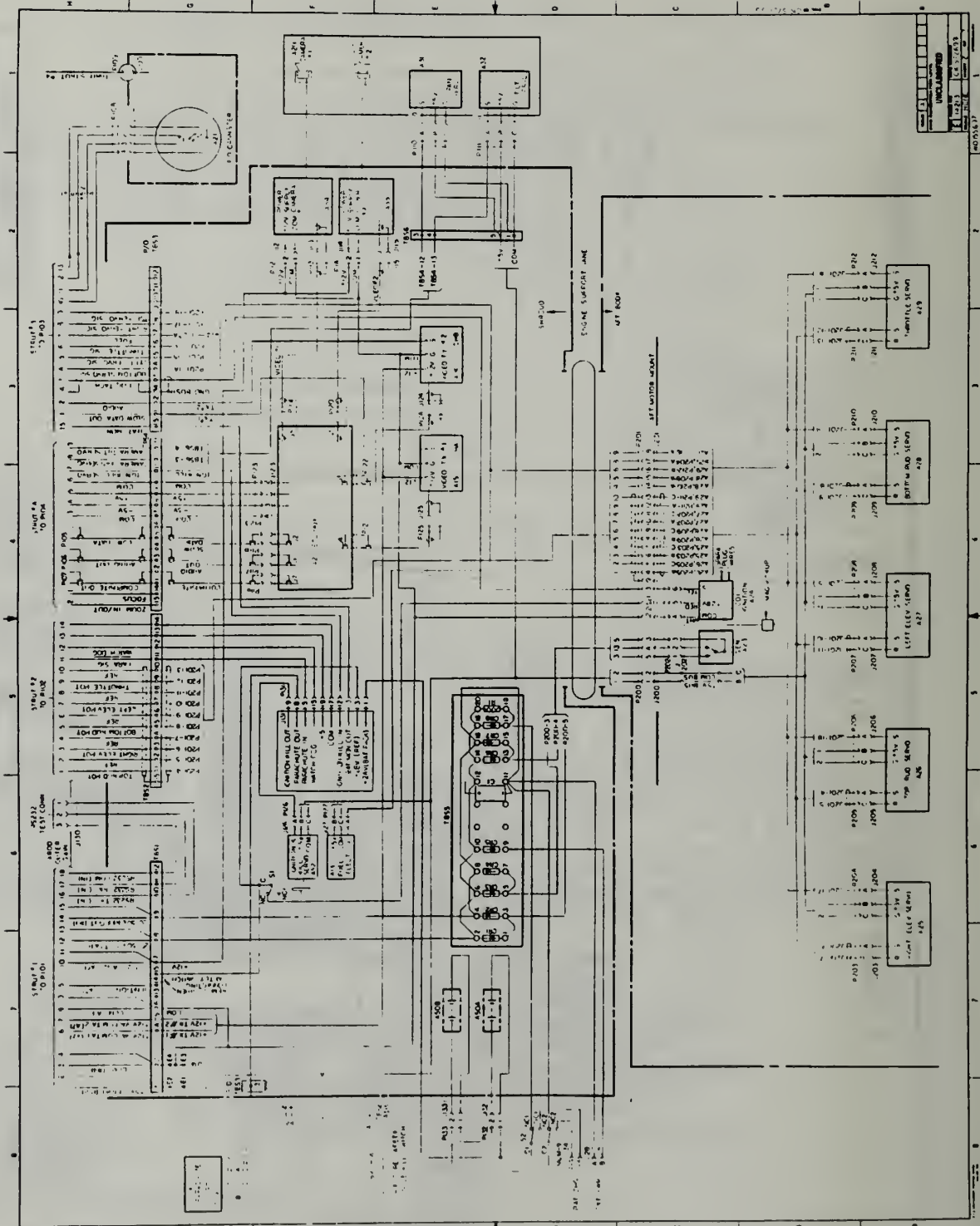
FEATURES: MS-747WB SERVO HAS A HEAVY DUTY
OUTPUT SHAFT WITH BALL BEARING AND
O-RING SEAL RUGGED EXTRA-THICK
GEARS, ARM AND DISK. EXCELLENT
MECHANICAL AND ELECTRONICS QUALITY.

Condor RC MS-747WB Servo Specifications

APPENDIX C: AROD SCHEMATICS- AROD-3 FOREBODY & SHEET 2 OF 2

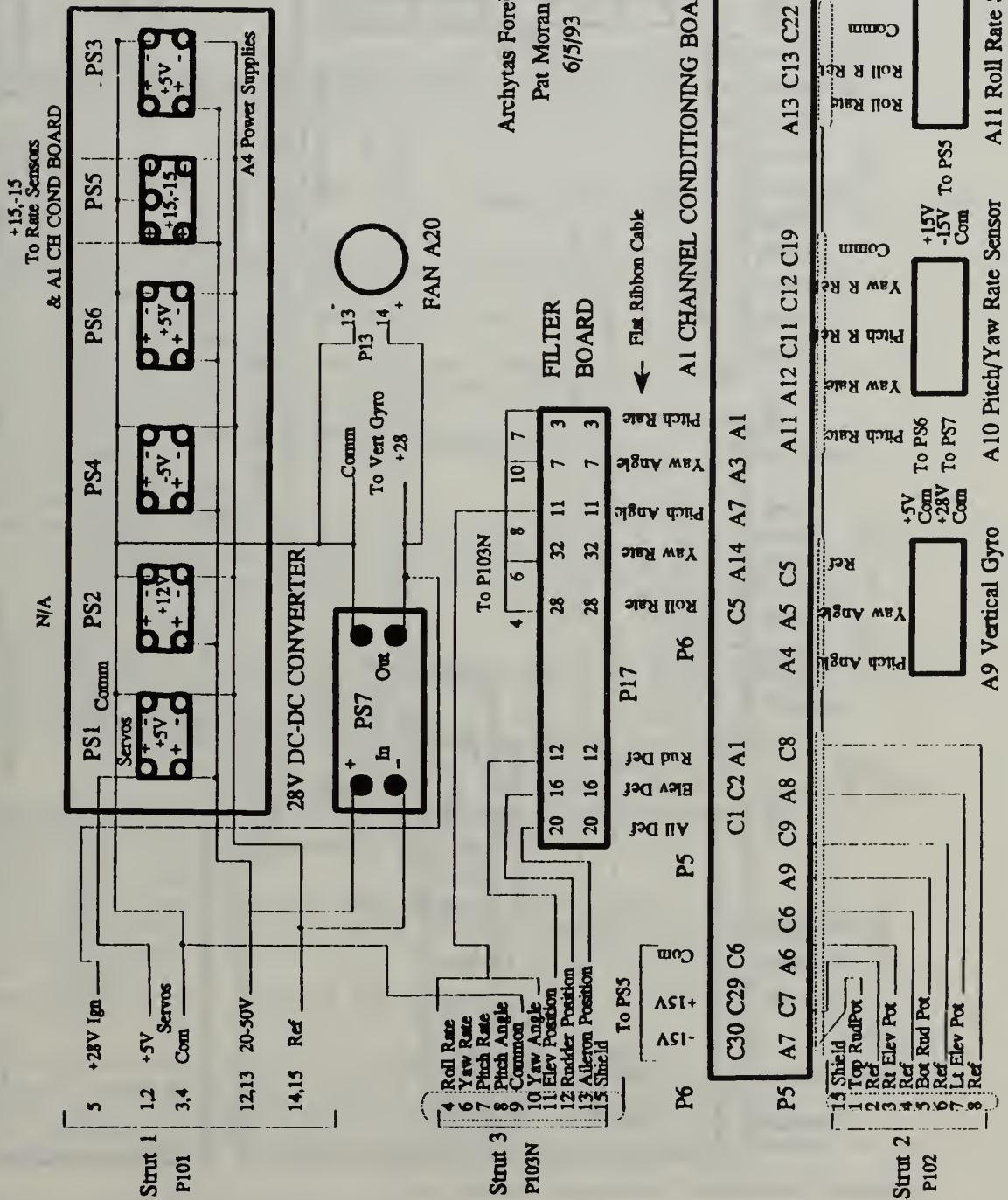


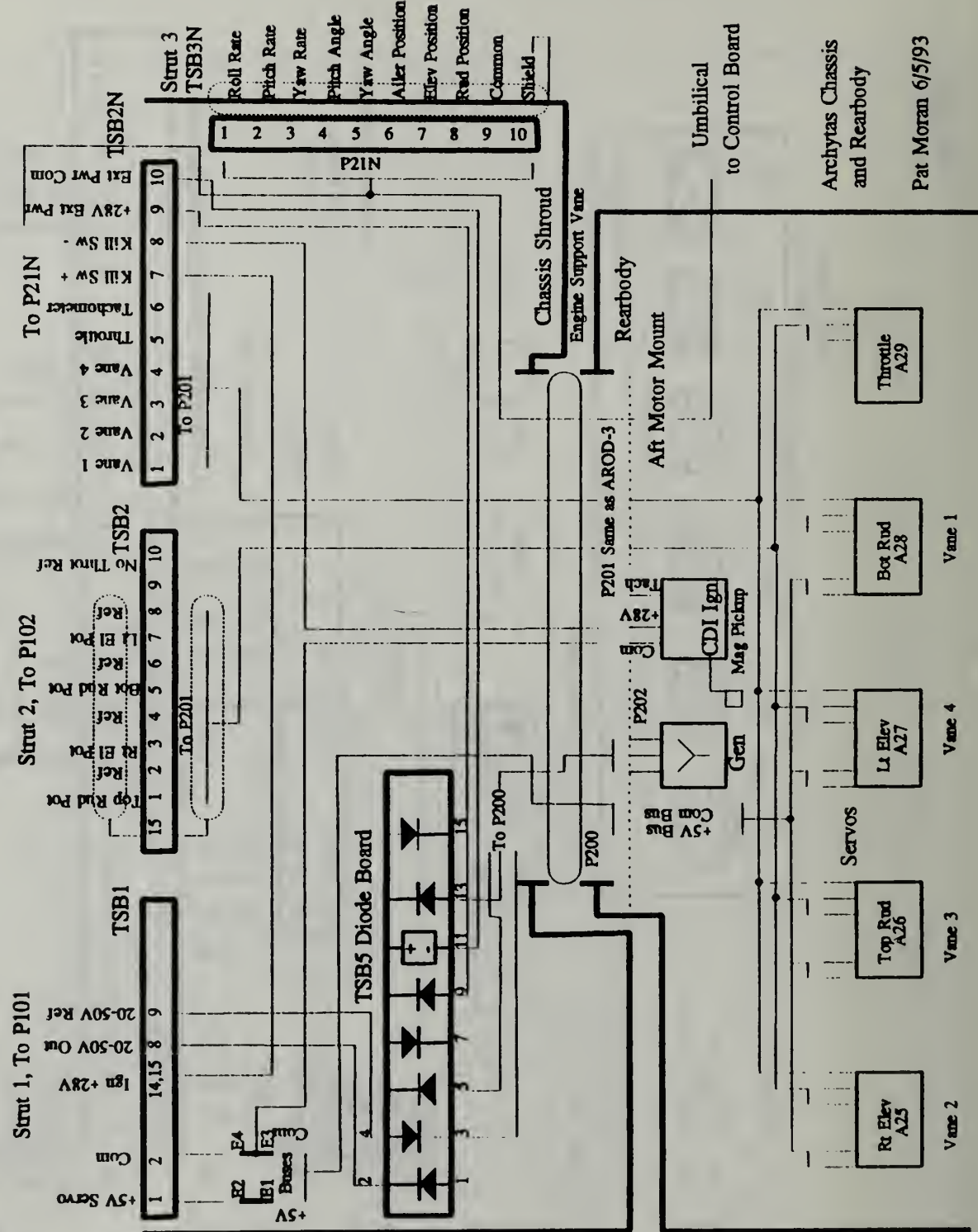
AROD-3 Forebody Schematic, Sheet 1 of 2



AROD-3 Forebody Schematic, Sheet 2 of 2

Archytas Forebody Schematic, Sheet 1 of 2





Archytas Forebody Schematic, Sheet 2 of 2

APPENDIX D: ARCHYTAS UAV ENGINE RUN CHECKLIST

ARCHYTAS ENGINE RUN CHECKLIST

1/22/93 PJM

Setup

Keys for Bldg 249

Vehicle/stand to Bldg 249 (at least 2 people if pushing, or pull w/truck)

Computer setup

Oscilloscope w/probes & cord

Voltmeter w/probes (runs on battery if desired)

External power supply 28 VDC

Tools- allen wrenches, screw drivers, etc

Gasoline- premixed w/oil

Fuel pump (pressurize gas can to feed fuel)

Extension cords (1 already at Bldg 249, bring 1)

Video camera w/film

Ear protection: Foamies/MickeyMouse ears

Safety glasses

Electrical tape

Paper towels

Soldering Gun & solder

Other items: _____

Engine Runs

Notify Prof Howard (X2870) of run/times (phone in Bldg 230- Don has key)

Run area swept clean

Engine stand jacks raised

Personnel rqrd: computer operator (kill switch during start)

brakeman (set brake with tie wrap if no roll rqrd)

starter (assume kill switch duty when engine started)

All duties clearly-defined, primary operator designated

Hand signals understood by all (due to noise)

Hearing & eye protection

Computer up & running

General vehicle security walkaround- no loose panels, wires, etc.

Fire extinguisher nearby (hanging outside entrance to Bldg 249)

Golf course clear

Camera running

Extra observers well forward of vehicle

Duties

Computer operator- throttle, joystick, kill switch (primary operator)

Brakeman- stand by brake, (may be omitted if no roll rqrd)

Starter- pull start cord, (man kill switch once engine started)

Camera operator- safety obsrvr, stand by fire ext (omit w/camera on auto)

MINIMUM PERSONNEL: 2 (camera running, no roll rqrd)

Reminder: KEYS FOR BLDG 249

LIST OF REFERENCES

1. Kaminer, I. I., "Avionics Systems Design AE 4276 Class Notes," Naval Postgraduate School, Monterey, CA, March, 1993.
2. Merz, P. V., *Development and Testing of the Digital Control System for the Archytas Unmanned Air Vehicle*, Master's Thesis, Naval Postgraduate School, Monterey, CA, December, 1992.
3. Davis, J. P., *Design of a Robust Autopilot for the Archytas Prototype using Linear Quadratic Synthesis*, Master's Thesis, Naval Postgraduate School, Monterey, CA, December, 1992.
4. Munson, K., *World Unmanned Aircraft*, Jane's Publishing Co., 1988.
5. Department of Defense, *Unmanned Aerial Vehicles (UAV) Master Plan 1992*, pp. 34-6, 15 April 1992.
6. Draft Proposal, "Development of a Robust Autopilot/Autoland System for the Close-Range Unmanned Air Vehicle", by R. M. Howard and I. I. Kaminer, Naval Postgraduate School, Monterey, CA, 1992.
7. Brynestad, M.A., *Investigation of the Flight Control Requirements of a Half-scale Ducted Fan Unmanned Air Vehicle*, Master's Thesis, Naval Postgraduate School, Monterey, CA, 1992.
8. *AROD Development Status, System Description and Technical Considerations*, Sandia National Laboratory, December, 1986.
9. Stoney, R. B., *Design and Fabrication of a Vertical Attitude Takeoff and Landing Unmanned Air Vehicle*, Master's Thesis, Naval Postgraduate School, Monterey, CA, June, 1992.
10. Humphrey Inc. Product Summary Catalog, June 1992.
11. MAST Project, *Technical Report #1*, by A. P. Pascoal, IST, Lisbon, Portugal, COWIconsult, Copenhagen, Denmark, and ORCA Instrumentation, Brest, France, March, 1992.

12. Kuechenmeister, D. R. *A High-fidelity Non-linear Simulation of an Autonomous Unmanned Air Vehicle*, Master's Thesis, Naval Postgraduate School, Monterey, CA, June, 1993.
13. *Webster's Ninth New Collegiate Dictionary*, p. 1076, Merriam-Webster Inc., 1986.
14. Kaltenberger, B. R., *Design of a Robust Autopilot for the Archytas Prototype in Hover Mode via LQR Synthesis*, Master's Thesis in progress, Naval Postgraduate School, Monterey, CA, to be published September, 1993.
15. Phone Conversation with Mr. C. Cross, Futaba RC Inc., Irvine, CA, April, 1993.
16. Brand, D., "Understanding PCM for Model Radio Control," *Heliscene Magazine*, Issue 3, pp. 60-64, Early Summer, 1991.
17. Hoffman, A., Letter to Archytas Project Working Group, dated 2 March 1993.
18. Kelly, A., and Pohl, I., *A Book on C: Programming in 'C'*, Second Edition, Benjamin/Cummings, 1990.
19. Franklin, G.F., Powell, J.D., and Emami-Naeini, A., *Feedback Control of Dynamic Systems*, Second Edition, Addison-Wesley, April, 1991.

INITIAL DISTRIBUTION LIST

| | No. Copies |
|---|------------|
| 1. Defense Technical Information Center Cameron Station Alexandria VA 22304-6145 | 2 |
| 2. Library, Code 052 Naval Postgraduate School Monterey CA 93943-5002 | 2 |
| 3. Chairman, Code AA Department of Aeronautics and Astronautics Naval Postgraduate School Monterey, CA 93943-5100 | 1 |
| 4. LCDR Patrick J. Moran Commandant (G-EAE-3) U.S. Coast Guard Headquarters 2100 2nd St. SW. Washington, DC 20150 | 1 |
| 5. Professor Richard M. Howard, Code AA/Ho Department of Aeronautics and Astronautics Naval Postgraduate School Monterey, CA 93943-5100 | 2 |
| 6. LCDR Michael K. Shields, Code EC/Sh Department of Electrical and Computer Engineering Naval Postgraduate School Monterey, CA 93943-5100 | 2 |
| 7. Professor Isaac I. Kaminer, Code AA/Ka Department of Aeronautics and Astronautics Naval Postgraduate School Monterey, CA 93943-5100 | 1 |

- | | | |
|-----|--|---|
| 8. | Mr. Don Meeks UAV Lab, Building 214 Naval Postgraduate School Monterey, CA 93943-5100 | 1 |
| 9. | CDR B. J. Niesen Commandant (G-aOLE) U.S. Coast Guard Headquarters 2100 2nd St. SW. Washington, DC 20150 | 1 |
| 10. | CDR R. Renoud Commandant (G-EAE-4) U.S. Coast Guard Headquarters 2100 2nd St. SW. Washington, DC 20150 | 1 |
| 11. | LT Paul Merz 2709 State St. Gautier, MS 39553 | 1 |

DUDLEY KNOX LIBRARY
NAVAL POSTGRADUATE SCHOOL
MONTEREY CA. 93943-5101



DUDLEY KNOX LIBRARY



3 2768 00308585 3